UNIVERSITÀ DELLA CALABRIA

UNIVERSITA' DELLA CALABRIA

Dipartimento di Matematica e Informatica

Scuola di Dottorato

Archimede in Scienze, Comunicazione e Tecnologie

Indirizzo

Scienze e Tecnologie dei Sistemi complessi

CICLO

XXVI

TITOLO TESI

Hydrodynamical models for charge transport in compound semiconductors

Settore Scientifico Disciplinare MAT/07-FISICA MATEMATICA

Direttore: Ch.mo Prof. Pietro Pantano

Supervisori: Ch.mo Prof. Giovanni Mascali

Ch.mo Prof. Giuseppe Alì

Dottoranda: Dott.ssa Rosa Claudia Torcasio

UNIVERSITA DELLA CALABRIA

UNIVERSITA' DELLA CALABRIA

Dipartimento di Matematica e Informatica

Scuola di Dottorato

Archimede in Scienze, Comunicazione e Tecnologie

Indirizzo

Scienze e Tecnologie dei Sistemi complessi

CICLO

XXVI

TITOLO TESI

Hydrodynamical models for charge transport in compound semiconductors

Settore Scientifico Disciplinare MAT/07-FISICA MATEMATICA

Direttore: Ch.mo Prof. Pietro Pantano

Firma Pietro Pantano

Supervisori: Ch.mo Prof. Giovanni Mascali

Firma Giovanni Mascali

Ch.mo Prof. Giuseppe Alì

Firma Giuseppe Alì

Dottoranda: Dott.ssa Rosa Claudia Torcasio

Firma Rosa Claudia Torcasio

Contents

Introduction

Semiconductor materials are employed in different fields, e.g. electronical an microelectronical devices, laser, solar cells. In particular, in microelectronics they have a wide range of applications, including computers, telecomunications, etc.
The most commonly used material for these applications is silicon. There are several examples in literature about the description of its physical properties. Moreover, mathematical models have been developed in order to describe the physical properties that characterize the transport phenomena in this semiconductor. However, since silicon devices operate in a low power range, under current development there are research activities related to technologies and power devices which take into consideration new materials, more appropriate for these applications. In this setting compound semiconductors have found wide use. One of the first compound semiconductor to be used was Gallium arsenide (GaAs), employed, for instance, for infrared LED, lasers or solar cells.
The advantages of GaAs with respect to Si are that it has a higher saturation electron velocity and a higher mobility, and therefore it is important for devices functioning at frequencies higher than 250GHz.
Recently wider bandgap semiconductors, like Gallium nitride (GaN) and Silicon carbide (SiC), have also attracted great interest, since they have a high breakdown field, a low thermal generation rate, and a good thermal conductivity and stability. These properties are useful for high power and high temperature devices.

As a consequence there is an increasing demand of models which can accurately forecast the performance of these devices, analyzing the main physical processes involved in these new materials.
From an industrial point of view, the importance of these models is mainly due to the fact that simulations give the possibility of saving on production costs.
For compound semiconductors, in literature can be found Monte Carlo models [19][29][30], but there is a certain lack of macroscopical models, which are computationally less expensive and then useful for computer aided design (CAD)[20].
The aim of this work is exactly the development of hydrodynamical models for charge transport in compound semiconductors.
These models can be obtained starting from the semiclassical kinetic description of charge transport, taking into account the band structure of the semiconductors of interest. Specifically, one has to consider a number of populations of charge carriers equal to the number of valleys (in the band structure of the material) where the carriers involved in the conductivity live. The state of each carrier population can be described by a distribution function, whose time evolution is determined by a Boltzmann transport equation [11][15][31]. The Poisson equation for the self-consistent electric field is coupled to the Boltzmann equation. The Boltzmann equation is an integro-differential equation which needs to be solved numerically. Since Monte Carlo model and finite difference schemes are computationally very expensive [31][42], hydrodynamical models have been introduced. These models, starting from Bolzmann equation, consider a certain number of moments of the distribution function, obtained multiplying the distribution function by a weight function and integrating over the first Brillouin zone [11]. The weight functions are usually chosen in such a way that they give rise to physically meaningful moments, such as, for example, density, mean velocity, mean energy, etc.
The set of evolution equations related to the moments, which are obtained

from the Boltzmann equation by integration, is a not closed system since the number of unknowns is higher than the number of equations.
In the past, the closure of these hydrodynamical models has been obtained with ad hoc closure relations, sometimes containing parameters without any physical justification [40]. For this reason, alternative methods have been researched, which are based on first physical principles. One of the most used among these is the maximum entropy principle [23][32][36][37][41], which is based on the fact that, if one has a certain amount of information about a physical system, the least biased distribution functions, which can be used for evaluating the unknown moments, are those extremizing the entropy of the system, under the constraint that they reproduce the known information.
This thesis consists of four chapters. In order to better understand the derivation of the models, in the first two chapters we present very briefly some basic concepts of semiconductor physics and charge transport theory.
In particular Chapter 1 starts from the definition of crystals and lattices, continuing with the derivation and the description of the energy band structure of crystals, which allows the introduction of conduction and valence bands. On the basis of width of the gap between these two bands, materials are then classified into insulators, conductors and semiconductors. The chapter ends with the introduction of the main analytic approximations employed for the carrier energy in the valleys and of the concepts of lattice vibrations and phonons, these latters being fundamental for the charge transport description.
In Chapter 2 we derive the Boltzmann equation for electrons, first without collisions, then taking into account the main scattering processes, which can be described by means of suitable collision operators. In fact, we present the main mechanisms of interaction that can occur between electrons and phonons, and electrons and impurities. In conclusion the moments method is introduced together with the closure method based on the maximum entropy principle.
In the last two chapters we describe the two hydrodynamical models re-

spectively developed in [9] and [26]. The objective of both chapters is the construction of macroscopic models which are able to describe the charge transport in a generic compound semiconductor material. In fact the models are constructed in such a way that they can be applied to any semiconductor material with few adjustments, once the physical parameters of the material and the number of valleys in the conduction bands have been identified. In Chapter 3 we present an isotropic model, while in Chapter 4 an anisotropic one. All the main scattering mechanisms are considered in these models, i.e. charge interaction with acoustical and polar optical phonons and impurities as regards the intravalley scattering, and with non polar optical phonons for the intervalley processes.

In semiconductors, the charges which give the most contribution to conduction are the electrons that occupy states around the minima of the lower conduction bands and the holes around the maxima of the higher valence bands. It is then important to construct models which make use of the best possible approximations for the energy dispersion relations for these charges.

In Chapter 3, we consider isotropic energy dispersion relations. The approximation is spherical and non parabolic. In this chapter we show numerical results for bulk GaN and 4H-SiC. The obtained results are in good agreement with those found in literature, based on kinetic models.

However for highly anisotropic semiconductors, better approximations are needed.

In Chapter 4, for this reason, we make use of more general energy dispersion relations, employing an ellipsoidal approximation. This approximation is useful to describe charge transport in semiconductors for which electron masses along the principal axes are consistently different, implying different carrier drift velocities along different directions. At the end of the chapter we show the results of numerical simulation for bulk 4H-SiC and 6H-SiC, that are, also in this case, in good agreement with those found in literature. The model presented in this chapter can be considered as an improvement of the previous one, described in Chapter 3. In fact several comparisons are

made between the isotropic model and the anisotropic one for the case of bulk 4H-SiC. The differences which are found for the valley occupancies, the total mean energy and above all the total drift velocity show the importance of taking into account the anisotropy.

Chapter 1

Semiconductor physics

1.1 Crystal Structures

1.1.1 Crystals and lattices

Definition 1 *Crystals are solids in which atoms are arranged in ordered patterns. Ideal crystals are translation invariant. Defining three vectors* $\boldsymbol{a}_1$,$\boldsymbol{a}_2$ *and* $\boldsymbol{a}_3$ *not lying in the same plane, the crystal remains identical if translated by a vector*

$$\boldsymbol{T} = n_1\boldsymbol{a}_1 + n_2\boldsymbol{a}_2 + n_3\boldsymbol{a}_3, \tag{1.1}$$

with n_1,n_2 *and* n_3 *are any three relative integers [1].*

Along with translations, there are also other symmetry operations found in crystals. For instance they can be rotations, reflections, rotaryreflections and inversions. The space group of a crystal is defined as the set of all its symmetry operations.

Definition 2 *The translation vectors in (1.1) define a set of points called "Bravais lattice" or simply "lattice". The parallelepiped formed by the vectors* $\boldsymbol{a}_1$,$\boldsymbol{a}_2$ *and* $\boldsymbol{a}_3$ *is a primitive unit cell. The lattice in (1.1) can be also called*

"direct lattice", so that it can be distinguished from the "reciprocal lattice" [1].

There is no unique way of choosing a primitive cell. The most common choice is that of the Wigner-Seitz cell, which keeps the symmetry of the Bravais lattice.

Definition 3 *The Wigner-Seitz primitive cell of a lattice is formed by all points closer to one of the lattice points than to any other [1].*

1.1.2 Reciprocal lattice

The concept of reciprocal lattice has a fondamental role in the theory of solid state. Let $\mathbf{a}_1, \mathbf{a}_2, \mathbf{a}_3$ be unit vectors of a direct lattice, we can associate to these vectors, the corresponding three unit vectors $\mathbf{b}_1, \mathbf{b}_2, \mathbf{b}_3$ for the reciprocal lattice, defined by

$$\mathbf{b}_1 = 2\pi \frac{\mathbf{a}_2 \times \mathbf{a}_3}{V_c}, \mathbf{b}_2 = 2\pi \frac{\mathbf{a}_3 \times \mathbf{a}_1}{V_c}, \mathbf{b}_3 = 2\pi \frac{\mathbf{a}_1 \times \mathbf{a}_2}{V_c},$$

where $V_c = \mathbf{a}_1 \cdot \mathbf{a}_2 \times \mathbf{a}_3$ is the volume of the unit cell of the direct lattice. It follows immediately that between the unit vectors of the direct lattice and those of the reciprocal lattice the following condition holds:

$$\mathbf{a}_i \cdot \mathbf{b}_j = 2\pi\delta_{ij}, \quad i = 1, 2, 3, \tag{1.2}$$

where δ_{ij} is the Kronecker delta symbol:

$$\delta_{ij} = 0, \quad i \neq j,$$

$$\delta_{ij} = 1, \quad i = j.$$

Noting that the reciprocal lattice is a Bravais lattice, it is possible to derive its reciprocal lattice. Of course this is the original direct lattice.
The set of all vectors in the reciprocal lattice satisfies the relation

$$e^{i\mathbf{T}\cdot\mathbf{G}} = 1,$$

for $\mathbf{T} = n_1\mathbf{a}_1 + n_2\mathbf{a}_2 + n_3\mathbf{a}_3$ in the direct lattice and $\mathbf{G} = m_1\mathbf{b}_1 + m_2\mathbf{b}_2 + m_3\mathbf{b}_3$ in the reciprocal lattice, being $\mathbf{T}\cdot\mathbf{G}$ given by

$$\mathbf{T}\cdot\mathbf{G} = 2\pi(n_1m_1 + n_2m_2 + n_3m_3).$$

The volume, in reciprocal space, of the reciprocal lattice primitive cell, is the analogous of that of the direct lattice, using now the unit vectors of the reciprocal lattice and employing the formula for the vector triple product:

$$\mathbf{b}_1\cdot\mathbf{b}_2\times\mathbf{b}_3 = \left(\frac{2\pi}{V_c}\right)^3(\mathbf{a}_2\times\mathbf{a}_3)\cdot[(a_3\times\mathbf{a}_1)\times(\mathbf{a}_1\times\mathbf{a}_2)] = \frac{(2\pi)^3}{V_c}.$$

Definition 4 *The first Brillouin zone of a lattice is formed by all points of the reciprocal space closer to one of the points of the reciprocal lattice than to any other [2].*

So, the first Brillouin zone (BZ) is the Wigner-Seitz cell of the reciprocal lattice.

1.2 The Schroedinger equation for external electrons

Electron transport in semiconductors deals with the behaviour of electrons, which can move inside the crystal, under the application of external forces. Therefore a fundamental problem is to determine the states available to the electrons in the crystal and their energies. This is a multiparticle problem which, in principle, requires the solution of a Schroedinger equation

$H\psi = E\psi$, where the Hamiltonian H and the wave function ψ depend on the coordinates of all particles.

We start considering a system composed by N nuclei with masses M_I and charges $Z_I e, I = 1, ..., N$ and n electrons with mass m and charge -e. We indicate by $\mathbf{R}_I$ the position coordinate of the I-th nucleum, and by $\mathbf{r}_i$ the coordinate of the i-th electron. The wave function of electrons and nuclei is of the form $\psi(\mathbf{r}, \mathbf{R}, \mathbf{t})$, where $\mathbf{R} \equiv (R_1, ..., R_N)$ and $\mathbf{r} \equiv (r_1, ..., rn)$.

We now consider the Schroedinger equation:

$$H(\mathbf{r}, \mathbf{R})\psi(\mathbf{r}, \mathbf{R}) = \mathbf{E}\psi(\mathbf{r}, \mathbf{R}). \tag{1.3}$$

The Hamiltonian can be written as:

$$H = T_e + T_N + V_{ee} + V_{NN} + V_{eN} \tag{1.4}$$

where

$T_e = -\sum_{i=1}^{n} \frac{\hbar^2}{2m}\nabla_i^2$ is the electron kinetic energy operator

$T_N = -\sum_{I=1}^{N} \frac{\hbar^2}{2M_I}\nabla_I^2$ is the nuclear kinetic energy operator

$V_{ee} = \frac{1}{2}\sum_{i,j\ i\neq j} \frac{e^2}{|\mathbf{r}_i - \mathbf{r}_j|}$ is the electron-electron potential operator

$V_{NN} = \frac{1}{2}\sum_{I,J\ I\neq J} \frac{Z_I Z_J e^2}{|\mathbf{R}_I - \mathbf{R}_J|}$ is the nuclear-nuclear interaction potential operator

$V_{eN} = \sum_{I,J} \frac{Z_I e^2}{|\mathbf{r}_i - \mathbf{R}_I|}$ is the electron-nuclear interaction potential operator.

An equation of the form (1.3) with Hamiltonian (1.4), obviously cannot be solved analitically and so approximations are needed.

We make then use of the Born-Oppenheimer approximation [3][5].

First of all it must be said that electrons are thousand times lighter than nuclei, and so they can be considered as particles that follow the nuclear motion adiabatically. Hence the adiabatic method can be applied to equation (1.3) separating the function $\psi(\mathbf{r}, \mathbf{R})$ in the product of two functions:

$$\psi(\mathbf{r}, \mathbf{R}) = \phi(\mathbf{r}, \mathbf{R})\theta(\mathbf{R}) \tag{1.5}$$

where ϕ and θ are respectively elecronic and nuclear wave fuctions the former being parametrized by the nuclear positions.

Substituting (1.5) into (1.3) and using the approximation $\nabla_I \theta(\mathbf{R}) \gg \nabla_I \phi(\mathbf{x}, \mathbf{R})$, which is another consequence of the difference in masses between electrons and nuclei, and dividing by $\theta(\mathbf{R})\phi(\mathbf{r}, \mathbf{R})$ we have:

$$T_e \frac{\phi(\mathbf{R}, \mathbf{r})}{\phi(\mathbf{R}, \mathbf{r})} + V_{ee} + V_{eN} = E - T_N \frac{\theta(\mathbf{R})}{\theta(\mathbf{R})} - V_{NN} \tag{1.6}$$

The three terms at the left hand side can be considered as a function of $\mathbf{R}$, say $\mathcal{E}_n(\mathbf{R})$, so:

$$T_e \frac{\phi(\mathbf{R}, \mathbf{r})}{\phi(\mathbf{R}, \mathbf{r})} + V_{ee} + V_{eN} = \mathcal{E}_n(\mathbf{R}). \tag{1.7}$$

Moreover, from the definition of $\mathcal{E}$, in correspondence of each eigenvalue $\mathcal{E}_n$ of (1.7) one has

$$T_N \frac{\theta(\mathbf{R})}{\theta(\mathbf{R})} + V_{NN} + \mathcal{E}_n(\mathbf{R}) = E. \tag{1.8}$$

This yields a set of two coupled equations, (1.7) and (1.8), the first one is an electronic eigenvalue equation, the second one is a nuclear eigenvalue equation. The term $\mathcal{E}_n(\mathbf{R})$, the electron energy, gives a contribution to the potential for nuclei motion.

Equation (1.7) cannot be solved exactly, so further approximations are made, supposing that the electron wave function can be written as the antysimmetrized product of functions of a single electron. In this approximation, so called Hartree-Fock, one obtains the following equations

$$H_{HF}(\mathbf{r}_i)\psi_i(\mathbf{r}_i) = \mathcal{E}_i \psi_i(\mathbf{r}_i),$$

where H_{HF} is the Hartree-Fock Hamiltonian, see [3]. Supposing in addition that the Hamiltonian does not depend on the particular state ψ_i, the above set of N dependent equations reduce to the single particle equation:

$$H(\mathbf{r})\psi(\mathbf{r}) = E\psi(\mathbf{r})$$

with

$$H(\mathbf{r}) = \frac{p^2}{2m} + U(\mathbf{r}),$$

where U is the mean potential of the crystal on each electron which takes into account the effect of the nuclei, of the core electrons and of all the other external electrons. In principle the solution of this equation is an answer to the problem we started with in this section.

1.3 The periodic potential and Bloch's theorem

We now consider an electron in a potential $U(\mathbf{r})$ satisfying the periodicity condition:

$$U(\mathbf{r}+\mathbf{R}) = U(\mathbf{r}) \tag{1.9}$$

for all vectors $\mathbf{R}$ in the direct lattice.
This means that the potential is periodic with the same periodicity of the direct lattice, i.e. is translation invariant with respect to the lattice.
Now, let us consider the Schroedinger equation for a single electron in a periodic potential. This equation has the form

$$H\psi = \left(-\frac{\hbar^2}{2m}\nabla^2 + U(\mathbf{r})\right)\psi = \mathcal{E}\psi. \tag{1.10}$$

The solution of this equation depends on the potential. If the potential U has the periodicity (1.9), the stationary states of Bloch electrons, i.e., of those electrons which satisfy equation (1.10), have a very important property:

Theorem 1 ***Bloch's Theorem.***
The eigenstates ψ of the one-electron Hamiltonian (1.10) , where $U(\mathbf{r}+\mathbf{R}) = U(\mathbf{r})$ for all $\mathbf{R}$ in a Bravais lattice, can be chosen to have the form of the product of a plane wave with a function with the periodicity of the Bravais lattice:

$$\psi(\boldsymbol{r}) = e^{i\boldsymbol{k}\cdot\boldsymbol{r}}u(\boldsymbol{r}), \tag{1.11}$$

where

$$u(\mathbf{r}+\mathbf{R}) = u(\boldsymbol{r}) \tag{1.12}$$

for all $\boldsymbol{R}$ *in the Bravais lattice [2].*

(1.11) are called Bloch waves.
Another way of stating Bloch's theorem is:

$$\psi(\mathbf{r}+\mathbf{R}) = e^{i\mathbf{k}\cdot\mathbf{R}}\psi(\mathbf{r}). \tag{1.13}$$

This follows immediately from equations (1.11) e (1.12).
Proof
Let us define a translation operator:

$$T_{\mathbf{R}}\psi = \psi(\mathbf{r}+\mathbf{R}) \tag{1.14}$$

Using the hypothesis (1.9) and the definition (1.14) it can be proved that H and $T_{\mathbf{R}}$ commute, in fact the Laplacian operator is translation invariant and the potential is periodic. It means that for each ψ we have

$$T_{\mathbf{R}}H\psi = HT_{\mathbf{R}}\psi.$$

Also any two translation operators commute. It follows that the set of operators consisting of the Hamiltonian and the translation operators forms a set of commuting operators. From a theorem of quantum mechanics the eigenstates of H can be chosen to be also eigenstates of translation operators. Therefore, H and $T_{\mathbf{R}}$ admit a common set of eigenstates:

$$H\psi = \mathcal{E}\psi$$

$$T_{\mathbf{R}}\psi = c(\mathbf{R})\psi.$$

Since the translation operators commute and

$$T_{\mathbf{R}}T_{\mathbf{R}'} = T_{\mathbf{R}+\mathbf{R}'}; \tag{1.15}$$

we have that for the eigenvalues $c(\mathbf{R})$ of the translation operators the property

$$c(\mathbf{R}+\mathbf{R}') = c(\mathbf{R})c(\mathbf{R}') \tag{1.16}$$

holds, where $\mathbf{R}$ is a vector in the Bravais lattice, having the form

$$\mathbf{R} = n_1\mathbf{a}_1 + n_2\mathbf{a}_2 + n_3\mathbf{a}_3,$$

with $\mathbf{a}_i,\ i = 1, 2, 3$ three primitive vectors.
We can always write $c(\mathbf{a}_i)$ in the form:

$$c(\mathbf{a}_i) = e^{2\pi i x_i}$$

by a suitable choice of the x_i, which in general are complex numbers. Using (1.16) it follows:

$$c(\mathbf{R}) = e^{2\pi i(n_1x_1+n_2x_2+n_3x_3)} \tag{1.17}$$

Defining $\mathbf{k} = x_1\mathbf{b}_1 + x_2\mathbf{b}_2 + x_3\mathbf{b}_3$, with $\mathbf{b}_i\ i = 1, 2, 3$, satisfing (1.2), we have $\mathbf{k}\cdot\mathbf{R} = 2\pi(n_1x_1 + n_2x_2 + n_3x_3)$, then (1.17) is equivalent to

$$c(\mathbf{R}) = e^{i\mathbf{k}\cdot\mathbf{R}}.$$

In conclusion we have

$$T_{\mathbf{R}}\psi = \psi(\mathbf{r} + \mathbf{R}) = c(\mathbf{R}) = e^{i\mathbf{k}\cdot\mathbf{R}}\psi.$$

1.4 Semiclassical dynamics

An electron in a superposition of Bloch states (wavepacket) strongly peaked around a value $\mathbf{k}_0$ changes its position and wave-vector (also named crystal momentum) under the effect of an external electric field. By using standard results in quantum mechanics [1], it can be proved that the electric field is "sufficiently" slow varying in space the semiclassical approximation holds according to which electrons can be considered as classical particles whose motion is governed by the following equations

$$\mathbf{r} = \mathbf{v}_{\mathbf{k}}^{n} = \frac{1}{\hbar}\nabla_{\mathbf{k}}\mathcal{E}_n(\mathbf{k}), \tag{1.18}$$

$$\hbar\mathbf{k} = -q\mathbf{E}, \tag{1.19}$$

with $\mathbf{r}$ the electron position and $\mathbf{E}$ the electric field.

1.5 Energy bands and group velocity

In principle we can solve equation (1.10) for each different value of $\mathbf{k}$ in the first Brillouin zone, obtaining the eigenvalues $\mathcal{E}_n(\mathbf{k})$ of the states corresponding to the vector $\mathbf{k}$.
$\mathcal{E}_n(\mathbf{k})$ represents the total energy, kinetic and potential, of an electron in the Bloch eigenstate $\psi_n(\mathbf{k})$. The functions $\mathcal{E}_n(\mathbf{k})$ are called energy bands and identify the energetic levels that can be occupied by electrons in a lattice. Energy bands can intersect each other or can be separated by gaps, called energy band gaps. In energy gaps there appear forbidden energies that cannot be reached by electrons moving in the crystal.
From the Planck-Einstein relation, for each $\mathbf{k}$, $\mathcal{E}_n(\mathbf{k})$ is related to a frequency

$$\omega(\mathbf{k}) = \frac{1}{\hbar}\mathcal{E}_n(\mathbf{k}).$$

Therefore, the n-th energy band $\mathcal{E}_n(\mathbf{k})$ can be considered as the dispersion relation of a wavepacket, given by overlapping Bloch waves, whose's corresponding group velocity is

$$\mathbf{v}_n(\mathbf{k}) = \frac{1}{\hbar}\mathcal{E}_n(\mathbf{k}).$$

1.6 Energy bands and material classification

1.6.1 Band occupation

An energy band can be empty, partially filled or completely filled of electrons. If a band is completely filled it cannot conduct. In fact being the Schroedinger

equation invariant under a time reversal transformation, in each band, for each state $\mathbf{k}$ there exists a state $-\mathbf{k}$ such that

$$\mathcal{E}(\mathbf{k}) = \mathcal{E}(-\mathbf{k}).$$

It also holds:

$$\mathbf{v}(\mathbf{k}) = \frac{1}{\hbar}\nabla_{\mathbf{k}}\mathcal{E}(\mathbf{k}) = -\frac{1}{\hbar}\nabla_{\mathbf{k}}\mathcal{E}(-\mathbf{k}) = -v(-\mathbf{k}),$$

since, being the function $\mathcal{E}$ even, its gradient, which is related to the electron group velocity, is odd. So we have

$$\sum_{\mathbf{k}\in BZ} \mathbf{k} = 0, \sum_{\mathbf{k}\in BZ} \mathbf{v}(\mathbf{k}) = 0.$$

Now applying a constant, uniform, electric field, electrons in a completely filled band move as described in the previous section and those exiting from one side of the BZ reenter from the opposite side in such a way that the total occupation is analtered and no charge current is generated.
At zero temperature electrons occupy available states starting from the band with the lowest energy. When the last band occupied is completely filled it is called valence band, while the lowest empty band is called conduction band. The gap between these two bands is the energy gap.

At temperatures higher than zero, a certain number of electrons, by thermal excitation, will move to the conduction band leaving an equal number of empty states in the valence band. Electrons in the conduction band, by the effect of an external electric field, can then move to the higher empty states, and so participate to conduction. Also the empty states left by these electrons in the valence band participate to conduction, because they are available states electrons in valence band can move to. These empty states can be considered as occupied by positively charged particles moving in the direction opposite to that of electrons. These fictitious particles are called holes. While at equilibrium electrons tend to occupy states with lower energy, holes tend to occupy states with higher energy.

Therefore, we can say that a material conductivity is due to electrons in the states near to the lowest energy minima in conduction bands and to holes near the highest energy maxima in valence bands.

1.6.2 Fermi - Dirac distribution

In equilibrium conditions the probability of occupation of an electronic state in a semiconductor is given by the Fermi-Dirac distribution:

$$f(\mathcal{E}) = \frac{1}{e^{\left(\frac{\mathcal{E}-\mu}{k_B T}\right)} + 1}, \tag{1.20}$$

where k_B is the Boltzmann costant, T is the absolute temperature and μ is the chemical potential. This probability depends only on the energy of the state. The Fermi-Dirac distribution is not related to a particular physical system, in fact each system of fermions, i.e. particles that cannot occupy the same state, satisfies (1.20).
From (1.20) it follows that the probability of occupation of a state with energy $\mathcal{E} = \mu$ is $\frac{1}{2}$. This value is called Fermi energy ($\mathcal{E}_F$).

1.6.3 Insulators, conductors, semiconductors

The classification of materials as insulators, conductors and semiconductors can be obtained considering the width of the energy gap:

- if the gap, at zero temperature, between the valence and the conduction band is much higher than $k_B T$, where T is the room temperature, the conduction band remains almost empty also at room temperature because the thermal energy can drive only few electrons from one band to the other. Such a material, in absence of impurities, is an *insulator* (Figure 1.1).

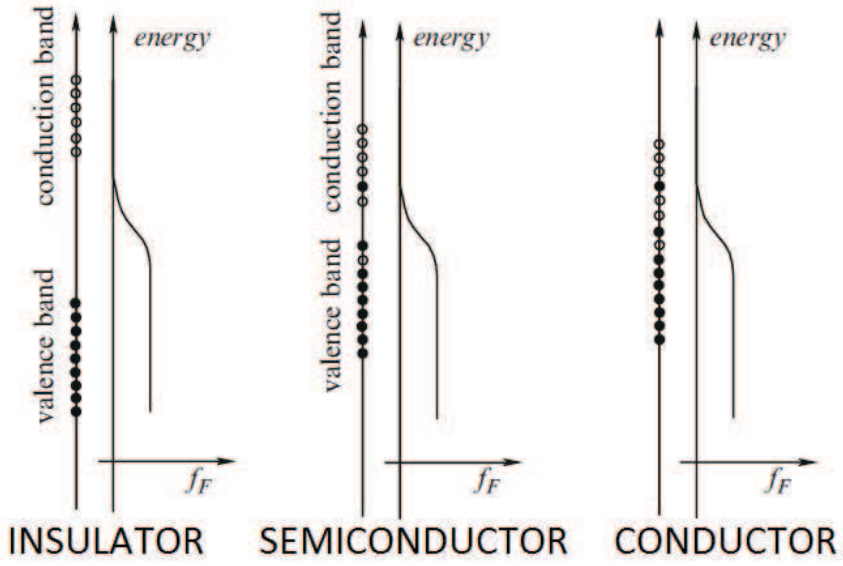

Figure 1.1: Bands and Fermi-Dirac distribution functions in insulators, semiconductors and conductors. The occupied states are represented by coloured circles, the empty states by not coloured ones [1].

- If at zero temperature the valence band is completely filled and the conduction band is empty and their energy gap can be compared with $k_B T$, some electrons are driven to the conduction band by thermal energy. Such a material is called a *semiconductor* (Figure 1.1).
- If at zero temperature the last occupied band is not completely filled or if the gap between the conduction and the valence band is zero, the material is a *conductor* (Figure 1.1).

1.6.4 Doped semiconductors

Doping is useful to increase a semiconductor conductivity. It consists of the increasing of the number of electrons or holes by adding to the semiconductor the so called impurities. If the result is the increasing of the number of electrons in the conduction band the impurities are called donors, while

if the doping produces an increase of holes the impurities are called acceptors. These impurities are ionized, because their atoms donate or accept an electron, so that they can be positively or negatively charged. From ionized donors we have free electrons in a semiconductor, that is called a doped semiconductor of n type. Ionized acceptors yield instead free holes in a semiconductor, in this case called doped semiconductor of p type.

1.7 Band approximation

Generally energy bands as functions of the wave vector $\mathbf{k}$ can be found only numerically, therefore it is often necessary to consider a simple analytical approximations. We consider the regions around the minima of the conduction band, called valleys, or around the maxima of the valence band, also called valleys. We start taking into account the parabolic approximation, in which the conduction band is a paraboloid around the energy minimum of each valley. In this case the function $\mathcal{E}(\mathbf{k})$ is approximated by a quadratic form, that can be one of the following:

$$\mathcal{E}(\mathbf{k}) = \frac{\hbar^2 k^2}{2m};\ (\textit{spherical bands}) \tag{1.21}$$

$$\mathcal{E}(\mathbf{k}) = \frac{\hbar^2}{2}\left[\frac{k_1^2}{m_1} + \frac{k_2^2}{m_2} + \frac{k_3^2}{m_3}\right];\ \ (\textit{ellipsoidal bands}) \tag{1.22}$$

$$\mathcal{E}(\mathbf{k}) = ak^2[1 \mp g(\theta, \psi)].\ \ (\textit{warped bands}) \tag{1.23}$$

In the above equations, $\mathbf{k}$ is measured from the bottom (top) of the band as well as $\mathcal{E}$.
In the first equation the band is locally isotropic around the minimum (maximum). In this case bands have spherical equienergetic surfaces with mass m (Figure 1.2). The second equation represents the anisotropic case considering a band with ellipsoidal isoenergetic surfaces. $1/m_1$, $1/m_2$ and $1/m_3$ are the three eigenvalues of the inverse effective mass tensor defined as

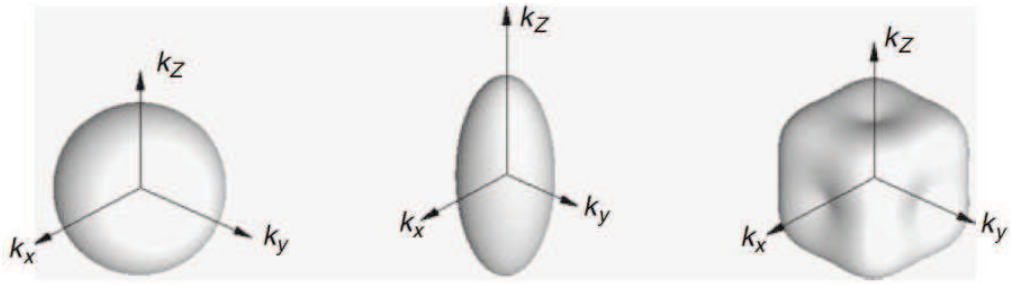

Figure 1.2: Surfaces for spherical, ellipsoidal and warped bands [1]

$M_{ij}^{-1} := \hbar^{-2}\frac{\partial^2 \mathcal{E}}{\partial k_i \partial k_j}$. When using ellipsoidal bands one can consider a trasformation from ellissoids to spheres, given by:

$$\tilde{k_i} = \sqrt{\frac{m^*}{m_i^*}} k_i$$

with $m^* = \sqrt[3]{m_1^* m_2^* m_3^*}$ $i = 1, 2, 3$. This is called the Herring-Vogt transformation and it can be useful to make calculations more simple. In the third equation warped equienergetic surfaces are considered, which are used for holes in valence bands (Figure 1.2). The valence band is warped around its minima because of anisotropy, the expression of the function g can be found in [1].

If we now consider the case in which the values of $\mathbf{k}$ are away from the minima of the conduction band or from the maxima of the valence band, the above expression are no more valid. Therefore, a more accurate approximation is needed:

$$\mathcal{E}(1 + \alpha\mathcal{E}) = \gamma(\mathbf{k}),$$

where α is called nonparabolicity parameter and $\gamma(\mathbf{k})$ can assume one of the forms in (1.21)-(1.23).

In the nonparabolic approximation, also called Kane approximation, the group velocity is given by

$$\mathbf{v} = \frac{1}{\hbar}\nabla_{\mathbf{k}}\mathcal{E} = \frac{\hbar\mathbf{k}}{m(1 + 2\alpha\mathcal{E})}.$$

1.8 Lattice vibrations and phonons

Since a crystal is an elastic medium, elastodynamic waves can propagate in it. There can by two types of elastodynamic waves: the acoustical waves and the optical ones. These waves are generated from displacement of atoms from their equilibrium position, which produces a perturbation of the periodic potential of the lattice.

This displacement, in certain semiconductors, can be coupled with a rearrangement of the charges in the atoms [4]. In these cases we have the so called piezoelectric effect, in which electric fields are produced by stresses and deformations. These fields yield the polar interaction, while the non polar interaction is given, as said, by the potential generated by atoms displacement.

To describe elastodynamic waves is necessary a study from the quantum mechanics point of view. The quantization of the elastodynamic field yields to the concept of phonons, which can be considered as the analogous to photons for the magnetic waves. Of course there can be acoustical and optical phonons.

Equilibrium phonon occupation number is given by the Bose-Einstein distribution [3]

$$N(\hbar\omega) = \frac{1}{e^{\frac{\hbar\omega}{k_B T_L}} - 1}$$

where ω is the phonon frequency and T_L the lattice temperature.

A complete description of electron-phonon interaction requires the second quantization and goes well beyond the scope of this thesis.

In the Born approximation [1], this interaction reduces to two elementary scattering processes: the absorption and the emission of a phonon, which will be discussed with greater details in the next chapter.

Chapter 2

Electronic interactions and Boltzmann equation

2.1 The distribution function

Let us consider a gas of N particles.

Definition 5 *If f(*$\mathbf{x}$*,*$\mathbf{v}$*,t) is a one particle distribution function,*

$$f(\mathbf{x}, \mathbf{v}, t)d\mathbf{x}d\mathbf{v}$$

is the number of particles with positions in the volume $d\mathbf{x}$ *around* $\mathbf{x}$ *and velocities in* $d\mathbf{v}$ *around* $\mathbf{v}$*, at time t [24].*

Then, the normalization condition of the distribution function can be written as [1]

$$\int_V d\mathbf{x} \int_{\mathbb{R}^3} d\mathbf{v} f(\mathbf{x}, \mathbf{v}, t) = N.$$

where V is the space region occupied by the gas.
In the case of electrons in crystals, we consider the distribution function $f(\mathbf{x}, \mathbf{k}, t)$ for a single particle, where the variable $t \in \mathbb{R}^+$ is the time, $\mathbf{x} \in \Omega$ is the position in the crystal, Ω is the volume of the crystal and $\mathbf{k}$ is the wave number defined in the first Brillouin zone $\mathcal{B}$.
In such a case

$$f(\mathbf{x}, \mathbf{k}, t)d\mathbf{x}d\mathbf{k}$$

is the number of electrons in $d\mathbf{x}d\mathbf{k}$ and normalization condition is

$$\int_{\Omega} d\mathbf{x} \int_{\mathcal{B}} d\mathbf{k} f(\mathbf{x}, \mathbf{k}, t) = N,$$

where N is the number of electrons in the conduction band in the sample volume Ω.

2.2 The Boltzmann equation

2.2.1 The Boltzmann equation without collisions

The purpose is to find the kinetic equation govering the time evolution of the electron distribution function[1].
For now we suppose that equations (1.18)-(1.19) give a complete description of the electron dinamics. This means that we are neglecting the effect of collisions between electrons themselves and with phonons.

All the electrons that at the time $t = 0$ are in the volume $d\mathbf{x}_0 d\mathbf{k}_0$ centered in the point $(\mathbf{x}_0, \mathbf{k}_0)$, will move with the same trajectory satisfing equations (1.18)-(1.19). Therefore at the time t those electrons will be in the volume $d\mathbf{x}d\mathbf{k}$ centered in the point $(\mathbf{x}(t), \mathbf{k}(t))$. This implies that

$$f(\mathbf{x}(t), \mathbf{k}(t), t) d\mathbf{x} d\mathbf{k} = f(\mathbf{x}_0, \mathbf{k}_0, 0) d\mathbf{x}_0 d\mathbf{k}_0. \tag{2.1}$$

Moreover according to the Liouville theorem [7], the volume element in the phase space $(\mathbf{x}, \mathbf{k})$ is conserved during the motion, i.e. $d\mathbf{x}d\mathbf{k} = d\mathbf{x}_0 d\mathbf{k}_0$.
Therefore equation (2.1) becomes

$$f(\mathbf{x}(t), \mathbf{k}(t), t) = f(\mathbf{x}_0, \mathbf{k}_0, 0). \tag{2.2}$$

Differentiating with respect to time equation (2.2) and applying the chain rule for differerentiation we obtain:

$$\frac{\partial f}{\partial t} + \frac{d\mathbf{x}}{dt} \cdot \nabla_{\mathbf{x}} f + \frac{d\mathbf{k}}{dt} \cdot \nabla_{\mathbf{k}} f = 0$$

[1] We are neglecting holes and considering n-type devices in which conduction is essentially due to electrons.

Reminding that $(\mathbf{x}(t), \mathbf{k}(t))$ is solution of (1.18)-(1.19), the last equation writes:

$$\frac{\partial f}{\partial t} + \mathbf{v}(\mathbf{k}) \cdot \nabla_{\mathbf{x}} f - \frac{q}{\hbar} \mathbf{E} \cdot \nabla_{\mathbf{k}} f = 0 \tag{2.3}$$

Equation (2.3) is called the Vlasov equation or the collisionless Boltzmann equation and is valid at any t and for each couple of values $(\mathbf{x}, \mathbf{k})$.

2.2.2 The Boltzmann equation with collisions

The Boltzmann equation (2.3) derived in the previous section gives the conservation of the number of electrons in the volume $d\mathbf{x}d\mathbf{k}$. Let $\delta(dN)$ denote the variation of the particle number in the above volume in the time interval dt:

$$\delta(dN) = dN(\mathbf{x}(t+dt), t+dt, \mathbf{k}(t+dt)) - dN(\mathbf{x}, \mathbf{k}) \tag{2.4}$$

where

$$dN(\mathbf{x}, \mathbf{k}, t) = f(\mathbf{x}, \mathbf{k}, t) d\mathbf{x}d\mathbf{k} \tag{2.5}$$

is the number of electrons in the volume $d\mathbf{x}d\mathbf{k}$ at time t [4]. If there are no collisions, $\delta(dN) = 0$, otherwise if collisions occur, $\delta(dN) \neq 0$.
We can write

$$\delta(dN) = \delta(dN)^{in} - \delta(dN)^{out}, \tag{2.6}$$

since because of the scatterings there will be particles entering the volume, thus originating the gain term $\delta(dN)^{in}$ and particles leaving it, giving rise to the loss term $\delta(dN)^{out}$.
We define $P(\mathbf{k}', \mathbf{k}) d\mathbf{k}' dt$ as the probability that after a collision an electron moves from the state $\mathbf{k}'$ to the state $\mathbf{k}$. To find the value of $\delta(dN)^{in}$ we then need to integrate over all possible values of $\mathbf{k}'$ in the first Brillouin zone. In order not to contraddict the Pauli exclusion principle [1], we also need to multiply the previous quantity by $(1 - 4\pi^3 f(\mathbf{x}, t, \mathbf{k}))^2$, i.e. by the probability

[2] $4\pi^3 f$ is the occupation number of the state [1]

that the final state is empty. So doing we obtain:

$$\delta(dN)^{in} = \left(\int_{\mathcal{B}} P(\mathbf{k}', \mathbf{k}) dN(\mathbf{x}, \mathbf{k}') \right) (1 - 4\pi^3 f(\mathbf{x}, t, \mathbf{k}) d\mathbf{k}' dt$$

and, analogously,

$$\delta(dN)^{out} = \left(\int_{\mathcal{B}} (1 - 4\pi^3 f(\mathbf{x}, t, \mathbf{k}')) P(\mathbf{k}, \mathbf{k}') d\mathbf{k}' \right) dN(\mathbf{x}, \mathbf{k}) dt.$$

Substituting the last two equations in (2.6), using definitions (2.4) and (2.5), reminding the Liouville theorem, and letting dt go to zero, we have

$$\frac{\partial f}{\partial t} + \mathbf{v} \cdot \nabla_{\mathbf{x}} f + \frac{q}{\hbar} \mathbf{E} \cdot \nabla_{\mathbf{k}} f = \mathcal{C}(\mathbf{x}, t, \mathbf{k}), \tag{2.7}$$

$$\mathcal{C}(\mathbf{x}, \mathbf{k}, t) = \int_{\mathcal{B}} P(\mathbf{k}', \mathbf{k}) f'(1 - 4\pi^3 f) - P(\mathbf{k}, \mathbf{k}') f(1 - 4\pi^3 f') d\mathbf{k}'$$

where $f := f(\mathbf{x}, \mathbf{k}, t)$ and $f' := f(\mathbf{x}, \mathbf{k}', t)$. $\mathcal{C}(f)$ is called the collision operator and depends on the scattering mechanisms occurring in the semiconductor, because these give the expressions for the various $P(\mathbf{k}, \mathbf{k}')$.
In fact in $\mathcal{C}(f)$ there appears a sum over all types of collisions.
Equation (2.7) is called the Boltzmann equation with collisions and represents the Boltzmann equation for charge transport in semiconductors. The first term at the right hand side represents a gain, of the number of carriers in $(\mathbf{x}, \mathbf{k})$, while the second term represents a loss.
In the semiclassical description, the Boltzmann equation is coupled to the Poisson equation for the electrostatic potential:

$$\nabla_{\mathbf{x}} \cdot \mathbf{E} = -\Delta\phi = \frac{q}{\epsilon} [N_+(\mathbf{x}, t) - N_-(\mathbf{x}, t) + n(\mathbf{x}, t) - p(\mathbf{x}, t)]$$

where ϕ is the electric potential, ϵ is the dielectric constant, depending on the material, and $n(\mathbf{x}, t)$, $p(\mathbf{x}, t)$, $N_+(\mathbf{x}, t)$, $N_-(\mathbf{x}, t)$, are the density of electrons, holes, acceptor dopants and donor dopants respectively.

2.3 Electronic interactions

2.3.1 Scattering mechanisms

As said, the displacement of atoms from their equilibrium position, due to lattice vibrations, yields a perturbation of the periodic potential of the lattice, which is source of scattering.
In a many valley model, electronic scattering can be classified into two classes:

- *intravalley*, if electron after the collision remains in the same valley as before;
- *intervalley*, if the electron after the collision is brought into another valley.

There are several types of collision mechanisms that can be classified as follows. Electrons can interact with:

- *phonons*, producing an absorbtion or emission of a phonon. Of course we need to consider both acoustical and optical phonons.
- *Impurities*, whose effect is relevant at low temperature, when phonons are less effective.
- *Other electrons*, whose effect is relevant at high electron concentrations.

For each kind of collision, the principle of detailed balance holds [1]:

$$P(\mathbf{k}', \mathbf{k}) = P(\mathbf{k}, \mathbf{k}')e^{-\frac{\mathcal{E}(\mathbf{k})-\mathcal{E}(\mathbf{k}')}{\mathbf{k}_B T_L}},$$

which assures that in equilibrium the collision term vanishes.
In order to study electron transitions between two Bloch states, it is convenient to consider the system as separated into the electron of interest and the rest of the crystal. By doing so, the Hamiltonian can be written as

$$H = H_e + H_c + H'.$$

Here H_e is the electron Hamiltonian (1.10), while H_c is the Hamiltonian of the rest of the crystal and H' is the perturbation Hamiltonian, which describes the interaction between the two systems. Therefore the Hamiltonian of the unperturbed system is given by

$$H = H_e + H_c$$

and its eigenstates can be written as direct products of the form

$$|\mathbf{k}, c\rangle = |\mathbf{k}\rangle \, |c\rangle$$

where $|\mathbf{k}\rangle$ and $|c\rangle$ represent the unperturbed states of the electron and the crystal respectively.
The transition probability from the state $|\mathbf{k}, c\rangle$ to the state $|\mathbf{k}', c'\rangle$ is given by the Fermi golden rule [1]

$$P(\mathbf{k}, c, \mathbf{k}', c') = \frac{V}{4\pi^2\hbar} \left|\langle \mathbf{k}', c'| \, H' \, |\mathbf{k}, c\rangle\right|^2 \delta(\mathcal{E}(\mathbf{k}', c') - \mathcal{E}(\mathbf{k}, c)), \tag{2.8}$$

with V the volume of the crystal, $\mathcal{E}(\mathbf{k}, c)$ the unperturbed energy of the state $|\mathbf{k}, c\rangle$.
H' acts on the electron coordinate $\mathbf{r}$ and on the variables $\mathbf{y}$ which describe the state of the crystal.
Expanding H' in Fourier series one has

$$H'(\mathbf{r}, \mathbf{y}) = \frac{1}{\sqrt{V}} \sum_{\boldsymbol{\xi}} \left[\mathcal{A}(\boldsymbol{\xi}, \mathbf{y}) e^{i\boldsymbol{\xi}\cdot\mathbf{r}} + \mathcal{A}^*(\boldsymbol{\xi}, \mathbf{y}) e^{i\boldsymbol{\xi}\cdot\mathbf{r}}\right], \tag{2.9}$$

with $\boldsymbol{\xi}$ wave vector of the reciprocal space, and $\mathcal{A}^*$ the adjoint of $\mathcal{A}$. Considering for now only the first addend of the last expression, the term $\langle \mathbf{k}', c'| \, H' \, |\mathbf{k}, c\rangle$ in (2.8) becomes

$$\langle \mathbf{k}', c'| \, H' \, |\mathbf{k}, c\rangle = \frac{1}{\sqrt{V}} \sum_{\boldsymbol{\xi}} \langle c' \, |\mathcal{A}(\boldsymbol{\xi}, \mathbf{y})| \, c\rangle \int_V \psi^*_{\mathbf{k}'}(\mathbf{r}) e^{i\boldsymbol{\xi}\mathbf{r}} \psi_{\mathbf{k}}(\mathbf{r}) d\mathbf{r}$$

where $\psi_{\mathbf{k}}(\mathbf{r})$ are the Bloch eigenfunctions given by (1.11).
The integral I at the right hand side of the last formula can be decomposed

in the sum of integrals over the cells of the direct lattice. These integrals are all equal to

$$I = \sum_j e^{i(\mathbf{k}-\mathbf{k}'+\boldsymbol{\xi})\cdot\mathbf{R}_j} \int u^*_{\mathbf{k}'}(\mathbf{r}')u_{\mathbf{k}}(\mathbf{r}')e^{i(\mathbf{k}-\mathbf{k}'+\boldsymbol{\xi})\cdot\mathbf{r}'}d\mathbf{r}'.$$

where $\mathbf{R}_j$ are the vectors of the direct lattice which locate the cells. Moreover

$$\sum_j e^{i(\mathbf{k}-\mathbf{k}'+\boldsymbol{\xi})\cdot\mathbf{R}_j} = \delta_{\mathbf{G},\mathbf{k}-\mathbf{k}'+\boldsymbol{\xi}}N$$

where N is the number of cells in the crystal, and $\mathbf{G}$ is a vector of the reciprocal lattice which is null in the intravalley scatterings. The transitions in which $\mathbf{G} = 0$ are called *normal* or *non-umklapp* or *N-processes*, while if $\mathbf{G} \neq 0$ they are called *umklapp* or *U-processes*. The Kronecher δ expresses the conservation of the crystal momentum up to $\mathbf{G}$. Finally, considering in a similar way also the second addend in (2.9), the transition rate (2.8) becomes

$$P(\mathbf{k}, c; \mathbf{k}', c') = \frac{1}{4\pi^2\hbar}\left|\sum_{\boldsymbol{\xi}} \langle c' \left|\mathcal{A}(\boldsymbol{\xi}, \mathbf{y})\right| c\rangle\right|^2 \mathcal{G}(\mathbf{k}, \mathbf{k}', \mathbf{G})\delta(\mathcal{E}(\mathbf{k}', c') - \mathcal{E}(\mathbf{k}, c)). \tag{2.10}$$

Here $\mathcal{G}$ is the overlap integral, given by

$$\mathcal{G}(\mathbf{k}, \mathbf{k}', \mathbf{G}) = \left|N \int u^*_{\mathbf{k}}(\mathbf{r}')u_{\mathbf{k}}(\mathbf{r}')e^{i(\mathbf{G}\cdot\mathbf{r})}d\mathbf{r}\right|^2.$$

2.3.2 Electron-Phonon scattering-Deformation potential

Now we want to apply the results of the last section to the interaction between electrons and phonons. In absence of polarization fields, only the deformation of the lattice needs to be considered. In this case the perturbation Hamiltonian is given by

$$H' = \sum_{ij} E_{ij}\frac{\partial y_i}{\partial r_j}, \tag{2.11}$$

where the $\frac{\partial y_i}{\partial r_j}$ represent the deformation of the crystal due to vibrations, and E_{ij} is the deformation potential tensor costant, which depends on the

material.

In the continuous medium approximation, $\mathbf{y}$, indicating the displacement of the atoms, can be written in terms of the phonon creation and annihilation operators [1], $a^*_{-\boldsymbol{\xi}}$ and $a_{-\boldsymbol{\xi}}$, as follows

$$\mathbf{y}(\mathbf{r}) = \sum_{\boldsymbol{\xi},l} \mathbf{e}_{\boldsymbol{\xi}l} \left(\frac{\hbar}{2\rho V \omega_l(\boldsymbol{\xi})} \right)^{\frac{1}{2}} \left\{ a_{\boldsymbol{\xi}l} + a^*_{-\boldsymbol{\xi}l} \right\} e^{i\boldsymbol{\xi}\cdot\mathbf{r}}$$

where ρ is the density of the crystal, $\mathbf{e}_{\boldsymbol{\xi}l}$ is the polarization vector and $\omega_l(\boldsymbol{\xi})$ is the phonon angular frequency.

Employing the last expression, the Hamiltonian in (2.11) becomes

$$H' = \sum_{ij} E_{ij} \sum_{\boldsymbol{\xi}l} [\mathbf{e}_{\boldsymbol{\xi}l}]_i i\boldsymbol{\xi}_j \left(\frac{\hbar}{2\rho V \omega(\boldsymbol{\xi})} \right)^{\frac{1}{2}} \left\{ a_{\boldsymbol{\xi}l} + a^*_{-\boldsymbol{\xi}l} \right\} e^{i\boldsymbol{\xi}\cdot\mathbf{r}}.$$

This is an explicit forn of the Fourier transform indicated in (2.9). Only two terms containing the creation and annihilation operators give a contribution in the sum over $\boldsymbol{\xi}$ in (2.10) [1]. These terms correspond to the emission or the absorption of a phonon. In the first case a phonon with wave vector $\boldsymbol{\xi}$ and energy $\hbar\omega$ is absorbed by an electron of wave vector $\mathbf{k}$ and energy $\mathcal{E}(\mathbf{k})$. Therefore the wave vector and the energy of the electron after interaction satisfy the following conditions:

$$\mathbf{k}' + \mathbf{G} = \mathbf{k} + \boldsymbol{\xi},$$

$$\mathcal{E}(\mathbf{k}') = \mathcal{E}(\mathbf{k}) + \hbar\omega.$$

In the second case, an electron with wave vector $\mathbf{k}$ and energy $\mathcal{E}(\mathbf{k})$ emits a phonon of wave vector $\boldsymbol{\xi}$ and energy $\hbar\omega$, and its final wave vector and energy are given by

$$\mathbf{k}' + G = \mathbf{k} - \boldsymbol{\xi},$$

$$\mathcal{E}(\mathbf{k}') = \mathcal{E}(\mathbf{k}) + \hbar\omega.$$

From the above results, the transition probability per unit time from the

state $\mathbf{k}$ to the state $\mathbf{k}'$ reads

$$P(\mathbf{k},\mathbf{k}') = \frac{1}{8\pi^2\omega_l(\boldsymbol{\xi})}\begin{bmatrix} N_{\boldsymbol{\xi}l} \\ N_{\boldsymbol{\xi}l}+1 \end{bmatrix}\mathcal{G}\left|\sum_{ij} E_{ij}\boldsymbol{\xi}_j[\mathbf{e}_{\boldsymbol{\xi}l}]_i\right|^2 \delta[\mathcal{E}(\mathbf{k}')-\mathcal{E}(\mathbf{k})\mp\hbar\omega_l(\boldsymbol{\xi})], \tag{2.12}$$

where $N_{\boldsymbol{\xi}l}$ and $N_{\boldsymbol{\xi}l}+1$ refer to absorption and emission, respectively.

2.3.3 Main electron-phonon scattering mechanisms

In this section the main scattering phenomena are presented.

- **Intravalley scattering by acoustic phonons** is usually considered as an elastic process. In this case the phonon polulation $N_{\boldsymbol{\xi}}$ is approximated by [1]

  $$N_{\boldsymbol{\xi}} = \frac{1}{e^{\hbar\xi v_s}/k_BT-1} \approx \frac{k_BT}{\hbar\xi v_s} - \frac{1}{2}$$

  The expression for the scattering probability given by (2.12) becomes:

  $$P^{(ac)}(\mathbf{k},\mathbf{k}') = \frac{\xi E_1^2}{8\pi^2\rho v_s^2}\left[\frac{k_BT_L}{\hbar\xi v_s}\mp\frac{1}{2}\right]\delta(\mathcal{E}(\mathbf{k}')-\mathcal{E}(\mathbf{k}))$$

  where k_B is the Boltzmann constant, T_L is the lattice temperature, and v_s is the sound velocity. The tensor E_{ij} in this case has a diagonal form with equal diagonal elements and therefore is treated as a constant E_1. Moreover the overlap integral $\mathcal{G}$ is constant and therefore included in E_1.

  In the elastic approximation there are no differences between final states coming from absorption or emission processes, then the probabilities per unit time can be summed, to yield

  $$P^{(ac)}(\mathbf{k},\mathbf{k}') = \mathcal{K}^{(ac)}\delta(\mathcal{E}(\mathbf{k}')-\mathcal{E}(\mathbf{k})),$$

  where $\mathcal{K}^{(ac)} = \frac{k_BT_LE_1^2}{4\pi^2\hbar\rho v_s^2}$.

  Since it is not direction dependent the acoustic scattering is an isotropic process.

- **Scattering by polar optical phonon** is present in compound semiconductors and is an inelastic process. It gives rise to an intravalley transition whose scattering rate can be found with a procedure which is shown in [1] and is given by:

$$P^{(p)}(\mathbf{k},\mathbf{k}') = \frac{\mathcal{K}^{(p)}}{|\mathbf{k}-\mathbf{k}'|^2}\,\mathcal{G}(\mathbf{k},\mathbf{k}')\begin{bmatrix} N^{(p)} \\ N^{(p)}+1 \end{bmatrix}\delta(\mathcal{E}'-\mathcal{E}\mp\hbar\omega^{(p)}),$$

where $\mathcal{K}^{(p)} = \frac{q^2\omega^{(p)}}{8\pi^2}\left(\frac{1}{\epsilon_\infty}-\frac{1}{\epsilon_s}\right)$. $N^{(np)}$ is the polar optical phonon occupation number, ϵ_∞ is the high frequency dielectric constant, ϵ_s is the material permittivity. In this expression there appears the overlap integral $\mathcal{G}$, which for materials which have the minimum of the conduction band at the center of the Brillouin zone, is given by [10]

$$\mathcal{G}(\mathbf{k},\mathbf{k'}) = (aa' + cc'cos\beta)$$

with

$$a = \sqrt{\frac{1+\alpha\mathcal{E}}{1+2\alpha\mathcal{E}}}, \qquad a' = \sqrt{\frac{1+\alpha\mathcal{E}'}{1+2\alpha\mathcal{E}'}},$$
$$c = \sqrt{\frac{\alpha\mathcal{E}}{1+2\alpha\mathcal{E}}}, \qquad c' = \sqrt{\frac{\alpha\mathcal{E}'}{1+2\alpha\mathcal{E}'}},$$

and β the angle between $\mathbf{k}$ and $\mathbf{k}'$.

- **Scattering by non polar optical phonons**. In this case the scattering rate can also be written, by an extension of the deformation theory, starting from (2.12) and replacing $E_1^2\boldsymbol{\xi}^2$ by a squared optical coupling constant $(D_tK)^2$ can also include the overlap integral. This scattering mechanism is an intervalley process and transition probability is finally given by:

$$P_0^{(np)}(\mathbf{k}_A,\mathbf{k}'_B) = \mathcal{K}_0^{(np)}\,Z_{AB}\begin{bmatrix} N^{(np)} \\ N^{(np)}+1 \end{bmatrix}\delta(\mathcal{E}'_B-\mathcal{E}_A-\Delta_{AB}\mp\hbar\omega_0^{(np)}),$$

where $\mathcal{K}_0^{(np)} = \frac{(D_tK)^2}{8\pi^2\rho\omega_0^{(np)}}$, A and B are the valleys involved in the transition, $\hbar\omega_0^{(np)}$ is the optical phonon energy, $\Delta_{AB} = \mathcal{E}_A^{(0)} - \mathcal{E}_B^{(0)}$ is the

difference between the energy minima of the valleys, Z_{AB} is the number of equivalent final valleys B as seen from the initial valley A.

2.3.4 Impurity scattering

Interactions between electrons and impurities are scattering processes of electrons by perturbations of the periodic potential due to the presence of impurities. At low impurity concentration, a scattering of an electron by one impurity can be considered as independent from other impurities.
It is an elastic mechanism of interaction whose transition rate reads:

$$P^{(im)}(\mathbf{k},\mathbf{k}') = \frac{\mathcal{K}^{(im)}}{\left[|\mathbf{k}-\mathbf{k}'|^2+\lambda^2\right]^2}\,\delta(\mathcal{E}'-\mathcal{E}),$$

where $\lambda = \sqrt{\frac{N_D q^2}{\epsilon_s k_B T_L}}$, with N_D ionized impurity density, is the inverse of the Debye length, and $\mathcal{K}^{(im)} = \frac{Z^2 N_D\, q^4}{4\pi\hbar\epsilon_s^2}$ with Z impurity charge number.

2.4 Moments method

The Boltzmann equation is an integro-differential equation in the seven indipendent variables $(\mathbf{x},\mathbf{k},t)$. Numerically this equation can be solved by the Monte Carlo method or finite difference schemes, which are accurate but computationally very expensive. For this reason, hydrodynamical models are introduced by using the moments method, described in the following.
We can consider macroscopical quantities that give some of the information included in the distribution function and can be expressed as integrals of the distribution function multiplied by a weight function ψ of the wave vector $\mathbf{k}$. These quantities are known as moments of the distribution function. A moment of the distribution function with respect to the weight $\psi = \psi(\mathbf{k})$ is expressed as:

$$M_\psi(\mathbf{x},\mathbf{t}) = \int_{\mathcal{B}} \psi(\mathbf{k}) f(\mathbf{x},\mathbf{k},\mathbf{t})\mathbf{dk}.$$

Some of the moments have a direct physical meaning. For example, we can use 1, $\mathbf{v}(\mathbf{k})$, $\mathcal{E}(\mathbf{k})$, $\mathcal{E}(\mathbf{k})\mathbf{v}(\mathbf{k})$, to which correspond the following macroscopic quantities [9]
$n = M_1$, electron density
$\mathbf{V} = \frac{1}{n} M_{\mathbf{v}}$, electron mean velocity
$W = \frac{1}{n} M_{\mathcal{E}}$, electron mean energy
$\mathbf{S} = \frac{1}{n} M_{\mathcal{E}\mathbf{v}}$, electron mean energy flux.

We now want to find the evolution equations for the moments [6]. Starting from Boltzmann equation

$$\frac{\partial f}{\partial t} + \mathbf{v} \cdot \nabla_{\mathbf{x}} f - \frac{q}{\hbar} \mathbf{E} \cdot \nabla_{\mathbf{k}} f = \mathcal{C}[f] \tag{2.13}$$

and choosing a certain weight function ψ we want to find an equation for M_ψ. In order to do this we need to multiply equation (2.13) by ψ and to integrate over the Brillouin zone $\mathcal{B}$. We obtain:

$$\int_{\mathcal{B}} \psi \frac{\partial f}{\partial t} d\mathbf{k} + \int_{\mathcal{B}} \psi \mathbf{v} \cdot \nabla_{\mathbf{x}} f d\mathbf{k} - \frac{q}{\hbar} \mathbf{E} \cdot \int_{\mathcal{B}} \psi \nabla_{\mathbf{k}} f d\mathbf{k} = \int_{\mathcal{B}} \psi \mathcal{C}[f] d\mathbf{k}. \tag{2.14}$$

The first term at the left hand side in the last equation can be expressed as

$$\int_{\mathcal{B}} \psi \frac{\partial f}{\partial t} d\mathbf{k} = \frac{\partial}{\partial t} \int_{\mathcal{B}} \psi f d\mathbf{k} = \frac{\partial M_\psi}{\partial t},$$

while for the second term we have

$$\int_{\mathcal{B}} \psi \mathbf{v} \cdot \nabla_{\mathbf{x}} f d\mathbf{k} = \nabla_{\mathbf{k}} \cdot \int_{\mathcal{B}} \psi \mathbf{k} f d_{\mathbf{k}} = \nabla_{\mathbf{x}} \cdot M_{\psi \mathbf{v}}.$$

The third term can be written as

$$-\frac{q}{\hbar} \mathbf{E} \cdot \int_{\mathcal{B}} \psi \nabla_{\mathbf{k}} f d\mathbf{k} = \frac{q}{\hbar} \mathbf{E} \cdot \int_{\mathcal{B}} (\nabla_{\mathbf{k}} \psi f) d\mathbf{k} = q \mathbf{E} \cdot M_{\frac{1}{\hbar} \nabla_{\mathbf{k}} \psi},$$

where we have used the Gauss theorem and the periodicity of the integrand with respect to the Brillouin zone.
As regards the last term at the right hand side we define:

$$\mathcal{C}_\psi := \int_{\mathcal{B}} \psi \mathcal{C}[f] d\mathbf{k}.$$

Thus equation (2.14) becomes

$$\frac{\partial M_\psi}{\partial t} + \nabla_{\mathbf{x}} \cdot M_{\psi \mathbf{v}} + q\mathbf{E} \cdot M_{\frac{1}{\hbar}\nabla_{\mathbf{x}}\psi} = \mathcal{C}_\psi, \tag{2.15}$$

The last expression is the equation for the moment M_ψ.
We note that in this equation there appear moments different from M_ψ.
Adding equations for these other moments is not a solution to close the system, because so doing other unknown moments will be introduced.
Furthermore we don't have constitutive equations for the production terms.
To obtain a closed system, then, we start choosing a finite number of moments. Let these moments be $M_{\psi_1}, ..., M_{\psi_K}$, related to the weights $\psi_1, ..., \psi_K$.
These moments of course satisfy the system of n equations,

$$\frac{\partial M_{\psi_i}}{\partial t} + \nabla_{\mathbf{x}} \cdot M_{\psi_i \mathbf{v}} + q\mathbf{E} \cdot M_{\frac{1}{\hbar}\nabla_{\mathbf{k}}\psi_i} = \mathcal{C}_{\psi_i}, \quad i = 1, ..., K.$$

We need to express the quantities

$$M_{\psi_i \mathbf{v}}, \quad M_{\frac{1}{\hbar}\nabla_{\mathbf{k}}\psi_i}, \quad \mathcal{C}_{\psi_i} \quad i = 1, ..., K$$

as functions of the moments $M_{\psi_1}, ..., M_{\psi_K}$ chosen to describe the state of the system. This is the so called closure problem. In the past several hydrodynamical models have been introduced with ad hoc closure relations, without any physical justification. For this reason closure methods, based on first principles, have been researched. Among these methods there is the maximum entropy principle, which will be presented in the next section.

2.5 Maximum entropy principle

In this section a method to solve the closure problem is described.
We fix the weights ψ_i, $i = 1, ..., K$ and we consider the equations for the corresponding moments (2.15). This amounts to choose as main unknowns the following moments:

$$M_1 := M_{\psi_1}, ..., M_{\psi_k} := M_K. \tag{2.16}$$

We want to express the other moments appearing in the system of evolution equations as functions of the main unknowns (2.16). All these terms we want to find can be expressed as integrals in which there appears the distribution function f, that is solution of the Boltzmann equation. We don't know how this function looks like, but we need a function that depends on the fixed unknowns: $f_{clos} = f_{clos}(\mathbf{x}, \mathbf{k}, t; M_1, ..., M_K)$. With a function like that we can calculate the constitutive relations:

$$M^{clos}_{\psi_i \mathbf{v}}(M_1, ..., M_K) = \int_{\mathcal{B}} \psi_i \mathbf{v} f_{clos} d\mathbf{k},$$

$$M^{clos}_{\frac{1}{\hbar}\nabla_{\mathbf{k}}\psi_i}(M_1, ..., M_K) = \int_{\mathcal{B}} \frac{1}{\hbar} \nabla_{\mathbf{k}} \psi_i f_{clos} d\mathbf{k},$$

$$C^{clos}_{\psi_i}(M_1, ..., M_K) = \int_{\mathcal{B}} \psi_i \mathcal{C}[f_{clos}] d\mathbf{k}.$$

and use the closure relations.

In order to be coherent with the information we have, the following relations must hold:

$$\int_{\mathcal{B}} \psi_i f_{clos} d\mathbf{k} = M_i, \quad i = 1, ..., K. \tag{2.17}$$

Hence, choosing an appropriate closure distribution function f_{clos}, we obtain from (2.15) a closed system for $M_1, ..., M_K$:

$$\frac{\partial M_i}{\partial t} + \nabla_{\mathbf{x}} \cdot M^{clos}_{\psi \mathbf{v}} + q\mathbf{E} \cdot M^{clos}_{\frac{1}{\hbar}\nabla_{\mathbf{x}}\psi} = \mathcal{C}^{clos}_{\psi}, \quad i = 1, ..., K. \tag{2.18}$$

Now the problem is how to choose the distribution function.
A first condition, as said, is that such function has to satisfy (2.17).
From the H-theorem [8], we know that exists a function $S(f)$, related to the opposite of the entropy of the system, which has the property that cannot increase with time, but only decrease. Therefore, for the closure purpose, this property suggests to choose the distribution function for which the function S is minimal, i.e. the entropy is maximal. This idea is called Maximum Entropy Principle [6][11][34][35] and has origins in information theory [33].
The function S(f) can be written as:

$$S(f) = \int_{\mathcal{B}} \mathcal{S}(f) d\mathbf{k}, \qquad \mathcal{S}(f) = f(log 4\pi^3 f - 1). \tag{2.19}$$

Using the above functional, the problem we want to solve can be summarized as follows:
To find the distribution function f for which S(f) has its minimum, among all distribution functions for which (2.17) holds .

This constrained problem can be solved by using the Lagrange multipliers $\lambda_i,\ i = 1, ..., n$. In fact, solving the previous problem is equivalent to:

find a distribution function f and the Lagrange multipliers $\lambda_1, ..., \lambda_K$ *for which the function*

$$\widetilde{S}(f, \lambda_1, ..., \lambda_K) := S(f) + \sum_{i=1}^{K} \lambda_i \left(\int_{\mathcal{B}} \psi_i f d\mathbf{k} - M_i \right) \tag{2.20}$$

has its minimum.

Then we need to differentiate expression (2.20). We first rewrite $\widetilde{S}$ in the form:

$$\widetilde{S}(f, \lambda_1, ..., \lambda_K) = \int_{\mathcal{B}} \left(\mathcal{S}(f) + \sum_{i=1}^{K} \lambda_i \psi_i f \right) d\mathbf{k} - \sum_{i=1}^{K} \lambda_i M_i.$$

We can now calculate the functional derivative of $\widetilde{S}$ with respect to f, obtaining:

$$\frac{\partial \widetilde{S}}{\partial f}[\delta f] = \int_{\mathcal{B}} (S'(f) + \sum_{i=1}^{K} \lambda_i \psi_i) \delta f d\mathbf{k}. \tag{2.21}$$

Differentiating $\widetilde{S}(f)$ with respect to the λ_i, from the expression (2.20), we have:

$$\frac{\partial \widetilde{S}(f)}{\partial \lambda_i} = \int_{\mathcal{B}} \psi_i f d\mathbf{k} - M_i. \tag{2.22}$$

Putting the expressions (2.21) and (2.22) equal to zero, we obtain the conditions:

$$\mathcal{S}'(f) + \sum_{i=1}^{K} \lambda_i \psi_i = 0, \tag{2.23}$$

$$\int_{\mathcal{B}} \psi_i f d\mathbf{k} - M_i = 0, \quad i = 1, ..., K. \tag{2.24}$$

Since $\mathcal{S}(f) = f(log 4\pi^3 f - f)$, then $\mathcal{S}'(f) = log f$, so the first equation in (2.24) becomes:

$$log 4\pi^3 f + \sum_{i=1}^{K} \lambda_i \psi_i = 0,$$

from which

$$f = exp\left(- \sum_{i=1}^{K} \lambda_i \psi_i \right), \tag{2.25}$$

having redifined the Lagrange multipliers.
From the last expression we have the distribution function that we need to solve the problem (2.20). Eventually we need to express Lagrange multipliers as functions of the chosen unknowns $M_1, ..., M_K$. To do this it is sufficient to solve system (2.17).
Finally we have what we call f_{MEP}, where MEP stands for *Maximum Entropy Principle*:

$$f_{MEP} = exp\left(- \sum_{i=1}^{K} \lambda_i \psi_i \right) \tag{2.26}$$

with the Lagrange multipliers that solve the system

$$\int_{\mathcal{B}} \psi_i exp\left(- \sum_{i=1}^{K} \lambda_i \psi_i \right) = M_i, \quad i = 1, ..., K. \tag{2.27}$$

Using f_{MEP} we obtain a closed system of moments equations:

$$\frac{\partial M_i}{\partial t} + \nabla_{\mathbf{x}} \cdot M^{MEP}_{\psi_i \mathbf{v}} + q\mathbf{E} \cdot M^{MEP}_{\frac{1}{\hbar}\nabla_{\mathbf{x}}\psi} = \mathcal{C}^{MEP}_{\psi}, \quad i = 1, ..., K. \tag{2.28}$$

with

$$M^{MEP}_{\psi_i \mathbf{v}}(M_1, ..., M_K) = \int_{\mathcal{B}} \psi_i \mathbf{v} f_{MEP} d\mathbf{k},$$

$$M^{MEP}_{\frac{1}{\hbar}\nabla_{\mathbf{k}}\psi_i}(M_1, ..., M_K) = \int_{\mathcal{B}} \frac{1}{\hbar} \nabla_{\mathbf{k}} \psi_i f_{MEP} d\mathbf{k},$$

$$\mathcal{C}^{MEP}_{\psi_i}(M_1, ..., M_K) = \int_{\mathcal{B}} \psi_i C[f_{MEP}] d\mathbf{k},$$

where the maximum entropy function f_{MEP} is given by (2.26) and (2.27). This system is known as a hydrodynamical model for semiconductors based on the maximum entropy principle.

Chapter 3

An isotropic hydrodynamical model for compound semiconductors

3.1 Analytic approximation of the band structure

In this chapter we present a multivalley isotropic hydrodynamical model, by which it is possible to describe charge transport in a generic compound semiconductor.
In the following, for simplicity, only conduction bands are considered, but an analogous procedure can be done for valence bands.
As said, the main contribution to charge transport is given by those electrons which occupy states around the absolute minimum of the lowest conduction band, and at high fields also by those electrons which lie in states around the satellite minima in the lowest conduction bands, which are closest in energy to the absolute minimum. The dispersion relations in the neighbors of these minima, which are called valleys, are analitically approximated by ellipsoidal,

non parabolic expressions of the form (see section 1.7):

$$\mathcal{E}_A(\mathbf{k}_A)\left[1+\alpha_A\,\mathcal{E}_A(\mathbf{k}_A)\right]=\frac{\hbar^2}{2}\left[\frac{((\mathbf{k}_A)_1)^2}{(m_A^*)_1}+\frac{((\mathbf{k}_A)_2)^2}{(m_A^*)_2}+\frac{((\mathbf{k}_A)_3)^2}{(m_A^*)_3}\right], \qquad (3.1)$$

where the index A represents the valley that is taken into consideration, $\mathcal{E}_A$ is the electron energy in the A-th valley, measured from the bottom of the valley, $\mathbf{k}_A$ is the electron quasi-wave vector referred, for each valley, to the minimum of the valley, α_A is the non-parabolicity factor and $(m_A)_i^{-1}$ $i=1,2,3$ are the eigenvalues of inverse effective-mass tensor of the A-th valley.

Making use of the Herring-Vogt transformation

$$k_i^*=\sqrt{\frac{m^*}{(m_A^*)_i}}k_i$$

with $m^*=(m_1^*m_2^*m_3^*)^{\frac{1}{3}}$ density of states mass, the volume element in the $\mathbf{k}$-space can be written as

$$d\mathbf{k}=\frac{m^*\sqrt{2m^*}}{\hbar^3}\mathcal{N}(\mathcal{E},\alpha)d\mathcal{E}d\Omega, \quad \mathcal{N}(\mathcal{E},\alpha):=\sqrt{\mathcal{E}(1+\alpha\mathcal{E})}(1+2\alpha\mathcal{E}),$$

where $d\Omega$ is the solid angle element and we have dropped the valley index for simplicity. In this chapter we will make use of the isotropic approximation, which considers m^* as unique mass in any direction.

In this case, being the electron velocity given by

$$\mathbf{v}=\frac{1}{\hbar}\nabla_{\mathbf{k}}\mathcal{E}. \qquad (3.2)$$

$\mathbf{k}$, and $\mathbf{v}$ have the same direction, that is

$$k_i=\frac{\sqrt{2m^*}}{\hbar}\sqrt{\mathcal{E}(1+\alpha\mathcal{E})}n_i, \quad v_i=\sqrt{\frac{2}{m^*}}\frac{\sqrt{\mathcal{E}(1+\alpha\mathcal{E})}}{(1+2\alpha\mathcal{E})}n_i,$$

with $\mathbf{n}$ unit vector.

3.2 Hydrodynamical model

Conduction electrons are described as made of different populations, one for each valley. Thus, at a kinetic level, the electron state is represented by the distribution functions $f_A(\mathbf{x}, \mathbf{k}, t)$, where the index A identifies the considered valley.

The Boltzmann equations, which govern the time evolution of these functions, and which were introduced in the previous chapter, are here rewritten with an explicit reference to valleys:

$$\frac{\partial f_A(\mathbf{x}, \mathbf{k}, t)}{\partial t} + \mathbf{v} \cdot \nabla_{\mathbf{x}} f_A - \frac{q}{\hbar} \mathbf{E} \cdot \nabla_{\mathbf{k}} f_A = \mathcal{C}[f_A] + \sum_{B \neq A} \mathcal{C}_{AB}[f_A, f_B], \quad (3.3)$$

$$\nabla_{\mathbf{x}} \cdot (\epsilon_s \mathbf{E}) = q \left[N_-(\mathbf{x}, t) - n(\mathbf{x}, \mathbf{t}) \right], \qquad A, B = 1, 2, \ldots \quad (3.4)$$

the last equation being the Poisson equation for the self-consistent electric field to which the Boltzmann equations are coupled. In this case, the electron density n is given by

$$n = \sum_A \int_{\mathbb{R}^3} f_A(\mathbf{x}, \mathbf{k}, t) d\mathbf{k},$$

and ϵ_s indicates the dielectric constant of the semiconductor.

Comparing (3.4) with the expression reported in Chapter 2 we note that two terms are missing. This happens because we are neglecting holes and considering n-type devices. On the right-hand side of (3.3) there appear the collision operators, which can be divided into two classes: the first, denoted with $\mathcal{C}$ represents intravalley transitions, while the second one, corresponding to the terms $\mathcal{C}_{AB}$, refers to intervalley transitions.

As regards the first class, the collision operator in the non-degenerate approximation reads

$$\mathcal{C}_A[f] = \int_{\mathbb{R}^3} \left[P(\mathbf{k}', \mathbf{k}) f(\mathbf{k}') - P(\mathbf{k}, \mathbf{k}') f(\mathbf{k}) \right] d\mathbf{k}', \quad (3.5)$$

while the collision operators of the second class have the form

$$C_{A,B}[f_A, f_B] = \int_{\mathbb{R}^3} \left[P_{BA}(\mathbf{k}', \mathbf{k}) \, f'_B - P_{AB}(\mathbf{k}, \mathbf{k}') \, f_A \right] d\mathbf{k}' \quad (3.6)$$

where A and B are different valleys.
The scattering mechanisms considered here, with their related scattering rates, are those presented in section 2.3: acoustic scattering, polar optical phonon scattering and impurity scattering as regards intravalley transition, and non polar optical phonon scattering for intervalley transitions.
To all these processes, in the intervalley case, a first order correction to non-polar optical scattering rate must be added, which has the form

$$\begin{aligned} P_1^{(np)}(\mathbf{k}_A, \mathbf{k}'_B) &= \mathcal{K}_1^{(np)} |\mathbf{k}_A + \mathbf{k}_A^0 - \mathbf{k}'_B - \mathbf{k}_B^0|^2 Z_{AB} \begin{bmatrix} N^{(np)} \\ N^{(np)} + 1 \end{bmatrix} \\ &\times \delta(\mathcal{E}'_B - \mathcal{E}_A - \Delta_{AB} \mp \hbar\omega_1^{(np)}), \end{aligned} \tag{3.7}$$

with $A \neq B$, and $\mathcal{K}_1^{(np)} = \frac{(D_1)^2}{8\pi^2 \rho \omega_1^{(np)}}$. D_1 and $\omega_1^{(np)}$ respectively are the first-order intervalley deformation potential and phonon frequency. $\mathbf{k}_A^0$ and $\mathbf{k}_B^0$ are the centers of the A-th valley and of the B-th one, respectively. In order to find an approximation of the Boltzmann equations, the moments method needs now to be applied. Once the weights 1, $\mathbf{v}(\mathbf{k})$, $\mathcal{E}(\mathbf{k})$, $\mathcal{E}(\mathbf{k})\mathbf{v}(\mathbf{k})$ have been chosen and after multiplying the distribution functions by these weights, and integrating as in Chapter 2, the following moments are defined
$n = M_1$, electron density
$\mathbf{V} = \frac{1}{n} M_{\mathbf{v}}$, electron mean velocity
$W = \frac{1}{n} M_{\mathcal{E}}$, electron mean energy
$\mathbf{S} = \frac{1}{n} M_{\mathcal{E}\mathbf{v}}$, electron mean energy flux,
one set for each valley, and their evolution equations consist of the following set of balance equations

$$\frac{\partial n_A}{\partial t} + \frac{\partial (n_A \, V_A^j)}{\partial x^j} = n_A \, C_{n_A}, \tag{3.8}$$

$$\frac{\partial (n_A \, V_A^i)}{\partial t} + \frac{\partial (n_A \, F_A^{(0)ij})}{\partial x^j} + q \, E_j \, n_A \, G_A^{(0)ij} = n_A \, C_{V_A}^i, \qquad i = 1, 2, 3, \tag{3.9}$$

$$\frac{\partial (n_A \, W_A)}{\partial t} + \frac{\partial (n_A \, S_A^j)}{\partial x^j} + q \, E_j \, n_A V_A^j = n_A \, C_{W_A}, \tag{3.10}$$

$$\frac{\partial (n_A \, S_A^i)}{\partial t} + \frac{\partial (n_A \, F_A^{(1)ij})}{\partial x^j} + q \, E_j \, n_A \, G_A^{(1)ij} = n_A \, C_{S_A}^i, \qquad i = 1, 2, 3, \tag{3.11}$$

where

$$C_{n_A} = \frac{1}{n_A}\int \Big(C[f_A] + \sum_{B\neq A} C_{AB}[f_A, f_B]\Big) d\mathbf{k} \qquad \text{is the density production,}$$

$$\begin{aligned}
F_A^{(0)ij} &= \frac{1}{n_A}\int v_A^i v_A^j f_A d\mathbf{k} \qquad \text{is the velocity flux,}\\
G_A^{(0)ij} &= \frac{1}{n_A}\int \frac{1}{\hbar}\frac{\partial v_A^i}{\partial k^j} f_A d\mathbf{k},\\
C_{V_A}^i &= \frac{1}{n_A}\int v_A^i \Big(C[f_A] + \sum_{B\neq A} C_{AB}[f_A, f_B]\Big) d\mathbf{k} \quad \text{is the velocity production,}\\
C_{W_A} &= \frac{1}{n_A}\int \mathcal{E}_A(\mathbf{k})\Big(C[f_A] + \sum_{B\neq A} C_{AB}[f_A, f_B]\Big) d\mathbf{k} \text{ is the energy production,}\\
F_A^{(1)ij} &= \frac{1}{n_A}\int \mathcal{E}_A(\mathbf{k}) v_A^i v_A^j f_A d\mathbf{k} \qquad \text{is the flux of the energy flux,} \qquad (3.12)\\
G_A^{(1)ij} &= \frac{1}{n_A}\int \frac{1}{\hbar}\frac{\partial(\mathcal{E}_A v_A^i)}{\partial k^j} f_A d\mathbf{k},\\
C_{S_A}^i &= \frac{1}{n_A}\int \mathcal{E}_A v_A^i \Big(C[f_A] + \sum_{B\neq A} C_{AB}[f_A, f_B]\Big) d\mathbf{k} \text{ is the energy flux production.}
\end{aligned}$$

The system of equations (3.8)-(3.11) is not closed, since the number of unknowns is greater than the number of equations. In fact in this system there appear the fluxes $F_A^{(0)ij}$, $G_A^{(0)ij}$, $F_A^{(1)ij}$, $G_A^{(1)ij}$ and the production terms C_{n_A}, $C_{V_A}^i$, C_{W_A}, $C_{S_A}^i$, that need to be expressed as functions of the variables n_A, $\mathbf{V}_A$, W_A, and $\mathbf{S}_A$.

3.3 Closure by the maximum entropy principle

To get closure relations for the above system, we will make use of the maximum entropy principle.

According to this principle, already discussed in section 2.5, if a finite number of moments is known, then the distribution functions f_A^{MEP}, which can

be used for evaluating the unknown moments, correspond to the extremum of the entropy functional, under the costraints that those function reproduce the known moments

$$M_{\psi}^{A} = \int_{\mathbb{R}^3} \psi(\mathbf{k}) f_A^{MEP} d\mathbf{k}, \ \psi = 1, \mathbf{v}, \mathcal{E}, \mathcal{E}\mathbf{v}. \tag{3.13}$$

Here the maximum entropy distribution functions f_A^{MEP} and the moments M_{ψ}^{A} are written as depending on the index A, which represents the particular valley taken into consideration.

Since the phonon gas is considered as a thermal bath at constant temperature T_L, the Helmholtz free energy is a Liapunov functional [21] for the Boltzmann Poisson system, and it can be shown that the deriving optimization problem is equivalent to extremizing only the electron component of the entropy, under the condition that the average energy is one of the constraints. If the electron gas is sufficiently dilute, we can take the expression of the entropy obtained as limiting case of that arising in the Fermi statistics, then the entropy functional reads

$$\mathcal{S} = -k_B \sum_A \int_{\mathbb{R}^3} \left(f_A \log \frac{f_A}{y} - f_A \right) d\mathbf{k}, \quad y = \frac{2}{(2\pi)^3}.$$

Hence, appropriate distribution functions which extremize S under the constraints (3.13) have to be found. As said, in order to solve this constrained extremum problem, we need to make use of the Lagrangian multipliers. So doing we obtain the following maximum entropy distribution functions

$$f_A^{MEP} = \exp\left[- \left(\lambda^A + \lambda_{\mathbf{V}}^A \cdot \mathbf{v} + \left(\lambda_W^A + \lambda_{\mathbf{S}}^A \cdot \mathbf{v} \right) \mathcal{E}_A \right) \right], \quad A = 1, 2 \ldots$$

To close the equations, the Lagrange multipliers have to be expressed in terms of the fundamental variables, therefore the last expressions have to be substituted in (3.13). However an analytic inversion is impossible and a numerical one is not useful for numerical simulations of electron devices, because it needs to be performed at each time evolution of the state variables [14]. Therefore, only approximate expressions, under certain physical assumptions,

can be obtained. Using the same approach as in [11][15][16][17][38], we assume a small anisotropy of the distribution functions. Starting from the fact that the equilibrium state distribution functions are isotropic, i.e.

$$f_A^{MEP} = exp[-(\lambda^A + \lambda_W^A \mathcal{E})],$$

we suppose that the anisotropy of the f_A^{MEP} remain small also out of the equilibrium. This can be done by introducing a small parameter of anisotropy δ, assuming distribution functions to be analytic in δ and expanding them around δ up to the first order. Considering the representation theorems for isotropic functions, it follows that λ^A and λ_W^A are of zero order in δ, while $\lambda_{\mathbf{v}}^A$ and $\lambda_{\mathbf{S}}^A$ are of the first order in δ.
Therefore, so doing, the resulting approximate maximum entropy distribution functions read

$$f_A^{MEP} \approx \exp\left[-\lambda^A - \lambda_W^A \mathcal{E}_A\right]\left[1 - \delta\left(\lambda_{\mathbf{V}}^A \cdot \mathbf{v} + \lambda_{\mathbf{S}}^A \cdot \mathbf{v}\mathcal{E}_A\right)\right] + o(\delta). \quad (3.14)$$

In order to obtain the closure relations for the system (3.8)-(3.11) we consider only terms up to the first order in δ, then we can write

$$f_A^{MEP} \approx \exp\left[-\lambda^A - \lambda_W^A \mathcal{E}_A\right]\left[1 - \left(\lambda_{\mathbf{V}}^A \cdot \mathbf{v} + \lambda_{\mathbf{S}}^A \cdot \mathbf{v}\mathcal{E}_A\right)\right]. \quad (3.15)$$

Using these functions, the constraint relations can be inverted almost analitically.
Specifically, the equations to invert are the following

$$n_A = \int_{\Re^3} f_A^{MEP} d\mathbf{k}, \quad (3.16)$$

$$\mathbf{V}_A = \frac{1}{n_A}\int_{\Re^3} \mathbf{v}_A(\mathbf{k}_A) f_A^{MEP} d\mathbf{k}, \quad (3.17)$$

$$W_A = \frac{1}{n_A}\int_{\Re^3} \mathcal{E}(\mathbf{k}_A) f_A^{MEP} d\mathbf{k}, \quad (3.18)$$

$$\mathbf{S}_A = \frac{1}{n_A}\int_{\Re^3} \mathcal{E}(\mathbf{k}_A)\mathbf{v}_A(\mathbf{k}_A) f_A^{MEP} d\mathbf{k}, \quad (3.19)$$

where the f_A^{MEP} are given by (3.15).

For the densities and the energies we find

$$n = \frac{4\pi m^* \sqrt{2m^*}}{\hbar^3} \exp(-\lambda) \int_{\mathbb{R}^3} \exp(-\lambda_W \mathcal{E}) \mathcal{N}(\mathcal{E}, \alpha) d\mathcal{E},$$

$$W = \frac{4\pi m^* \sqrt{2m^*}}{\hbar^3 \, n} \exp(-\lambda) \int_{\mathbb{R}^3} \exp(-\lambda_W \mathcal{E}) \mathcal{E} \mathcal{N}(\mathcal{E}, \alpha) d\mathcal{E},$$

and defining

$d_0(\lambda_W, \alpha) := \int_{\mathbb{R}^3} \exp -(\lambda_W \mathcal{E}) \mathcal{N}(\mathcal{E}, \alpha) d\mathcal{E} = \frac{exp(\frac{\lambda_W}{2\alpha})}{2\lambda_W \sqrt{\alpha}} K_2(\frac{\lambda_W}{2\alpha})$

and

$d_n(\lambda_W, \alpha) := (-1)^n \frac{\partial}{\partial \lambda_W} d_0(\lambda_W, \alpha),$

where K_2 is the modified Bessel function of the second kind, one has

$$\lambda = -\log\left(\frac{\hbar^3 n}{4\,\pi\, m^*\, \sqrt{2\, m^*} d_0}\right),$$

$$\lambda_W = g^{-1}(W, \alpha),$$

where g^{-1} is the inverse function of $\frac{d_1(\lambda_W, \alpha)}{d_0(\lambda_W, \alpha)}$.

For the vector multipliers we obtain

$$\lambda_{V_i} = b_{11}(W, \alpha)\, V_i + b_{12}(W, \alpha)\, S_i, \qquad \lambda_{S_i} = b_{12}(W, \alpha)\, V_i + b_{22}(W, \alpha)\, S_i.$$

The b_{ij} are the elements of the matrix $\mathbf{B}$, which is the inverse of the symmetric matrix $\mathbf{A}$ of elements

$$a_{ij} = -\frac{2}{3m^*} \frac{p_{i+j-2}}{d_0},$$

with $p_n = p_n(W, \alpha) := \int_{\mathbb{R}^3} \frac{[\mathcal{E}(1+\alpha\mathcal{E})]^{\frac{3}{2}}}{1+2\alpha\mathcal{E}} \mathcal{E}^n \exp(-\lambda_W \mathcal{E})\, d\mathcal{E}$. The matrix B is symmetric, which reminds us of the Onsager relations [22].

Once the Lagrange multipliers are expressed as functions of the fundamental variables, the following step is to evalute the unknown moments present in the system (3.8)-(3.11), i.e. to get the closure relations for the fluxes and the production terms.

Closure relations for the fluxes. It is easy to show that

$$\begin{pmatrix} \mathbf{F}^{(0)} \\ \mathbf{F}^{(1)} \end{pmatrix} = \frac{2}{3m^* d_0} \begin{pmatrix} p_0 \\ p_1 \end{pmatrix} \mathbf{I},$$

with $\mathbf{I}$ the identity, and

$$\left(\begin{array}{c} \mathbf{G}^{(0)} \\ \mathbf{G}^{(1)} \end{array} \right) = \frac{1}{m^* d_0} \left[\int \left(\begin{array}{c} 1 - \frac{4}{3}\alpha \frac{\mathcal{E}(1+\alpha\mathcal{E})}{(1+2\alpha\mathcal{E})^2} \\ \mathcal{E} + \frac{2}{3} \frac{\mathcal{E}(1+\alpha\mathcal{E})}{(1+2\alpha\mathcal{E})^2} \end{array} \right) \exp\left(-\lambda_W \mathcal{E}\right) \sqrt{\mathcal{E}\left(1+\alpha\mathcal{E}\right)} d\mathcal{E} \right] \mathbf{I}.$$

Closure relations for the production terms

- **Acoustic phonon scattering**. Since the scattering is intravalley and elastic, the only non-zero production terms are those relative to the velocities and the energy fluxes. After some calculations in which we employ the following formula for angular integrals over the unit sphere S^2

$$\int_{S^2} n_{i_1} \cdots n_{i_k} \, d\Omega = \left\{ \begin{array}{ll} 0 & \text{if k is odd} \\ \frac{4\pi}{k+1} \delta_{(i_1 i_2} \cdots \delta_{i_{k-1} i_k)} & \text{if k is even,} \end{array} \right.$$

  we find

$$\left(\begin{array}{c} C^{(ac)}_{\mathbf{V}} \\ C^{(ac)}_{\mathbf{S}} \end{array} \right) = \mathbf{Q}^{(ac)} \mathbf{B} \left(\begin{array}{c} \mathbf{V} \\ \mathbf{S} \end{array} \right),$$

  where $\mathbf{Q}^{(ac)}$ is the matrix of elements

$$\begin{aligned} q^{(ac)}_{ij}(W,\alpha) &= \frac{8\pi\sqrt{2m^*}}{3\hbar^3 d_0} \frac{(i+j)!}{\lambda_W^{1+i+j}} \left[1 + 2\alpha(i+j+1)\lambda_W^{-1} \right. \\ &\quad \left. + \alpha^2 (i+j+2)(i+j+1)\lambda_W^{-2} \right]. \end{aligned}$$

- **Polar optical phonon scattering**. In this case the calculations are more involved, and make use also of the detailed balance principle, which here we rewrite in the general form valid for intervalley scattering too

$$P_{AB}(\mathbf{k}'_B, \mathbf{k}_A) = P_{AB}(\mathbf{k}_A, \mathbf{k}'_B) \exp\left(-\frac{\mathcal{E}_A - \mathcal{E}'_B + \Delta_{AB}}{k_B T_L} \right). \qquad (3.20)$$

For the density and the energy production terms we have

$$
\begin{aligned}
&C_n^{(p)} = 0,\\
&C_W^{(p)} = -\frac{2\pi m^* \omega^{(p)}}{\sqrt{2m^*}\, d_0} N^{(p)} \mathcal{K}^{(p)} \int_0^\infty \exp\left(-\lambda_W \mathcal{E}\right)\\
&\times \left(e^{-\hbar\omega^{(p)}\left(\lambda_W - \frac{1}{k_B T_L}\right)} - 1 \right) \Big[H_2(\mathcal{E}, \mathcal{E}^+, \alpha) H_3(\mathcal{E}, \mathcal{E}^+, \alpha)\\
&+ \alpha H_4(\mathcal{E}, \mathcal{E}^+, \alpha) \left(1 + \alpha \frac{H_1(\mathcal{E}, \alpha) + H_1(\mathcal{E}^+, \alpha)}{4 H_2(\mathcal{E}, \mathcal{E}^+, \alpha)} \right) \Big] d\mathcal{E},
\end{aligned}
$$

where $\mathcal{E}^+ := \mathcal{E} + \hbar\omega^{(p)}$, and the functions H_i, $i = 1, \ldots, 4$ are reported in Appendix A. As regards the production terms for the velocities and the energy fluxes, their expressions are similar to those of the previous case, with the elements of the matrix $\mathbf{Q}^{(ac)}$ this time given by

$$
\begin{aligned}
q_{ij}^{(ac)} = &-\frac{2\sqrt{2}\pi\, N^{(p)} \mathcal{K}^{(p)}}{3\hbar\sqrt{m^*} d_0} \int_0^\infty \Bigg[\frac{e^{-\hbar\omega^{(p)}\left(\lambda_W - \frac{1}{k_B T_L}\right)} \mathcal{E}^{i-1} (\mathcal{E}^+)^{j-1} + \mathcal{E}^{j-1} (\mathcal{E}^+)^{i-1}}{2(1 + 2\alpha\mathcal{E})(1 + 2\alpha\mathcal{E}^+)}\\
&\times H_2 \left(H_4 + \alpha \frac{H_4 \left(H_1(\mathcal{E}, \alpha) + H_1(\mathcal{E}^+, \alpha) \right)}{H_2} + \frac{\alpha^2}{12} \frac{H_5(\mathcal{E}, \mathcal{E}^+, \alpha)}{H_2^2} \right)\\
&- \left(\frac{e^{-\hbar\omega^{(p)}\left(\lambda_W - \frac{1}{k_B T_L}\right)} H_1(\mathcal{E}^+, \alpha) (\mathcal{E}^+)^{i+j-2}}{(1 + 2\alpha\mathcal{E}^+)^2} + \frac{H_1(\mathcal{E}, \alpha) \mathcal{E}^{i+j-2}}{(1 + 2\alpha\mathcal{E})^2} \right) \sqrt{H_2}\\
&\times \left(\sqrt{H_2} H_3 + \alpha \frac{H_4}{\sqrt{H_2}} + \frac{\alpha^2}{4} \frac{\left(H_1(\mathcal{E}, \alpha) + H_1(\mathcal{E}^+, \alpha) \right) H_4}{H_2^{\frac{3}{2}}} \right) \Bigg] e^{-\lambda_W \mathcal{E}}\, d\mathcal{E},
\end{aligned}
$$

where the function H_5 is also reported in Appendix A.

- **Impurity scattering**. The elements of the matrix $\mathbf{Q}^{(ac)}$ are given by

$$
q_{ij}^{(ac)} = \frac{\sqrt{2}\pi\hbar}{12 (m^*)^{\frac{3}{2}} d_0} \mathcal{K}^{(im)} \int_0^\infty e^{-\lambda_W \mathcal{E}} \mathcal{E}^{(i+j-1)} H_6(\mathcal{E}) \left(1 + \alpha\mathcal{E}\right) d\mathcal{E},
$$

with H_6 again given in Appendix A.

- **Non-polar phonon scattering**. We will consider both zeroth and the first order contributions to the intervalley scattering. For the density

and the energy production terms at the zero-order we find

$$\begin{pmatrix} n_A C_{n_A}^{(np),0} \\ n_A C_{W_A}^{(np),0} \end{pmatrix} = \frac{8\pi Z_{AB}(m_A^* m_B^*)^{\frac{3}{2}}}{\sqrt{2}\hbar^3} N^{(np)} \mathcal{K}_0^{(np)} \Bigg\{ \frac{n_B}{(m_B^*)^{\frac{3}{2}} d_0^B}$$
$$\times \Bigg[e^{-\lambda_W^B \Delta_{AB}^+ + \frac{\epsilon_0^{(np)}}{k_B T_L}} \int_0^\infty \begin{pmatrix} 1 \\ \mathcal{E} + a_{AB}^- \end{pmatrix} e^{-\lambda_W^B (\mathcal{E} + a_{AB}^-)}$$
$$\times H_7^{(0)}(\mathcal{E}, a_{AB}^-, \Delta_{AB}^+, \alpha_A, \alpha_B) d\mathcal{E} + e^{-\lambda_W^B \Delta_{AB}^-} \int_0^\infty \begin{pmatrix} 1 \\ \mathcal{E} + a_{AB}^+ \end{pmatrix}$$
$$\times e^{-\lambda_W^B (\mathcal{E} + a_{AB}^+)} H_7^{(0)}(\mathcal{E}, a_{AB}^+, \Delta_{AB}^-, \alpha_A, \alpha_B) d\mathcal{E} \Bigg] - \frac{n_A}{(m_A^*)^{\frac{3}{2}} d_0^A}$$
$$\times \Bigg[\int_0^\infty \begin{pmatrix} 1 \\ \mathcal{E} + a_{AB}^- \end{pmatrix} e^{-\lambda_W^A (\mathcal{E} + a_{AB}^-)} H_7^{(0)}(\mathcal{E}, a_{AB}^-, \Delta_{AB}^+, \alpha_A, \alpha_B) d\mathcal{E}$$
$$+ e^{\frac{\epsilon_0^{(np)}}{k_B T_L}} \int_0^\infty \begin{pmatrix} 1 \\ \mathcal{E} + a_{AB}^+ \end{pmatrix} e^{-\lambda_W^A (\mathcal{E} + a_{AB}^+)}$$
$$\times H_7^{(0)}(\mathcal{E}, a_{AB}^+, \Delta_{AB}^-, \alpha_A, \alpha_B) d\mathcal{E} \Bigg] \Bigg\},$$

where $d_0^A = d_0(\lambda_W^A, \alpha_A)$, $\epsilon_0^{(np)} = \hbar\omega_0^{(np)}$, $\Delta_{AB}^\pm = \Delta_{AB} \pm \epsilon_0^{(np)}$, $a_{AB}^\pm = max(0, -\Delta_{AB} \pm \epsilon_0^{(np)})$, and the function $H_7^{(0)}$ can be found in Appendix A.

In the last expression the two positive terms depend on the energy in the valley B and are gain terms, corresponding to the absorption and the emission of a phonon respectively. The negative terms depend on the energy in the valley A and are loss terms.

For this scattering mechanism the elements of the matrices $\mathbf{Q}_{AB}^{(np),0}$ read

$$q_{ij,\,AB}^{(np),0} = \frac{16\pi (m_B^*)^{\frac{3}{2}} Z_{AB}}{3\sqrt{2}\hbar^3 m_A^* d_0^A} N^{(np)} \mathcal{K}_0^{(np)} \int_0^\infty \Big[\left(\mathcal{E} + a_{AB}^-\right)^{i+j-2}$$
$$\times e^{-\lambda_W^A (\mathcal{E} + a_{AB}^-)} H_8^{(0)}(\mathcal{E}, a_{AB}^-, \Delta_{AB}^+, \alpha_A, \alpha_B) + \left(\mathcal{E} + a_{AB}^+\right)^{i+j-2}$$
$$\times e^{-\lambda_W^A (\mathcal{E} + a_{AB}^+) + \frac{\epsilon_0^{(np)}}{k_B T_L}} H_8^{(0)}(\mathcal{E}, a_{AB}^+, \Delta_{AB}^-, \alpha_A, \alpha_B) \Big] d\mathcal{E},$$

where the function $H_8^{(0)}$ is reported in Appendix A. As regards the first order production terms, if the valleys are centered at the same

k-point, nothing changes from the zero order ones, with the exception of $\mathcal{K}_0^{(np)}$, $\epsilon_0^{(np)}$, $H_7^{(0)}$, and $H_8^{(0)}$ that have to be respectively replaced by $\mathcal{K}_1^{(np)}$, $\epsilon_1^{(np)}$, $H_7^{(1)}$, and $H_8^{(1)}$. The functions $H_7^{(1)}$, and $H_8^{(1)}$ can be found in Appendix A. Moreover the terms relative to the velocities and the energy fluxes depend also on the velocities and the energy fluxes of the other valleys through the sum $\sum_{B\neq A} = Q_{AB}^{(np),1} B_B \begin{pmatrix} \mathbf{V}_A \\ \mathbf{S}_A \end{pmatrix}$, where the matrices $Q_{AB}^{(np),1}$ have elements

$$
\begin{aligned}
q_{ij,\,AB}^{(np),1} = {} & \frac{32\pi\sqrt{2}(m_A^*)^{\frac{3}{2}} Z_{AB}}{9\hbar^5 d_0^B} N^{(np)} \mathcal{K}_1^{(np)} \Bigg[e^{\frac{\epsilon_1^{(np)}}{k_B T_L}} \int_0^\infty e^{-\lambda_W^A \left(\mathcal{E}+\Delta_{AB}^+ + a_{AB}^-\right)} \\
& \times \left(\mathcal{E}+a_{AB}^-\right)^{i-1} \left(\mathcal{E}+\Delta_{AB}^+ + a_{AB}^-\right)^{j-1} H_9(\mathcal{E}, a_{AB}^-, \Delta_{AB}^+, \alpha_A, \alpha_B) \\
& + \left(\mathcal{E}+a_{AB}^+\right)^{i-1} \left(\mathcal{E}+\Delta_{AB}^- + a_{AB}^+\right)^{j-1} e^{-\lambda_W^A \left(\mathcal{E}+\Delta_{AB}^- + a_{AB}^+\right)} \\
& \times H_9(\mathcal{E}, a_{AB}^+, \Delta_{AB}^-, \alpha_A, \alpha_B) \Bigg] d\mathcal{E},
\end{aligned}
$$

where H_9 is in Appendix A.

3.4 Numerical simulations of GaN and SiC

In this section we present the results of numerical simulations regarding the case of bulk Gallium nitride (GaN) and Silicon carbide (SiC).

These two compound semiconductors are of great interest since they have a high breakdown field, a low thermal generation rate, and a good thermal conductivity and stability. For all these properties, these materials are very useful for high power and high temperature devices.

Bulk GaN. The model we used is that described in the previous sections. We consider the three valley conduction band used in [12] for wurtzite GaN (Figure 3.1). The parameters that have been used for the three valleys are reported in Table 3.1.

We take into account all the scattering mechanisms described before, except the first order intervalley interaction. The material parameters are listed in Table 3.2.

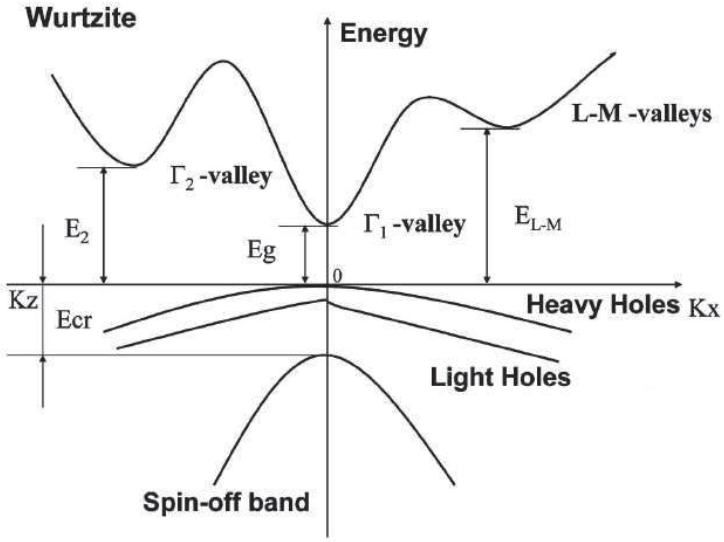

Figure 3.1: Analitycal band structure for wurtzite GaN [12].

Table 3.1: Parameters of the band structure of GaN and SiC

Material	GaN			SiC	
Conduction band valley	Γ_1	Γ_2	L-M	M,1st c.b.	M,2nd c.b.
Effective mass	$0.21m_e$	m_e	m_e	$0.38m_e$	$0.56m_e$
Valley energy minimum (eV)	0	1.9	2.1	0	0.14
Nonparabolicity factor (eV^{-1})	0.189	0.065	0.029	0.117	0.058
Number of equivalent valleys	1	1	6	3	3

If the initial velocities and energy fluxes are taken parallel to the electric field and the total electron density is considered equal to the donor concentration, the moment system becomes an ordinary differential equation system, where time is the only independent variable. Moreover, the Poisson equation is solved taking the total electron population equal to the doping concentration at all times, and the electrostatic potential with a linear profile between the two boundary values. If we choose the x-axis along the direction of the

Table 3.2: Bulk material parameters

	GaN	SiC	Units
ρ	6.15	3.2	$\left(\frac{g}{cm^3}\right)$
ϵ_s	8.9	9.7	ϵ
ϵ_∞	5.35	6.5	ϵ
v_s	6560	13730	(m/s)
Ξ_d	8.3	15	(eV)
$\hbar\omega^{(p)}$	92	120	(meV)
$\mathcal{E}_0^{(np)}$	92	85.4	(meV)
$\mathcal{E}_1^{(np)}$	-	33.2	(meV)
$D_t K$	1×10^9	7×10^8	$\left(\frac{eV}{cm}\right)$
D_1	-	5	(eV)

electric field, the moment system reduces to

$$\frac{dn_A}{dt} = n_A C_{n_A}(W_A) + \sum_{B \neq A} n_B C_{n_A}(W_B), \tag{3.21}$$

$$\frac{d}{dt}(n_A(\mathbf{V}_A)_x) + qE_x n_A(\mathbf{G}_A^{(0)})_{xx} = n_A c_{11}^A(W_A)(\mathbf{V}_A)_x + n_A c_{12}^A(W_A)(\mathbf{S}_A)_x, \tag{3.22}$$

$$\frac{dW_a}{dt} + qE_x n_A(\mathbf{V}_A)_x = n_A C_{W_A}(W_A) + \sum_{B \neq A} n_B C_{W_A}(W_B), \tag{3.23}$$

$$\frac{d}{dt}(n_A(\mathbf{S}_A)_x) + qE_x n_A(\mathbf{G}_A^{(1)})_{xx} = n_A c_{21}^A(W_A)(\mathbf{V}_A)_x + n_A c_{22}^A(W_A)(\mathbf{S}_A)_x, \tag{3.24}$$

where all the terms relative to the density and the energy productions have been summed into the first addenda in the equations (3.21) and (3.23), with the exception of the gain terms of the intervalley scattering, which depend on the energy in the other valleys involved in the scattering and are represented by the sums at left-hand sides of the equations. The integrals with respect to the microscopic energy, which appear in the fluxes and in the production terms, are numerically computed for a discrete number of values in a suitable range of the macroscopic energy, and after this stepwise linear interpolation

is used to approximate them in all the range. The system is numerically solved by a 4-th order Runge-Kutta method for sixty values of the applied electric field going from $10^{-3}V/\mu m$ to $100V/\mu m$.
The results are shown in Figures 3.2-3.5. They present all the main characteristics of GaN. The total velocity, Figure 3.4, increases with the electric field until it reaches a value of about $3.4 \times 10^7 cm/s$ at a threshold value of about 17 $V/\mu m$, which is in excellent agreement with [12]. The saturation velocity is instead higher and around $1.8 \times 10^7 cm/s$. The negative differential effect which can be seen in the Figure 3.4 is typical of the presence of the intervalley processes that, at high fields, increase the occupation of the upper, higher effective mass valleys, as can be seen in Figure 3.2. Instead at low fields, up to $2 - 3\, V/\mu m$, the behavior of the average velocity is high-slope linear. A low slope region follows (particularly for low doping, $N_D = 10^{15}/cm^3$, see the dashed curve), and at higher fields, before reaching the threshold value, there is a positive inflection [13] in the slope.

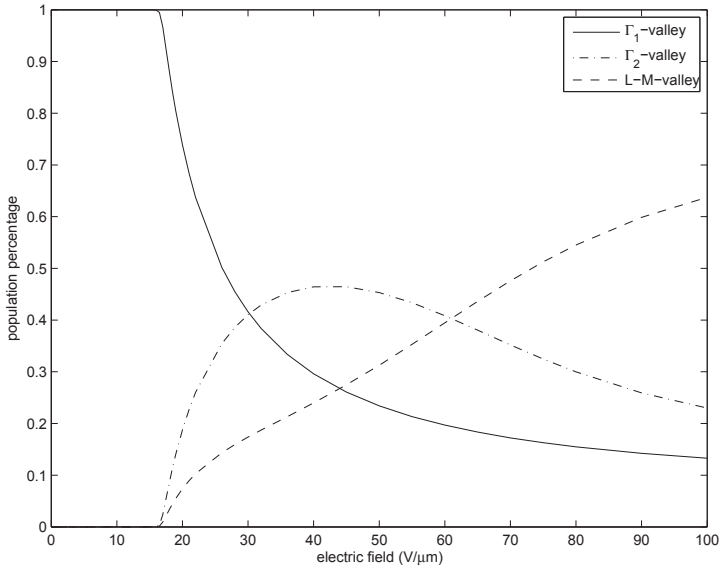

Figure 3.2: Valley occupancies vs the applied electric field.

As regards the valley occupancy, there is a first inversion between the Γ_1

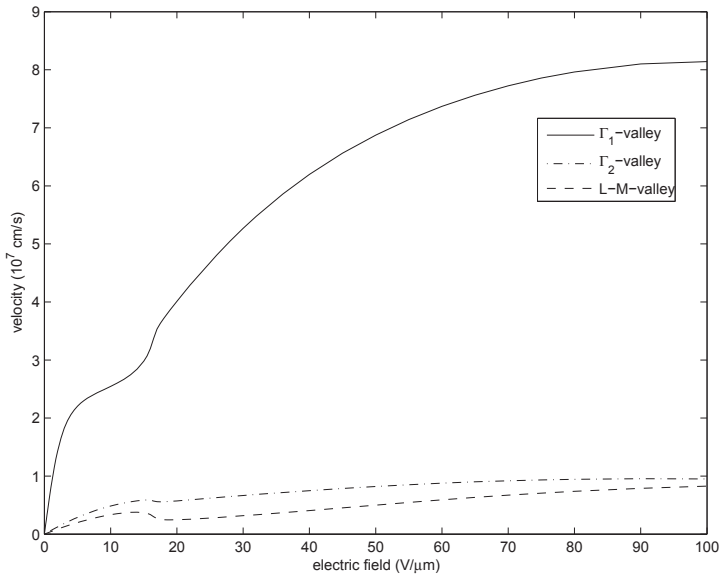

Figure 3.3: Valley velocities vs the applied electric field.

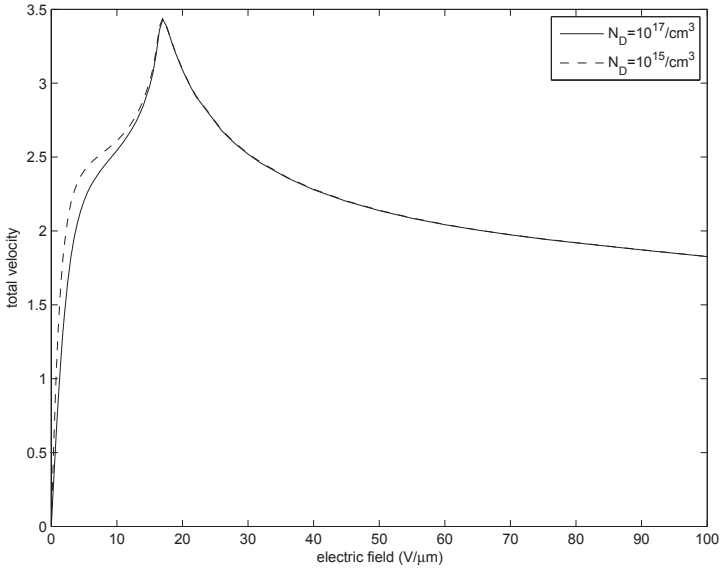

Figure 3.4: Total velocity vs the applied electric field.

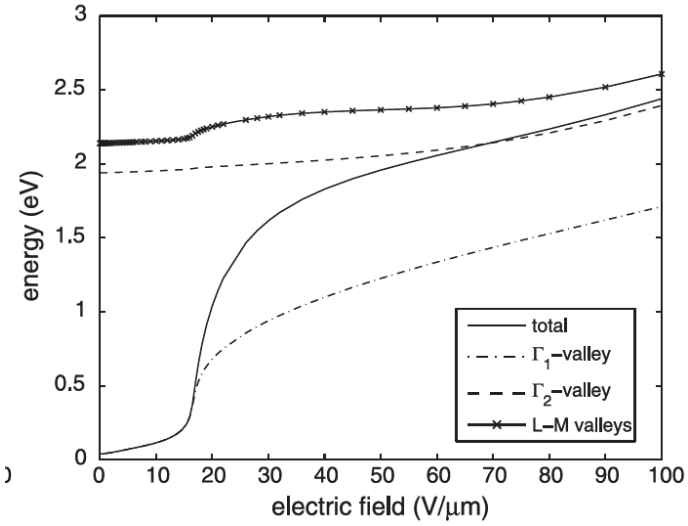

Figure 3.5: Valley energies and total average energy vs the applied electric field.

and the Γ_2 populations, and at higher fields there are two further inversions and at the end the most populated valleys are the 6 equivalent L-M ones. In Figure 3.5 we represent the behavior of the total mean energy. We notice the high slope at $10 - 35\, V/\mu m$, which corresponds to the rapid transfer of electrons from the Γ_1 to the Γ_2 and L-M valleys, in agreement with the results in [12].

Bulk SiC A procedure similar to that used for GaN has been applied also to the 4H-SiC polytype, which is the least anisotropic among the SiC polytypes. There are several results in literature about its band structure. Here we use those in [18] (Figure 3.6) .

The valleys around the minima at the symmetry points M of the lowest two conduction bands are considered. Because of the crystal symmetries there are 3 equivalent M points, therefore the total number of valleys, taken into account, is 6, and their parameters are reported in Table 3.2 . As regards the scattering mechanisms, we have considered also the first order intervalley interaction, which produces an enhancement of the population of the higher

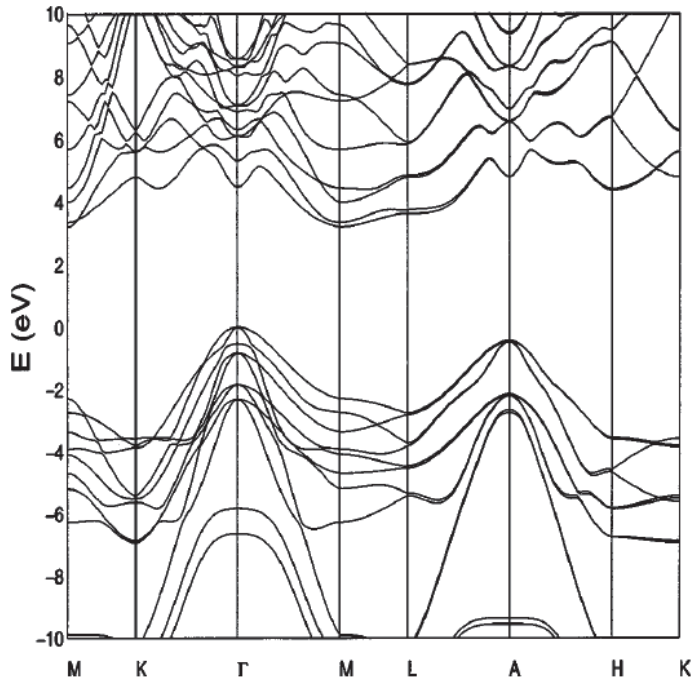

Figure 3.6: 4H-SiC bulk band structure.

valleys. The results are shown in Figures 3.7-3.10. In these figures, the label "with correction" means that also the first order correction to intervalley interactions is considered.

The behaviour of the total velocity is in good agreement with that in [25]. In literature we have not found results on the inversion of the electron populations in SiC, which is shown in Figure 3.7.

An improvement of these results by using ellipsoidal nonparabolic bands is the aim of the next chapter.

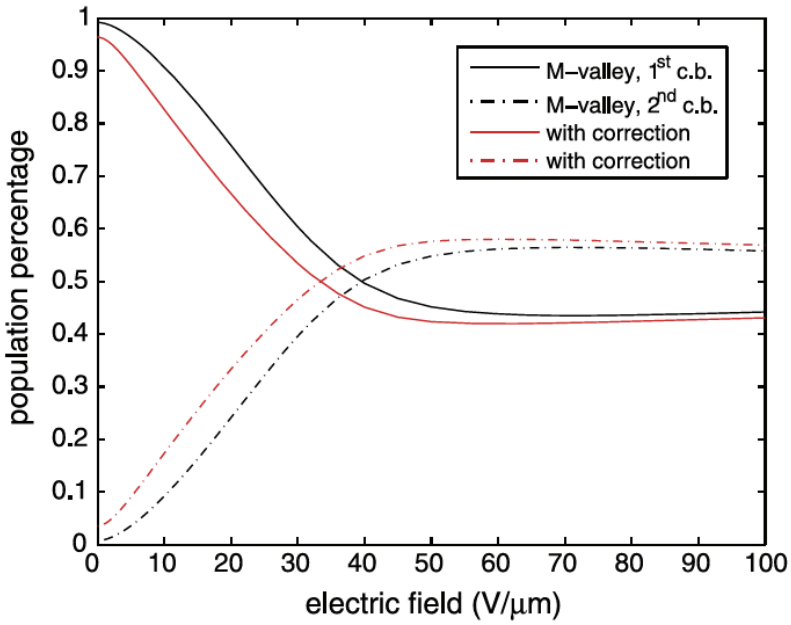

Figure 3.7: Valley occupancies vs the applied electric field.

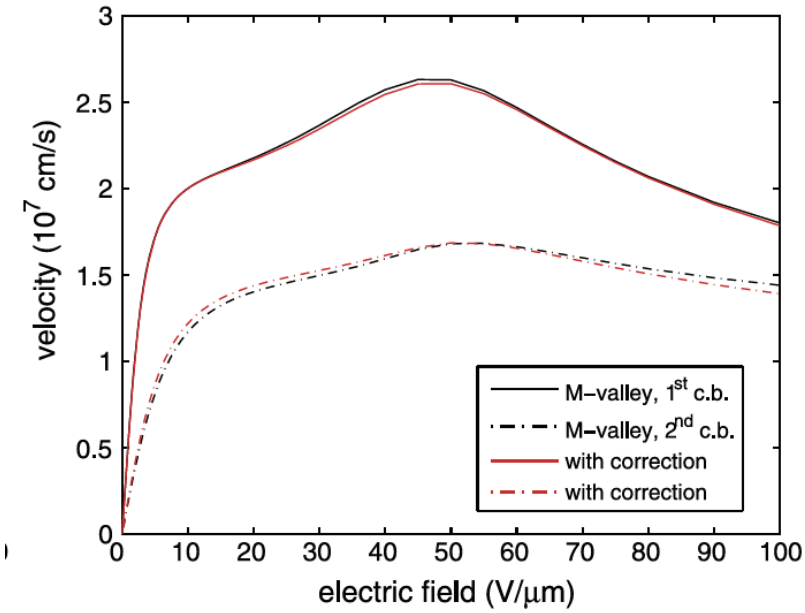

Figure 3.8: Valley velocities vs the applied electric field.

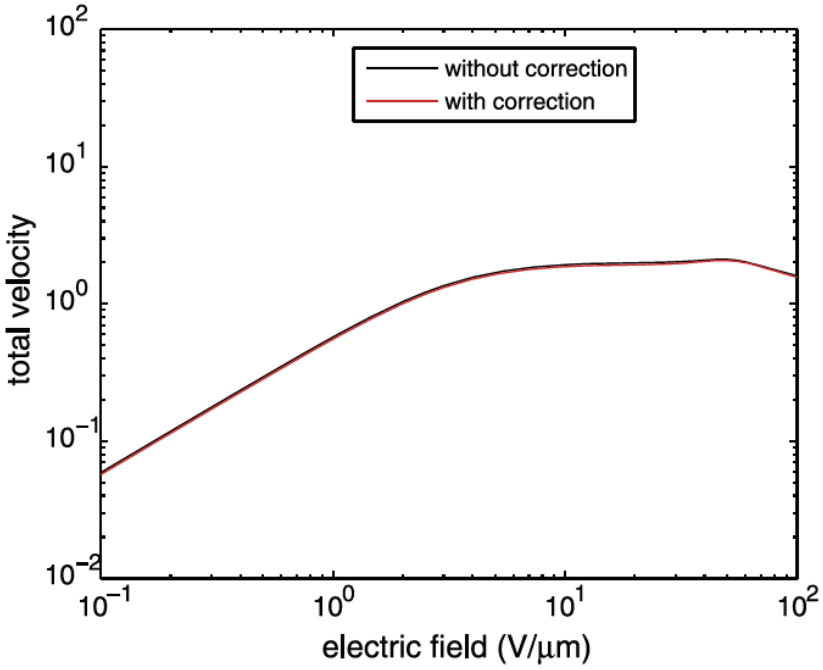

Figure 3.9: Total velocity vs the applied electric field.

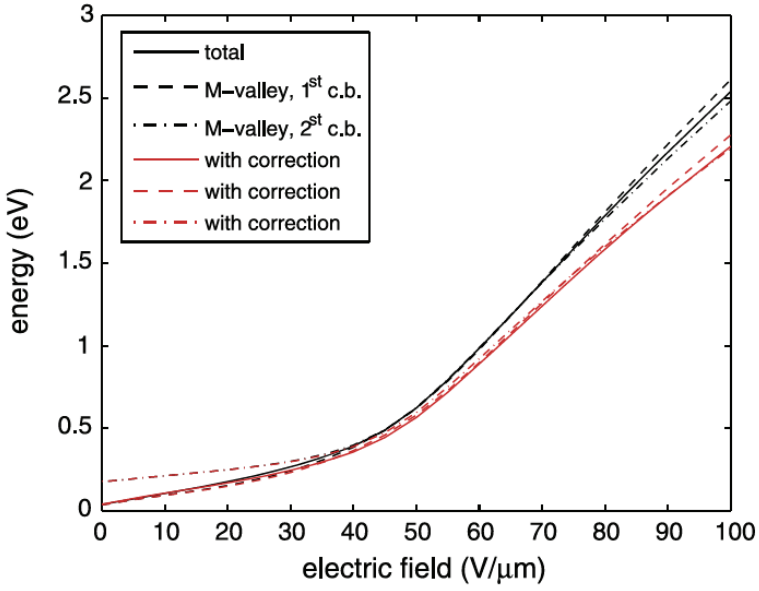

Figure 3.10: Valley energies and total average vs the applied electric field.

Chapter 4

An anisotropic hydrodynamical model for compound semiconductors

4.1 Analytic approximation of the band structure

In the previous chapter we presented a macroscopic model which is able to describe the behavior of compound semiconductor materials. In that model, a spherical analytical approximation was used for the energy dispersion relationships in the neighbors of the lowest minima of the conduction bands. For highly anisotropic semiconductors better approximations are needed.
In this chapter we will make use of a more generalized energy dispersion relation, employing an ellipsoidal approximation, which was used in [26]. The ellipsoidal approximation is very useful for the description of carrier transport in semiconductors for which electron masses along the principal axes are consistently different, implying different carrier drift velocities along different directions.
In particular, the non parabolic anisotropic dispersion relation taken into

account has the following form [27]

$$\mathcal{E}_{A}(\mathbf{k}_{A}) = \frac{\hbar^2 |\mathbf{k}_{A}|^2}{2\, m_e}\, \gamma_{A}(\mathcal{E}_{A})\, \psi_{A}^{-1}(\mathbf{n}_{A}), \tag{4.1}$$

where $\mathcal{E}_A$, $\mathbf{k}_A$, have, for each valley, the same meaning as in the previous chapter, and $\gamma_{A}(\mathcal{E}_{A}.)$ are generic non parabolicity factors. The index A runs over the considered valleys, and $\mathbf{n}_{A}$ is defined by $\mathbf{n}_{A} := \frac{\mathbf{k}_A}{|\mathbf{k}_A|}$. For electrons, in the ellipsoidal approximation, the dependence of ψ_A on $\mathbf{n}_{A}$ is given by

$$\psi_{A}^{-1} = \frac{((\mathbf{n}_{A})_1)^2}{(m_{A}^{*})_1} + \frac{((\mathbf{n}_{A})_2)^2}{(m_{A}^{*})_2} + \frac{((\mathbf{n}_{A})_3)^2}{(m_{A}^{*})_3},$$

where $(m_{A}^{*})_{i}^{-1}$, $i = 1, 2, 3$, are the diagonal elements (eigenvalues) of the inverse effective mass tensor of the A-th valley, multiplied by m_e, referred to an orthonormal basis of the tensor.

Analogously for holes, one has

$$\psi_{A}^{-1} = |A_{A}| \mp \sqrt{B_{A}^2 + \frac{C_{A}^2}{4}\left(\sin^4\vartheta \sin^2 2\varphi + \sin^2 2\vartheta\right)},$$

in the case of warped bands, with ϕ and θ respectively azimuthal and polar angle of $\mathbf{n}_{A}$ with respect to the main cristallographic axes. A_A, B_A and C_A, which depend on the specific material, are the inverse valence band parameters.

Each valley in the analytic approximation is extended to all $\mathbb{R}^3$ and the volume element in the $\mathbf{k}$-space can be written as

$$d\mathbf{k} = \frac{m_e\sqrt{2m_e}}{\hbar^3}\sqrt{\frac{\mathcal{E}}{\gamma^5(\mathcal{E})}}\Big(\gamma(\mathcal{E}) - \mathcal{E}\dot{\gamma}\,(\mathcal{E})\Big)\psi^{\frac{3}{2}}(\varphi,\theta)d\mathcal{E}d\Omega,$$

where the dot stays for derivative with respect to the argument of the function, and $d\Omega$ is the solid angle element. The charge velocity, given again by the quantum mechanichal formula (3.2), has the following expression in terms of the energy and the angular variables

$$v_i = \frac{\hbar}{2\, m_e}\frac{\gamma^{'2}(\mathcal{E})}{\gamma(\mathcal{E}) - \mathcal{E}\dot{\gamma}\,(\mathcal{E})}\, l_i,$$

where

$$l_i := \frac{\partial}{\partial k_i}(|\mathbf{k}|^2\,\psi^{-1}) = g(\mathcal{E})\eta_i(\varphi,\theta)n_i,$$

$$g := \frac{2\sqrt{2\,m_e\,\mathcal{E}}}{\hbar\,\sqrt{\gamma(\mathcal{E})}},$$

$$\eta_i := \frac{\sqrt{\psi}}{m_i^*}.$$

As in the previous chapter, also in this case, for the sake of simplicity, we will consider only the case in which conductivity is essentially due to electrons.

4.2 Hydrodynamical model

We consider again the Boltzmann-Poisson system given by equations (3.3) and (3.4) which describe the charge transport through the time evolution of the distribution functions $f_A(\mathbf{x},\mathbf{k},t)$. In these equations the collision terms at the right hand side are those in expressions (3.5) and (3.6), referring to the intravalley and intervalley interactions, in fact the scattering processes taken into consideration are those reported in Chapter 2.
Considering as usual the weights $1, \mathbf{v}(\mathbf{k}), \mathcal{E}(\mathbf{k}), \mathbf{v}(\mathbf{k})\mathcal{E}(\mathbf{k})$, we obtain the moments n, $\mathbf{V}$, W and $\mathbf{S}$, as reported in Chapter 2, for which equations (3.8)-(3.11) hold.
We have, also in this case, a set of equations that is not closed and we need then to apply the maximum entropy principle to close this system.

4.3 Closure by maximum entropy principle

Using the same procedure as in the previous chapter, the maximum entropy principle will again be applied to obtain a closed system. Taking into consideration the maximum entropy distribution functions (3.15) the purpose is that of inverting the constraints (3.16)-(3.19). Since, in general, the angular integration cannot be performed analitically when ellipsoidal approximations are used for the energy dispersion relations, computations are more involved

than those in [9], reported in the previous chapter.
First of all is useful to introduce a property that is employed for the calculations in this section.

Property 1 *If $\sigma(\mathbf{n})$ is an integrable even function of its argument then*

$$\int_{S^2} \sigma(\mathbf{n})\, n_i \, d\Omega = 0, \quad \int_{S^2} \sigma(\mathbf{n})\, n_i \, n_j \, d\Omega = 0, \;\; i,j = 1,2,3.$$

$$\int_{S^2} \sigma(\mathbf{n})\, n_i \, n_j \, n_k \, d\Omega = 0, \; \forall\, i,j,k = 1,2,3,$$

where S^2 is the unit sphere surface.

As regards the inversion of the constraints, the results are reported in the following.
From the scalar constraints, the densities and the energies are given by

$$n = \frac{m_e\sqrt{2m_e}J_0}{\hbar^3}\, e^{-\lambda} d_0(\lambda_W),$$
$$n\,W = \frac{m_e\sqrt{2m_e}J_0}{\hbar^3}\, e^{-\lambda} d_1(\lambda_W),$$

where

$$d_n(\lambda_W) := \int_0^\infty \mathcal{E}^n \exp(-\lambda_W \mathcal{E}) \sqrt{\frac{\mathcal{E}}{\gamma^5(\mathcal{E})}} \Big(\gamma(\mathcal{E}) - \mathcal{E}\dot{\gamma}\,(\mathcal{E})\Big)\, d\mathcal{E},$$

and

$$J_0 := \int_{S^2} \psi^{\frac{3}{2}} d\Omega.$$

Thus one has

$$\lambda = -\log\left(\frac{\hbar^3 n}{m_e\,\sqrt{2\,m_e}\,J_0\,d_0}\right) \tag{4.2}$$

$$\lambda_W = h^{-1}(W), \tag{4.3}$$

where h^{-1} is the inverse function of h, given by

$$h(\lambda_{_W}) := \frac{d_1(\lambda_W)}{d_0(\lambda_W)}.$$

Hereafter, λ_W will always be regarded as a function of W.
For the vector Lagrange multipliers, one has

$$\lambda_{V_i} = J_{1,i}^{-1}\big[b_{11}(W)\, V_i + b_{12}(W)\, S_i\big], \tag{4.4}$$

$$\lambda_{S_i} = J_{1,i}^{-1}\big[b_{12}(W)\, V_i + b_{22}(W)\, S_i\big]. \tag{4.5}$$

In the last equations $J_{1,i}$, $\quad i = 1, 2, 3$ is defined by

$$J_{1,i} := \int_{S^2} \psi^{\frac{3}{2}}\, \eta_i^2 n_i^2\, d\Omega,$$

the b_{ij} are the elements of the matrix $\mathbf{B}$, which is the inverse of the symmetric matrix $\mathbf{A}$ of elements

$$a_{ij} = -\frac{\hbar^2}{4m_e^2\, J_0}\frac{p_{i+j-2}}{d_0},\ i, j = 1, 2,$$

with

$$p_n = p_n(W) := \int_{\Re^3} \frac{\mathcal{E}^{n+\frac{1}{2}}}{\alpha(\mathcal{E}) - \mathcal{E}\dot{\alpha}\,(\mathcal{E})}\, \alpha^{\frac{3}{2}}(\mathcal{E}) g^2(\mathcal{E})\, e^{-\lambda_W \mathcal{E}} d\mathcal{E}.$$

As a consequence, also the matrix $\mathbf{B}$ is symmetric.
In this case, differently from the isotropic approximation, the relations (4.4) and (4.5) depend on the directions, since in their expressions appears the terms $J_{1,i}$, which in the anisotropic case vary with $i = 1, 2, 3$.
Once obtained expressions (4.2) and (4.3) for the scalar multipliers, (4.4) and (4.5) for vector ones, the Lagrange multipliers are expressed in terms of the fundamental variables. Therefore we are in condition to obtain closure relations for the fluxes and the production terms.
Closure relations for the fluxes. As regards the constitutive equations for the fluxes, one has

$$\begin{pmatrix} F_{ij}^{(0)} \\ F_{ij}^{(1)} \end{pmatrix} = \frac{\hbar^2\, J_{1,i}}{4m_e^2 J_0\, d_0} \begin{pmatrix} p_0 \\ p_1 \end{pmatrix} \delta_{ij}, \tag{4.6}$$

where δ_{ij} is the Kronecker delta symbol, and

$$G_{ij}^{(0)} = \frac{\hbar}{(2\, m_e)^{\frac{3}{2}} J_0\, d_0}\big[\frac{\hbar\, J_{1,i}}{\sqrt{2\, m_e}}\, \mathcal{G}_{1,0}(W) + (J_{3,i} - J_{2,i})\mathcal{G}_{2,0}(W)\big]\delta_{ij}, \tag{4.7}$$

$$G_{ij}^{(1)} = \frac{\hbar}{(2\,m_e)^{\frac{3}{2}}\,J_0\,d_0}\big[\frac{\hbar\,J_{1,i}}{\sqrt{2\,m_e}}\,\mathcal{G}_{1,1}(W)+(J_{3,i}-J_{2,i})\mathcal{G}_{2,1}(W)+\frac{\hbar\,J_{1,i}}{\sqrt{2\,m_e}}\mathcal{G}_{3,0}(W)\big]\delta_{ij}. \tag{4.8}$$

Here

$$\mathcal{G}_{1,n}(W) := \int_0^\infty \mathcal{E}^n \sqrt{\frac{\mathcal{E}}{\gamma(\mathcal{E})}}\; g(\mathcal{E})\,\dot{\beta}\,(\mathcal{E})\;\exp\left(-\lambda_{_W}\mathcal{E}\right)d\mathcal{E}$$

$$\mathcal{G}_{2,n}(W) := \int_0^\infty \mathcal{E}^n\, g(\mathcal{E})\;\exp\left(-\lambda_{_W}\mathcal{E}\right)d\mathcal{E},$$

$$\mathcal{G}_{3,n}(W) := \int_0^\infty \mathcal{E}^n \sqrt{\frac{\mathcal{E}}{\gamma(\mathcal{E})}}\; g(\mathcal{E})\,\beta(\mathcal{E})\;\exp\left(-\lambda_{_W}\mathcal{E}\right)d\mathcal{E},$$

$$J_{2\,,i} := \int_{S^2} (\eta_i - 2\,\frac{\partial \eta_i}{\partial n_i}) n_i^2 \psi\, d\Omega,$$

$$J_{3\,,i} := \int_{S^2} (\eta_i - 2\sum_j \frac{\partial \eta_i}{\partial n_j^2} n_j^2\, n_i^2) \psi\, d\Omega,$$

with $\beta := \frac{\gamma^2}{\gamma - \mathcal{E}\dot{\gamma}}\, g$.

Closure relations for the production terms.

- **Acoustic phonon scattering**. As said, since this scattering process is intravalley and approximately elastic, the only non-zero production terms are those relative to the velocities and the energy fluxes. The results of the calculations yield

$$\begin{pmatrix} C_{\mathbf{V}}^{(ac)} \\ C_{\mathbf{S}}^{(ac)} \end{pmatrix} = \mathbf{Q}^{(ac)} \begin{pmatrix} \mathbf{V} \\ \mathbf{S} \end{pmatrix}, \tag{4.9}$$

  where $\mathbf{Q}^{(ac)}$ is the matrix of elements

$$q_{ij}^{(ac)}(W) = \frac{1}{2\,\sqrt{2\,m_e}\hbar d_0}\mathcal{K}^{(ac)} \int_0^\infty \mathcal{E}^{i+j-1}\,\frac{g^2(\mathcal{E})}{\gamma(\mathcal{E})}\exp\left(-\lambda_{_W}\mathcal{E}\right)d\mathcal{E}. \tag{4.10}$$

  It can be noted that the contribution of the acoustic scattering is isotropic. This is due to the approximation used.

- **Polar optical phonon scattering**. For the polar optical scattering the calculations are even more complicated than in the isotropic case. First of all it is not possible to separate angular integration from the energy integration because of the presence of the overlap factor $\mathcal{G}$. Some assumptions on this factor are then needed. We assume that it depends on the carrier energies, $\mathcal{E}$ and $\mathcal{E}'$, and on the motion directions, $\mathbf{n}$ and $\mathbf{n}'$, through $\mathbf{k}$ and $\mathbf{k}'$, before and after the scattering.
  The first assumption is the following

  Assumption 1 *We will assume that $\mathcal{G}$ can depend on $\mathbf{n}$ and $\mathbf{n}'$ only through the scalar product $\mathbf{n}\cdot\mathbf{n}'$, even functions of n_i and n'_i, $i = 1, 2, 3$, and also through $n_z - n'_z$, as long as this latter dependence is even too.*

  This assumption is satisfied by the expression of $\mathcal{G}$ used by Fawcett et al [10], which is reported in Chapter 2, and also by the expression proposed by Nilsson et al. [28], which will be used in this chapter and which has the form

$$\mathcal{G}(\mathbf{k},\mathbf{k}') = 1 - (a_{01} + a_{02}\sin\chi)\left[1 - \exp\left[-(b_{01} + b_{02}\sin\chi)|\mathbf{q}|^{\mathbf{2}}\right]\right], \quad (4.11)$$

  where $\mathbf{q} = \mp(\mathbf{k}' - \mathbf{k})$ is the phonon quasi-wave vector and $\chi := \arccos\frac{q_z}{|\mathbf{q}|}$, while the constants a_{01}, a_{02}, b_{01}, and b_{02} can be found in table 4.1.

  Assumption 1 implies the following properties

Table 4.1: Parameter values used in the overlap model

Parameter	Value
a_{01}	0.873
a_{02}	0.0268
b_{01}	4.989×10^{-7} μm^2
b_{02}	-4.250 $\times10^{-7}$ μm^2

Property 2 *The function*

$$G^{s,p}(\mathcal{E},\mathcal{E}',\mathbf{n}) : = \int_{S^2} \frac{\mathcal{G}(\mathbf{k},\mathbf{k}')}{\frac{\mathcal{E}}{\gamma(\mathcal{E})}\psi(\mathbf{n})+\frac{\mathcal{E}'}{\gamma(\mathcal{E}')}\psi(\mathbf{n}')-2\sqrt{\frac{\mathcal{E}\mathcal{E}'}{\gamma(\mathcal{E})\gamma(\mathcal{E}')}\psi(\mathbf{n})\psi(\mathbf{n}')}\,\mathbf{n}\cdot\mathbf{n}'} \times\psi^{\frac{3}{2}}(\mathbf{n}')\,d\Omega'$$

is even with respect to n_i, $i=1,2,3$.

Property 3 *The functions*

$$G_i^{v,p}(\mathcal{E},\mathcal{E}',\mathbf{n}) : = \int_{S^2} \frac{\mathcal{G}(\mathbf{k},\mathbf{k}')}{\frac{\mathcal{E}}{\gamma(\mathcal{E})}\psi(\mathbf{n})+\frac{\mathcal{E}'}{\gamma(\mathcal{E}')}\psi(\mathbf{n}')-2\sqrt{\frac{\mathcal{E}\mathcal{E}'}{\gamma(\mathcal{E})\gamma(\mathcal{E}')}\psi(\mathbf{n})\psi(\mathbf{n}')}\,\mathbf{n}\cdot\mathbf{n}'} \times\psi^{\frac{3}{2}}(\mathbf{n}')\,\eta_i(\mathbf{n}')n_i'd\Omega', \quad i=1,2,3$$

are odd with respect to n_i *and even with respect to* n_j, $j\neq i$, $i,j=1,2,3$.

The function $G^{s,p}(\mathcal{E},\mathcal{E}',\mathbf{n})$ takes into account the angular integration of the core term $\frac{\mathcal{G}(\mathbf{k},\mathbf{k}')}{|\mathbf{k}-\mathbf{k}'|^2}$, appearing in the expression of $P^{(p)}(\mathbf{k},\mathbf{k}')$, given in Chapter 2. The function $G_i^{v,p}(\mathcal{E},\mathcal{E}',\mathbf{n})$ shows up in the angular integration of the term $\frac{\mathcal{G}(\mathbf{k},\mathbf{k}')}{|\mathbf{k}-\mathbf{k}'|^2}v_i(\mathbf{k})$. Then, the second angular integration, that with respect to the direction $\mathbf{n}$, which is needed for the evaluation of the production terms can be simplified by using Property 1. We also use the detailed balance principle, already employed in the previous chapter and given by expression (3.20).
After these assumptions, for the density and energy production terms we find

$$\begin{aligned} C_n^{(p)} &= 0, \\ C_W^{(p)} &= \frac{\sqrt{m_e}\,\omega^{(p)}}{\sqrt{2}\,J_0\,d_0}\,N^{(p)}\mathcal{K}^{(p)}\,n\int_0^\infty\Big(\int_{S^2}G^{s,p}(\mathcal{E},\mathcal{E}^+,\mathbf{n})\psi^{\frac{3}{2}}(\mathbf{n})\,d\Omega\Big) \\ &\quad\times H_{11}(\mathcal{E})H_{11}(\mathcal{E}^+)\left[1-e^{-\hbar\omega^{(p)}\left(\lambda_W-\frac{1}{k_BT_L}\right)}\right] \\ &\quad\times\exp\left(-\lambda_W\mathcal{E}\right)d\mathcal{E}, \end{aligned}$$

where $\mathcal{E}^+ := \mathcal{E} + \hbar\omega^{(p)}$, while the function H_{11} is reported in Appendix B.

As regards the production terms for velocities and energy fluxes, this time the contribution is anisotropic and given by

$$\begin{pmatrix} C_{V_i}^{(p)} \\ C_{S_i}^{(p)} \end{pmatrix} = J_{1,i}^{-1}\mathbf{Q}^{(p)}\mathbf{B}\begin{pmatrix} V_i \\ S_i \end{pmatrix}, \tag{4.12}$$

where $\mathbf{Q}^{(p)}$ is the matrix of elements

$$\begin{aligned} q_{ij}^{(p)} = {} & \frac{\hbar}{4\,m_e\sqrt{2m_e}J_0\,d_0}\,N^{(p)}\mathcal{K}^{(p)}\int_0^\infty \big[H_{12,\,i}(\mathcal{E},\mathcal{E}^+)\mathcal{E}^{i+j-1} \\ & + H_{13,\,i}(\mathcal{E},\mathcal{E}^+)(\mathcal{E}^+)^{i+j-1} - H_{14,\,i}(\mathcal{E},\mathcal{E}^+)\left(e^{\hbar\omega^{(p)}\left(\frac{1}{k_B T_L}-\lambda_W\right)}\right. \\ & \left.\times\mathcal{E}^{i-1}(\mathcal{E}^+)^{j-1} + (\mathcal{E}^+)^{i-1}\mathcal{E}^{j-1}\big)\big]\;e^{-\lambda_W\mathcal{E}}d\mathcal{E}. \end{aligned}$$

The functions $H_{12,\,i}$, $H_{13,\,i}$, and $H_{14,\,i}$, $i = 1, 2, 3$, are reported in Appendix B.

- **Impurity scattering**. In this case the procedure used is very similar to that employed for the polar optical scattering. In fact, for the functions

$$G^{s,im}(x,\mathbf{n}) := \int_{S^2}\frac{\mathcal{G}(\mathbf{k},\mathbf{k}')\psi^{\frac{3}{2}}(\mathbf{n}')}{\left[\frac{2\,m_e\,\mathcal{E}}{\hbar^2\,\alpha(\mathcal{E})}\left(\psi(\mathbf{n})+\psi(\mathbf{n}')-2\sqrt{\psi(\mathbf{n})\psi(\mathbf{n}')}\;\mathbf{n}\cdot\mathbf{n}'\right)+\lambda_D^2\right]^2}d\Omega',$$

$$\begin{aligned} G_i^{v,im}(x,\mathbf{n}) : \;=\; & \int_{S^2}\frac{\mathcal{G}(\mathbf{k},\mathbf{k}')\,\psi^{\frac{3}{2}}(\mathbf{n}')}{\left[\frac{2\,m_e\,\mathcal{E}}{\hbar^2\,\alpha(\mathcal{E})}\left(\psi(\mathbf{n})+\psi(\mathbf{n}')-2\sqrt{\psi(\mathbf{n})\psi(\mathbf{n}')}\;\mathbf{n}\cdot\mathbf{n}'\right)+\lambda_D^2\right]^2} \\ & \times\eta_i(\mathbf{n})n_i'd\Omega',\;\imath = 1,2,3. \end{aligned}$$

the Properties 2 and 3 hold.

These functions are used in the angular integration of $\frac{\mathcal{G}(\mathbf{k},\mathbf{k}')}{\left[|\mathbf{k}-\mathbf{k}'|^2+\lambda_D^2\right]^2}$ and $\frac{\mathcal{G}(\mathbf{k},\mathbf{k}')}{\left[|\mathbf{k}-\mathbf{k}'|^2+\lambda_D^2\right]^2}v_i(\mathbf{k})$.

Since this scattering process is elastic, we have $\mathcal{E}' = \mathcal{E}$, and then a

simplification can be made if compared with polar optical scattering. For the production terms relative to the velocities and the energy fluxes, the elements of the matrix $\mathbf{Q}^{(im)}$ are given by

$$q_{ij}^{(im)} = \frac{\mathcal{K}^{(im)}}{2\sqrt{2\,m_e}\,\hbar\,J_0\,d_0}\int_0^\infty \frac{\mathcal{E}^{(i+j-2)}\,g^2(x)}{\alpha(x)} H_{15}(\mathcal{E})e^{-\lambda_W\mathcal{E}}\,d\mathcal{E}, \qquad (4.13)$$

with H_{15} given in Appendix B.

- **Non-polar optical phonon scattering**. In this case the results are obtained after long and involved calculations. As regards the density and the energy production terms, we find

$$\begin{aligned}
&\begin{pmatrix} C_{n_A}^{(np)} \\ C_{W_A}^{(np)} \end{pmatrix} = \sum_{B\neq A} \frac{\sqrt{2}\,Z_{AB}(m_e)^{\frac{3}{2}}\,J_0^A\,J_0^B}{\hbar^3}\,N^{(np)}\,\mathcal{K}^{(np)}\Bigg\{\frac{n_B}{J_0^B d_0^B} \\
&\times\Bigg[e^{-\lambda_W^B\Delta_{AB}^+ + \frac{\varepsilon^{(np)}}{k_B T_L}}\int_0^\infty \begin{pmatrix} 1 \\ \mathcal{E}+a_{AB}^- \end{pmatrix} e^{-\lambda_W^B\left(\mathcal{E}+a_{AB}^-\right)} \\
&\times H_{16,AB}(\mathcal{E},a_{AB}^-,\Delta_{AB}^+)d\mathcal{E} + e^{-\lambda_W^B\Delta_{AB}^-}\int_0^\infty \begin{pmatrix} \mathcal{E}+a_{AB}^+ \end{pmatrix} e^{-\lambda_W^B\left(\mathcal{E}+a_{AB}^+\right)} \\
&\times H_{16,AB}(\mathcal{E},a_{AB}^+,\Delta_{AB}^-)d\mathcal{E}\Big] - \frac{n_A}{J_0^A\,d_0^A}\Bigg[\int_0^\infty \begin{pmatrix} 1 \\ \mathcal{E}+a_{AB}^- \end{pmatrix} e^{-\lambda_W^A\left(\mathcal{E}+a_{AB}^-\right)} \\
&\times H_{16,AB}(\mathcal{E},a_{AB}^-,\Delta_{AB}^+)d\mathcal{E} + e^{\frac{\varepsilon^{(np)}}{k_B T_L}}\int_0^\infty \begin{pmatrix} 1 \\ \mathcal{E}+a_{AB}^+ \end{pmatrix} e^{-\lambda_W^A\left(\mathcal{E}+a_{AB}^+\right)} \\
&\times H_{16,AB}(\mathcal{E},a_{AB}^+,\Delta_{AB}^-)d\mathcal{E},\Big]\Big\},
\end{aligned}$$

where

$$\begin{aligned}
d_0^A &= d_0(\lambda_W^A), \\
\varepsilon^{(np)} &= \hbar\omega^{(np)}, \\
\Delta_{AB}^{\pm} &= \Delta_{AB} \pm \varepsilon^{(np)}, \\
a_{AB}^{\pm} &= max(0, -\Delta_{AB} \pm \varepsilon^{(np)}),
\end{aligned}$$

and the function $H_{16,AB}$ can be found in Appendix B.

In the previous expression there are two positive terms and two negative ones. The positive terms are gain terms, corresponding to the absorption and the emission of a phonon respectively. These terms depend, through λ_W^B on the macroscopic energy in the valley B. The negative terms, are instead loss terms and they depend on the macroscopic energy in the valley A.

As regards the vector production terms, they are similar to those of acoustic scattering. In this case the elements of the matrices $\mathbf{Q}_{AB}^{(np)}$ are given by

$$q_{ij,\,AB}^{(np)} = \frac{J_0^B\, Z_{AB}}{2\,\hbar\,\sqrt{2\,m_e}\,J_0^A\,d_0^A} N^{(np)} \mathcal{K}^{(np)} \int_0^\infty \Big[\left(\mathcal{E} + a_{AB}^-\right)^{i+j-2} e^{-\lambda_W^A \left(\mathcal{E}+a_{AB}^-\right)} \times H_{17,\,B}(\mathcal{E}, a_{AB}^-, \Delta_{AB}^+) + \left(\mathcal{E} + a_{AB}^+\right)^{i+j-2} e^{-\lambda_W^A \left(\mathcal{E}+a_{AB}^+\right) + \frac{\varepsilon^{(np)}}{k_B T_L}} \times H_{17,\,B}(\mathcal{E}, a_{AB}^+, \Delta_{AB}^-) \Big] d\mathcal{E}, \tag{4.14}$$

where the function $H_{17,\,B}$ can be found in Appendix B.

In conclusion we report a Property which can be applied to drop the numerical computation time of the polar optical phonon and impurity terms by a factor of eight.

Property 4 *If $\nu(\mathbf{n}, \mathbf{n}')$ is an integrable function on $S^2 \times S^2$, such that*

- $\nu(-\mathbf{n}, -\mathbf{n}') = \nu(\mathbf{n}, \mathbf{n}')$,
- $\nu(-n_x, -n_y, n_z, n_x', n_y', n_z') = \nu(n_x, n_y, n_z, n_x', n_y', n_z')$,
- $\nu(-n_x, n_y, n_z, n_x', n_y', n_z') = \nu(n_x, n_y, n_z, n_x', n_y', n_z')$,

then

$$\int_{S^2 \times S^2} \nu(\mathbf{n}, \mathbf{n}')\, d\Omega\, d\Omega' = 8 \int_{Q^1 \times S^2} \nu(\mathbf{n}, \mathbf{n}')\, d\Omega\, d\Omega',$$

where Q^1 is the portion of the unit sphere surface which lies in the first octant of $\mathbb{R}^3$.

The integrands for the production terms of the polar optical phonon and impurity scattering satisfy the hypotheses under which Property 4 holds.

4.4 Numerical simulations of bulk 4H-SiC and 6H-SiC

Silicon carbide is an important semiconductor material, because of its high saturation velocity, large thermal conductivity, high breakdown voltages and high Schottky barriers. These properties are very important at high temperatures, at high frequency and for high power devices.

In the previous chapter were showed some results for 4H-SiC, produced

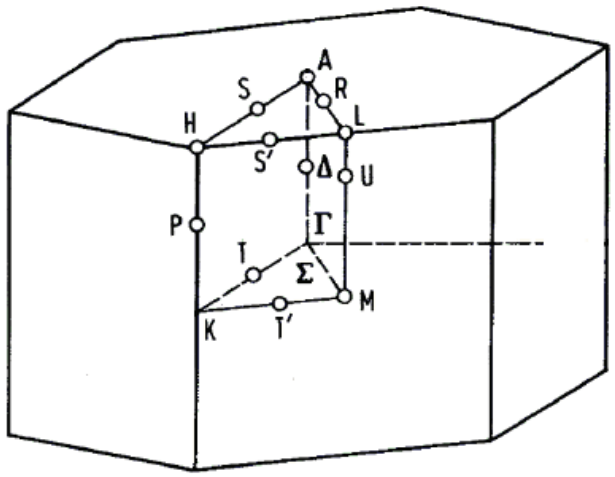

Figure 4.1: Hexagonal lattice

employing a model where an isotropic dispersion relation is used (we indicate this model as IB model). Here those results are compared with the new ones, obtained using a model that takes into account the anisotropic dispersion relations (in the following indicated as AB model). The aim is to show that the AB model is more appropriate to describe the behavior of anisotropic semiconductors, because the dependence of the drift velocity and the average energy on the applied the electric field strongly changes according to the direction of the latter. Among these anisotropic semiconductors

Table 4.2: Parameters of the band structure of 4H-SiC and 6H-SiC

Material	4H-SiC		6H-SiC	
Conduction band valley	M, 1^{st} c.b.	M, 2^{nd} c.b	L, 1^{st} c.b.	L, 2^{st} c.b.
Effective masses (m_e)	0.29, 0.58, 0.33	0.90, 0.58, 0.33	0.22, 0.90, 1.43	0.22, 0.90, 1.43
Valley energy minimum (eV)	0	0.14	0	0
α (eV^{-1})	0.117	0.058	0.039	0.039
Number of equivalent valleys	3	3	3	3

two hexagonal polytypes of silicon carbide, whose lattice is shown in Figure 4.1, are taken into consideration for simulations.

Bulk 4H-SiC

As in the previous chapter, for the band structure of 4H-SiC we have considered the results in [18]. Then the total number of valleys is again 6: 3 at the equivalent M points for each of the two lowest conduction bands. The parameters are those reported in Table 4.2.

In this table the masses along the principal directions M-K, M-Γ and M-L are reported and are indicated respectively with x, y and z. m_e is the free electron mass, and ϵ_0 the vacuum permittivity. In the bulk case, taking homogenoeous initial conditions, with initial velocities and energy fluxes equal to zero, the moment system, as seen, becomes a set of ordinary differential equations, where time is the only independent variable. The Poisson equation is, in this case, solved taking the total electron population equal to the doping concentration, and the electrostatic potential with linear profile between the two boundaries, while the moment system reduces to

$$\frac{dn_{_A}}{dt} = n_{_A} C_{n_{_A}}(W_A) + \sum_{B \neq A} n_{_B} C_{n_{_A}}(W_B), \tag{4.15}$$

$$\frac{d}{dt}(n_{_A}\mathbf{V}_{_A}) + q\mathbf{E}\cdot n_{_A}\mathbf{G}_{_A}^{(0)} = n_{_A} c_{11}^{A}(W_{_A})\mathbf{V}_{_A} + n_{_A} c_{12}^{A}(W_{_A})\mathbf{S}_{_A}, \tag{4.16}$$

$$\frac{d}{dt}(n_{_A}W_{_A}) + q\mathbf{E}\cdot n_{_A}\mathbf{V}_{_A} = n_{_A} C_{W_{_A}}(W_A) + \sum_{B \neq A} n_{_B} C_{n_{_A}}(W_B), \tag{4.17}$$

$$\frac{d}{dt}(n_{_A}\mathbf{S}_{_A}) + qq\mathbf{E}\cdot n_{_A}\mathbf{G}_{_A}^{(1)} = n_{_A} c_{21}^{A}(W_{_A})\mathbf{V}_{_A} + n_{_A} c_{22}^{A,i}(W_{_A})\mathbf{S}_{_A}, \tag{4.18}$$

where the indices A and B run over the valleys. All scattering mechanisms presentend in Chapter 2 are taken into account. The material parameters are reported in Table 4.3, following the data in [25]. Into the first addenda of the equations (4.15) and (4.17) are summed all the terms relative to the density and the energy productions, except the gain terms of the intervalley scattering, which depend on the energy of the other valleys, different from A, involved in the scattering and are represented by the sums at the right-hand sides of the equations. The production terms are numerically computed for a discrete number of values in a suitable range of the macroscopic energies and the values of interest during the numerical computation of the solution to the system (3.21-4.18) are evaluated by a stepwise linear interpolation. The computation of the production terms relative to the scattering with the polar optical phonons and with the impurities is very expensive, however these computations are done once for all and can be used for all kinds of devices. In particular, for the angular integration a suitable numerical method has been exploited, which has been tested verifying that, if the masses are equal, the results of the isotropic model are recovered. The ODE system is numerically solved by a 4-th order Runge-Kutta method for sixty values of the applied electric field going in modulus from $10^{-3}\, V/\mu m$ to $100\, V/\mu m$. Three directions of the field are considered, that is the principal directions of one of the three equivalent M-valleys.

The results are shown in Figures 4.2-4.5. All the main characteristics of 4H-SiC are qualitatively and quantitatively well described. At low fields, up to $4 \div 5\, V/\mu m$, the behavior of the total average velocity, which is defined as

$$\mathbf{V} = \frac{1}{n} \sum_{A} n_{A} \mathbf{V}_{A},$$

is high-slope linear, and the velocity reaches its maxima, which are about 2.04×10^7, 1.94×10^7 and 2.42×10^7cm/s respectively in the x, y and z direction, at about the fields 40, 40 and 32 $V/\mu m$. Considering this fact and inspecting Figure 4.3 it appears clear that taking into account the anisotropy of the energy dispersion relations is very important. In fact the differences

according to the direction of the electric field are relevant.

Also as regards the behavior of the valley occupancies, as shown in Figure 4.2, there are differences between the IB and AB model. In this case the population inversion occurs at a lower electric field than in the isotropic case. Furthermore, there is a remarkable discrepancy, as shown in Figure 4.4, between the predictions of the two models in the behavior of the total mean energy, which is given by

$$W = \frac{1}{n} \sum_{A} n_{A} \big(W_{A} + \mathcal{E}_{A}^{(0)} - \mathcal{E}_{1}^{(0)} \big).$$

This might be due also to the different overlap factor which has been used in this chapter as can be deduced from the fact that relevant differences in the energy production terms are present only for the polar optical scattering, see Figure 4.6-4.7. As regards the production terms for the velocities and the energy fluxes, the main differences can be found in the polar optical and impurity scattering which are anisotropic and for which the overlap factor is used, while for the acoustic and non polar optical scattering the differences are irrelevant, see Figures 4.11-4.14. At last in Figure 4.5, we show how the behavior of the drift velocity varies at different doping concentrations, and the model manages to capture the non-monotonicity with increasing impurity concentration typical of SiC.

6H-Bulk SiC

Also in this case for the band structure we have used the results in [18]. In particular we have considered the minima of the two lowest conduction bands to occur at the L symmetry point and used a number of equivalent valleys equal to three. Therefore also in this case the total number of valleys is 6, and furthermore the two lowest conduction bands are degenerate around L. The parameters are reported in Table 4.2, where in particular the masses along the principal directions L-H, L-A and L-M can be found. The results are shown in Figures 4.17-4.19 and are qualitatively analogous to those for 4H-SiC, therefore the same comments remain valid also in this case. For a better comparison with the experimental values found by von Muench [39],

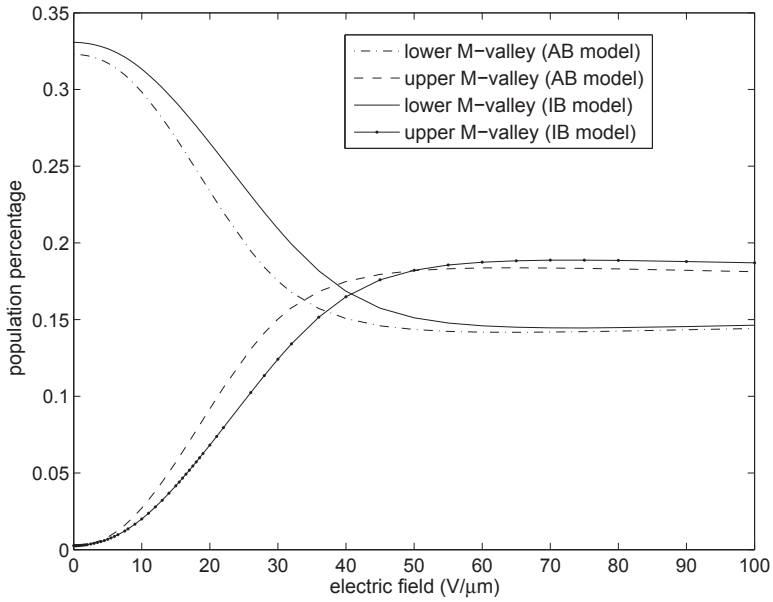

Figure 4.2: 4H-SiC. Valley occupancy vs the applied electric field directed along M-K. $N_D = 10^{19}/cm^3$

in Figure 4.17 we have highlighted by squares the velocities corresponding to the values of the electric field reported in [25]. Eventually Figure 4.20-4.21 shows that, as known, the anisotropy of 4H-SiC is lower than that of 6H-SiC.

Table 4.3: Bulk material parameters

	ρ	ϵ_s	ϵ_∞	v_s	Ξ_d	$\hbar\omega^{(p)}$	$\hbar\omega^{(np)}$	D_tK
4H-SiC	3.2	9.7	6.5	13730	15	120	85.4	7×10^8
6H-SiC	3.2	9.66	6.5	13730	17.5	120	85.4	$6{\times}10^8$
Units	$\frac{g}{cm^3}$	ϵ_0	ϵ_0	m/s	eV	meV	meV	meV

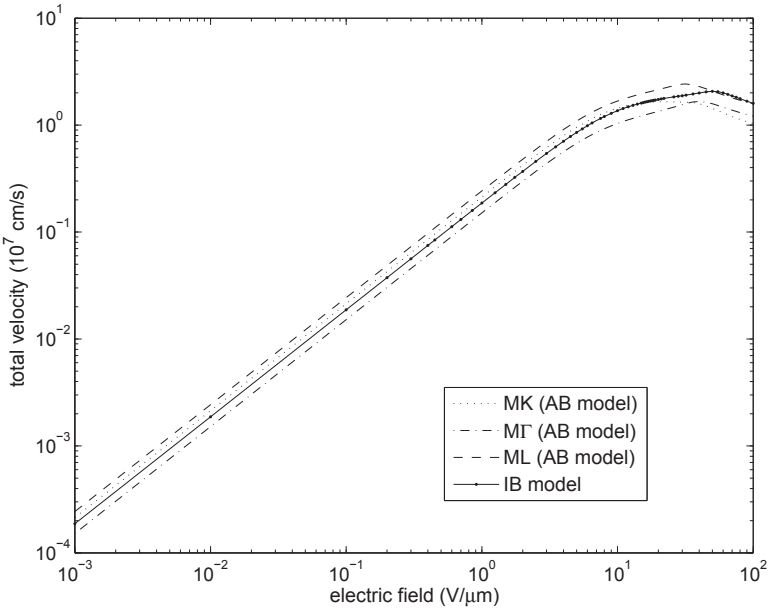

Figure 4.3: 4H-SiC. Total velocity vs the applied electric field. $N_D = 10^{19}/cm^3$

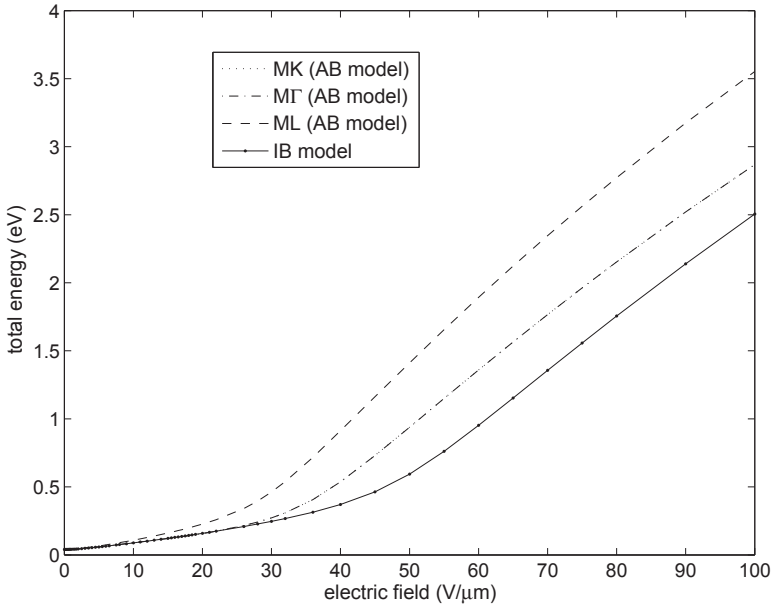

Figure 4.4: 4H-SiC. Total average energy (measured from the bottom of the 1^{st} M-valley) ve the applied electric field, $N_D = 10^{19}/cm^3$.

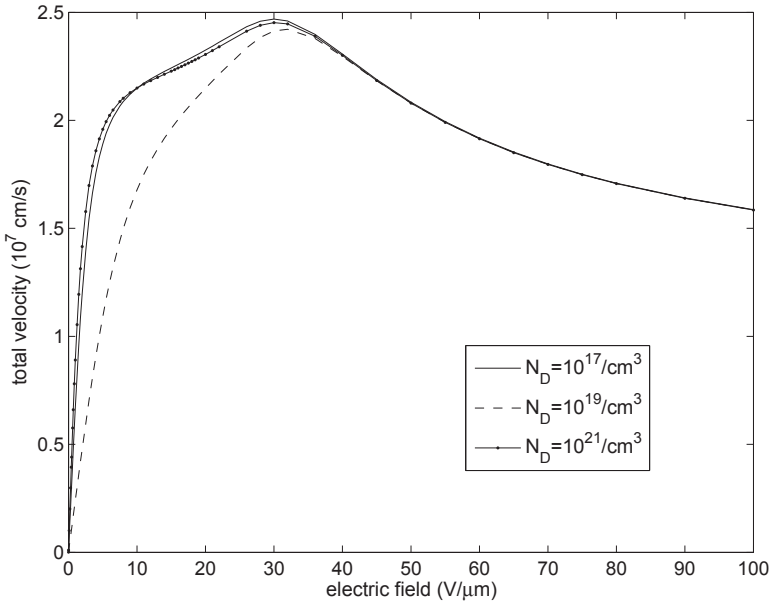

Figure 4.5: 4H-SiC. Total velocity vs the applied electric field. $N_D = 10^{19}/cm^3$

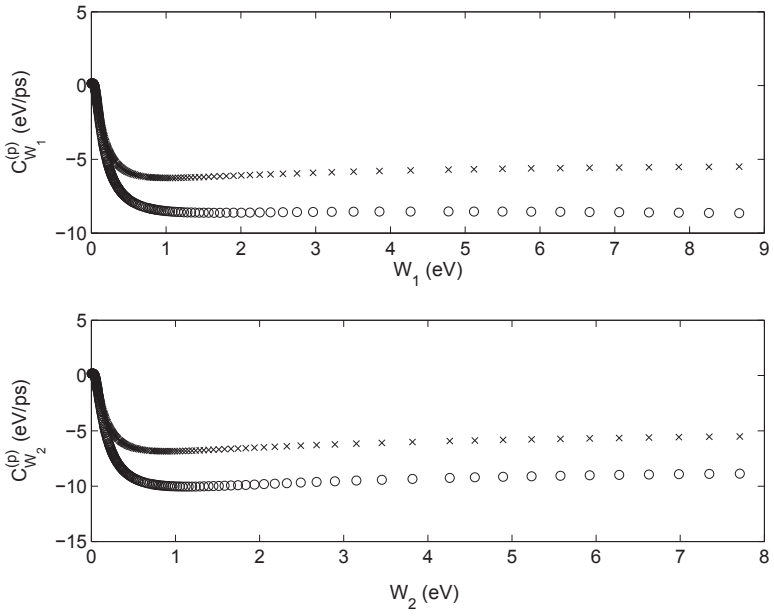

Figure 4.6: 4H-SiC. Polar optical energy production (for the two M-valleys). Circles refer to IB model, crosses to AB model.

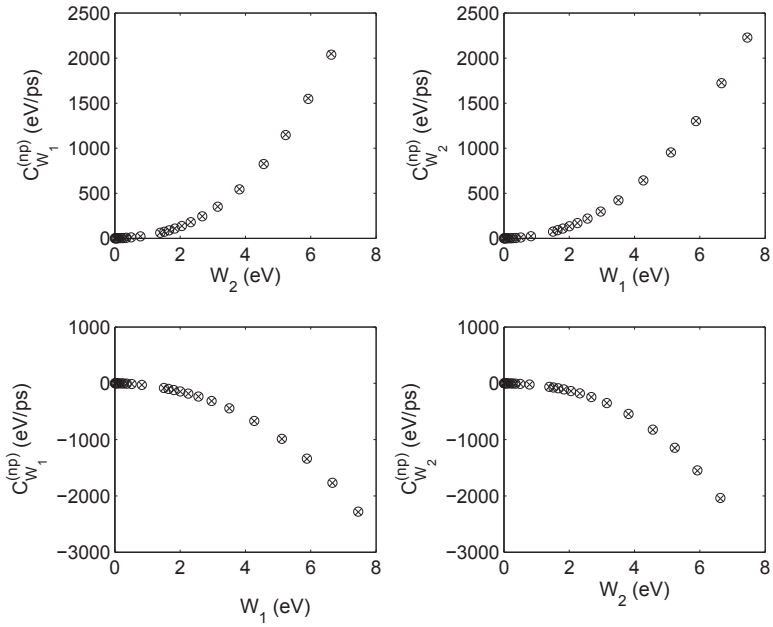

Figure 4.7: 4H-SiC. Non-polar optical energy productions (for the two M-valleys). Circles refer to IB model, crosses to AB model.

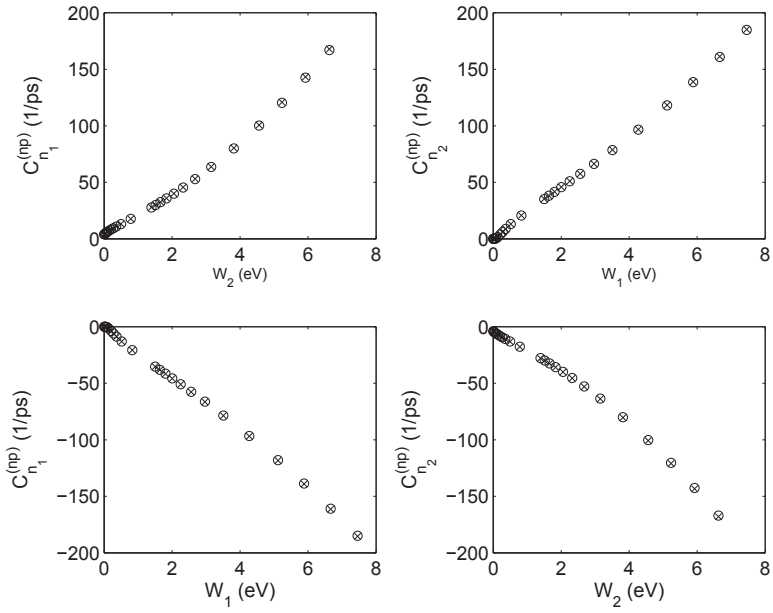

Figure 4.8: 4H-SiC. Non-polar optical density productions (for the two M-valleys). Circles refer to IB model, crosses to AB model.

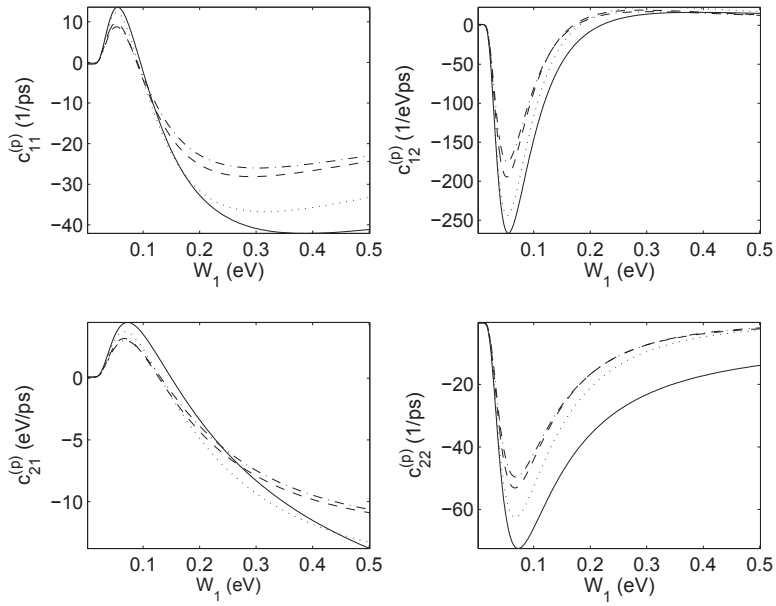

Figure 4.9: 4H-SiC. Polar optical scattering. Velocity and energy flux production terms (higher valley).

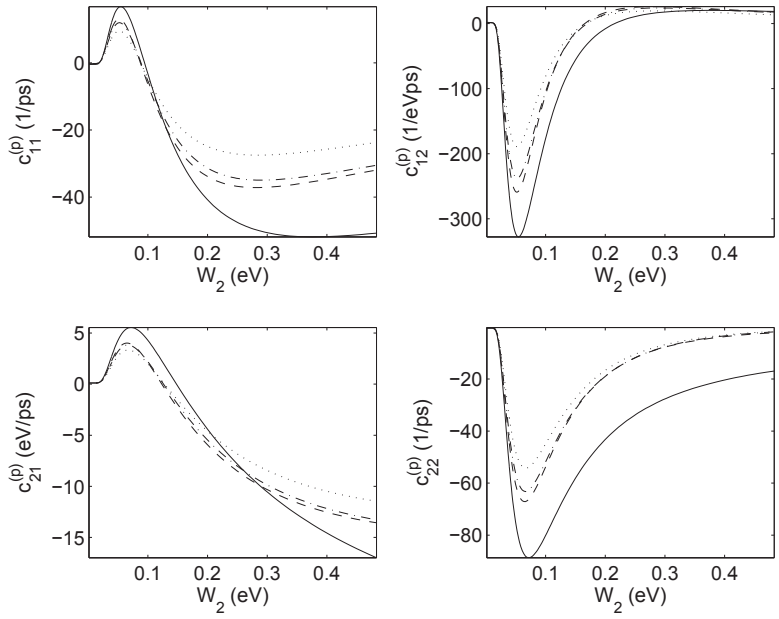

Figure 4.10: 4H-SiC. Polar optical scattering. Velocity and energy flux production terms (lower valley).

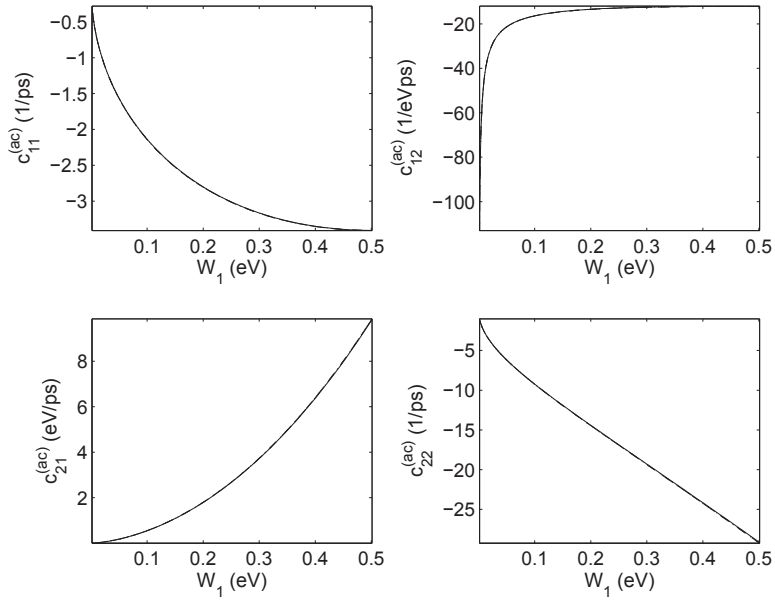

Figure 4.11: 4H-SiC. Acoustic scattering. Velocity and energy flux production terms (higher valley).

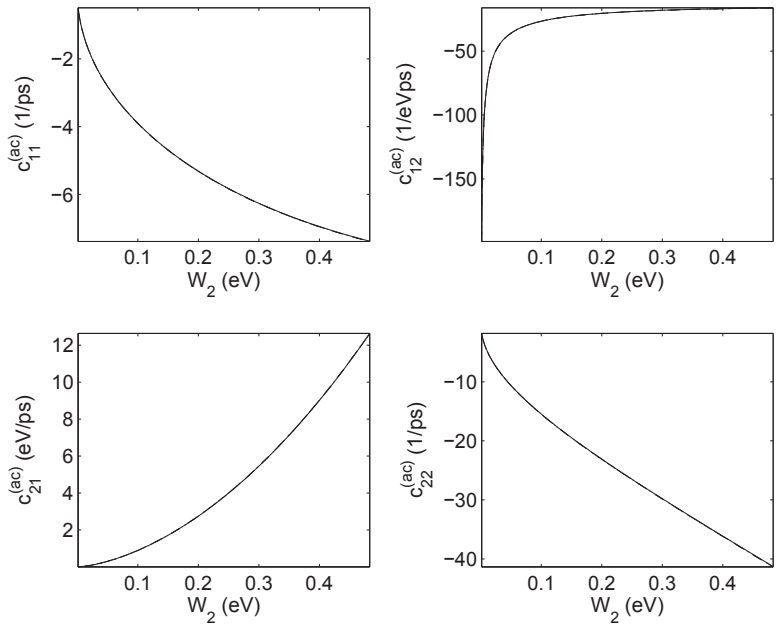

Figure 4.12: 4H-SiC. Acoustic scattering. Velocity and energy flux production terms (lower valley).

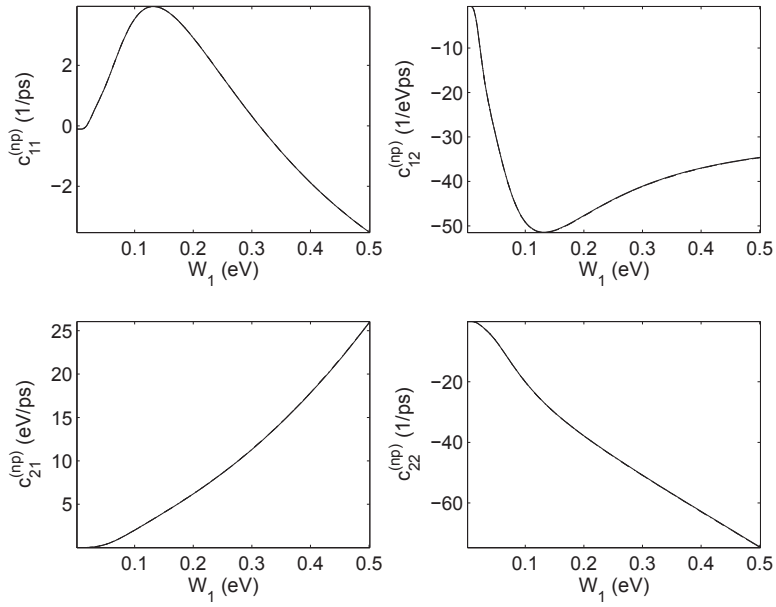

Figure 4.13: 4H-SiC. Non-polar optical scattering. Velocity and energy flux production terms (higher valley).

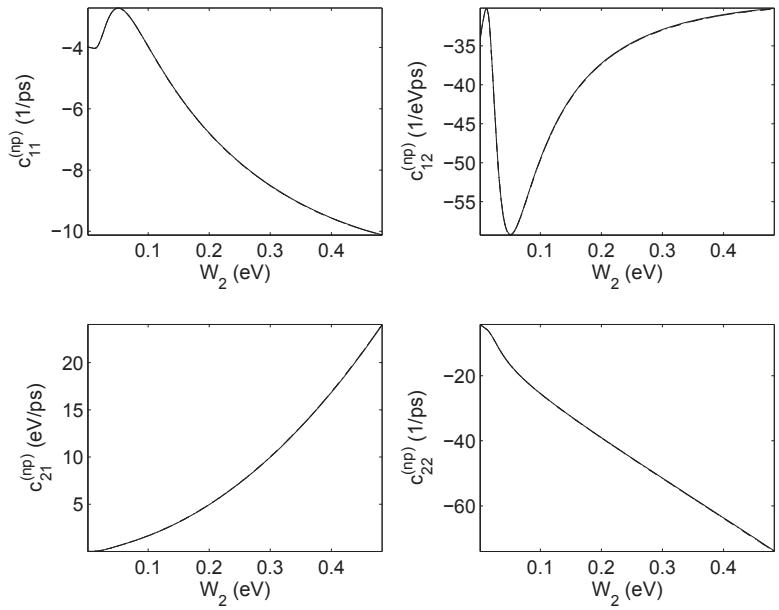

Figure 4.14: 4H-SiC. Non-polar optical scattering. Velocity and energy flux production terms (lower valley).

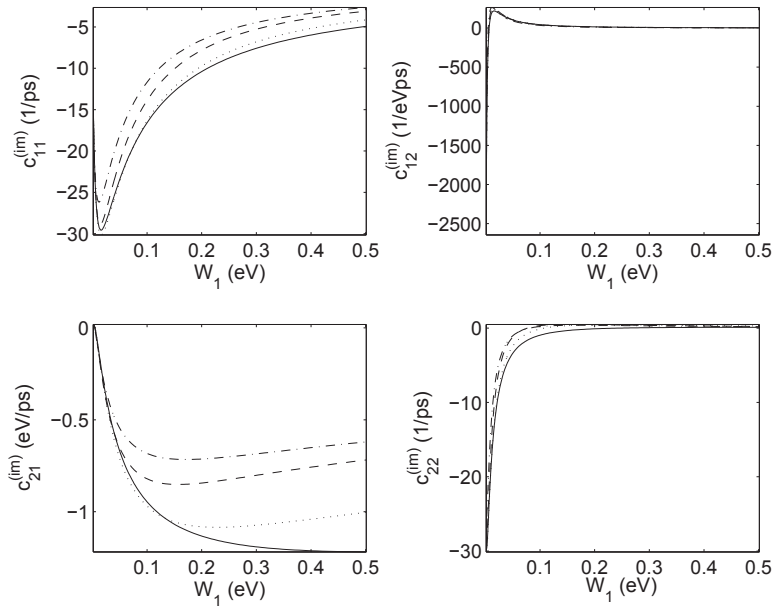

Figure 4.15: 4H-SiC. Impurity scattering. Velocity and energy flux production terms (higher valley)

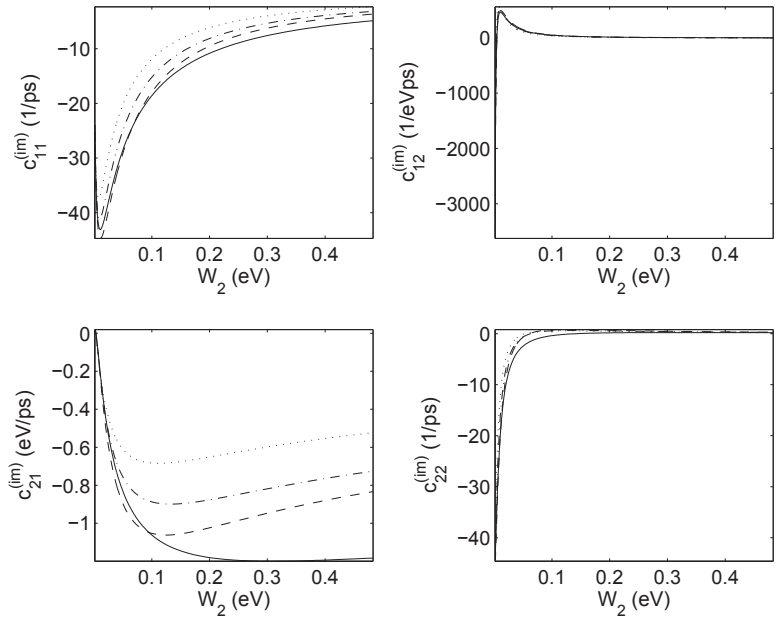

Figure 4.16: 4H-SiC. Impurity scattering. Velocity and energy flux production terms (lower valley).

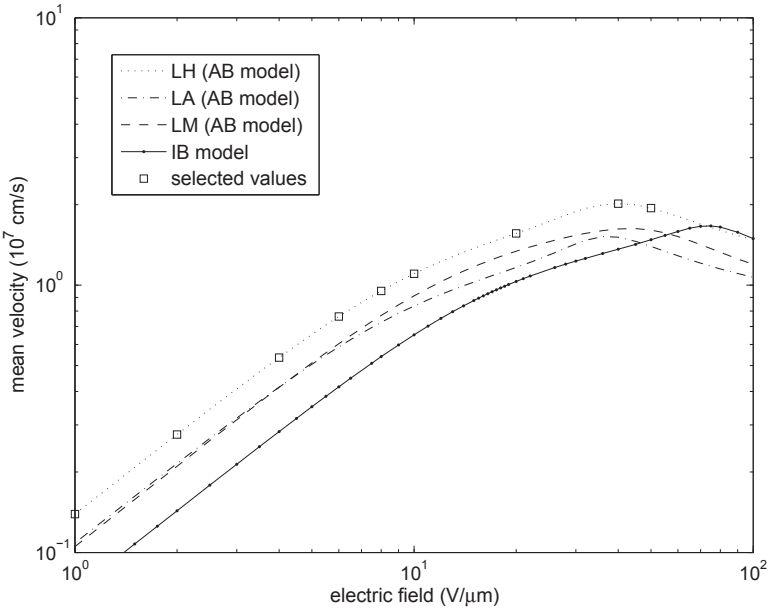

Figure 4.17: 6H-SiC. Total velocity vs the applied electric field.

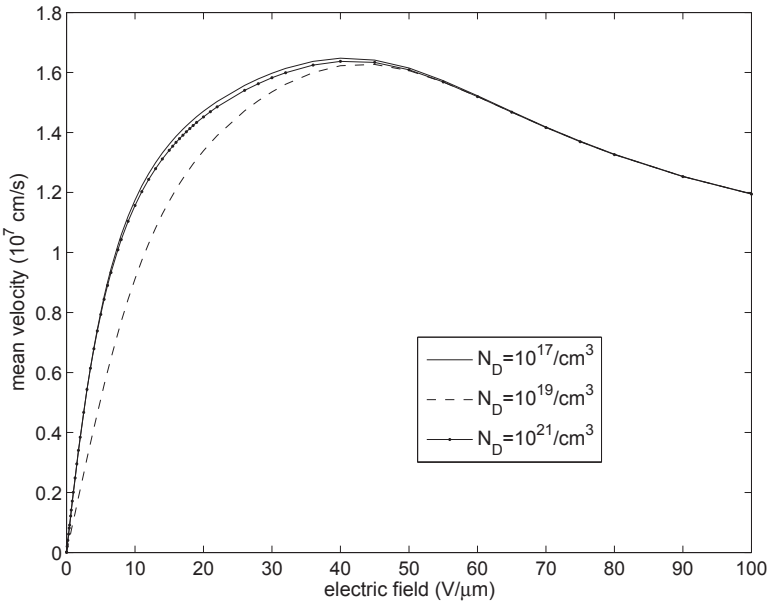

Figure 4.18: 6H-SiC. Total velocity vs the applied electric field directed along L-M, for the three values of N_D.

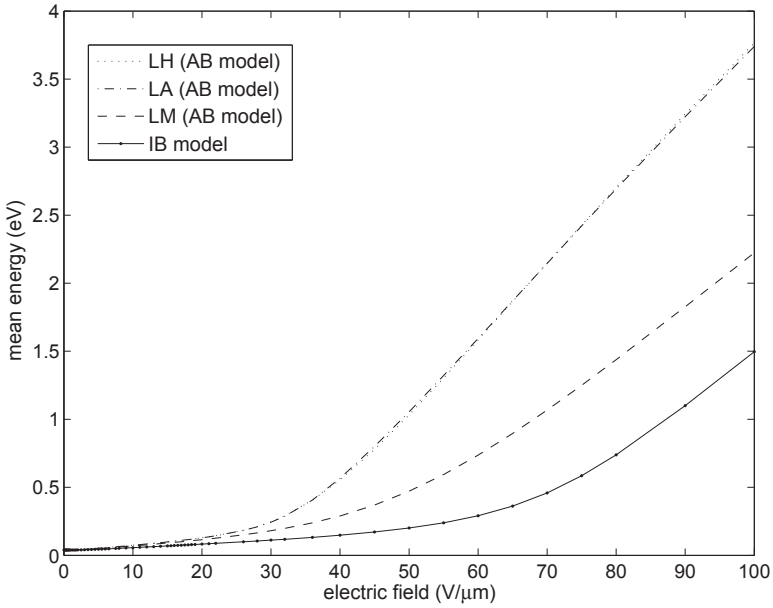

Figure 4.19: 6H-SiC. Total average energy (measured from the bottom of the first c.b.) vs the applied electric field along the three principal axes.

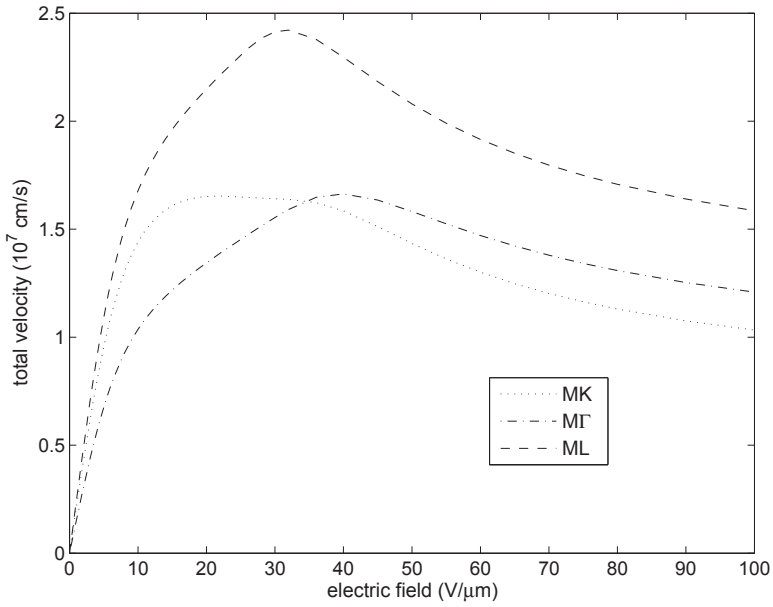

Figure 4.20: 4H-SiC, total velocity vs the applied electric field directed along the principal directions. N_D=10^{19}/cm^3.

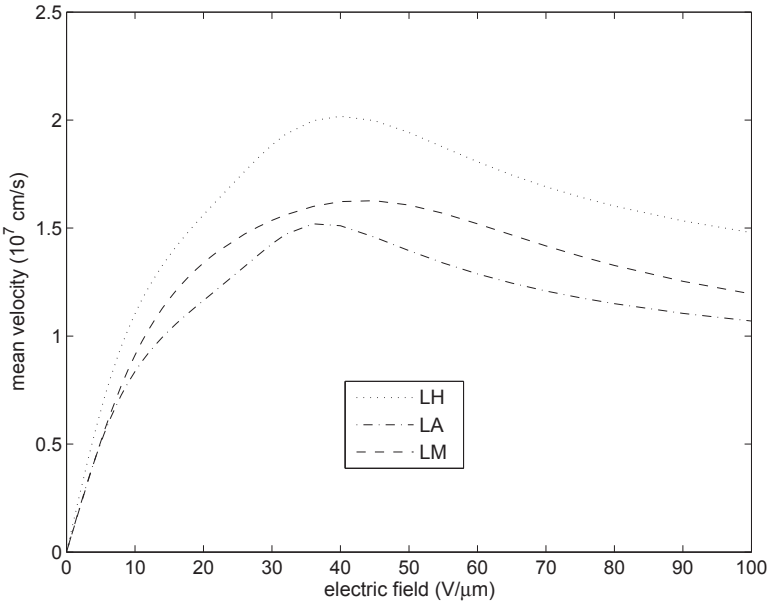

Figure 4.21: 6H-SiC, total velocity vs the applied electric field directed along the principal directions. N_D=10^{19}/cm^3.

Appendix A

In this section we report the functions which appear in the various production terms in Chapter 3.

$H_1(\mathcal{E},\alpha) = \mathcal{E}(1+\alpha\mathcal{E})$,

$H_2(\mathcal{E}_1,\mathcal{E}_2,\alpha) = (1+\alpha\mathcal{E}_1)(1+\alpha\mathcal{E}_2)$,

$H_3(\mathcal{E}_1,\mathcal{E}_2,\alpha) = ln\frac{\sqrt{H_1(\mathcal{E}_1,\alpha)}+\sqrt{H_1(\mathcal{E}_2,\alpha)}}{\left|\sqrt{H_1(\mathcal{E}_1,\alpha)}-\sqrt{H_1(\mathcal{E}_2,\alpha)}\right|}$,

$H_4(\mathcal{E}_1,\mathcal{E}_2,\alpha) = [(H_1(\mathcal{E}_1,\alpha)+H_1(\mathcal{E}_2,\alpha))H_3(\mathcal{E}_1,\mathcal{E}_2,\alpha) - 2\sqrt{\mathcal{E}_1\mathcal{E}_2H_2(\mathcal{E}_1,\mathcal{E}_2,\alpha)}]$,

$H_5(\mathcal{E}_1,\mathcal{E}_2,\alpha) = 3(H_1(\mathcal{E}_1,\alpha)+H_1(\mathcal{E}_2,\alpha))^3H_3(\mathcal{E}_1,\mathcal{E}_2,\alpha) - 8[\mathcal{E}_1\mathcal{E}_2H_2(\mathcal{E}_1,\mathcal{E}_2,\alpha)]^{\frac{3}{2}} - 6(h_1(\mathcal{E}_1,\alpha)+H_1(\mathcal{E}_2,\alpha))^2\sqrt{\mathcal{E}_1\mathcal{E}_2H_2(\mathcal{E}_1,\mathcal{E}_2,\alpha)}$,

$H_6(\mathcal{E},\alpha,m) = \frac{ln\left[1+\frac{8m}{\hbar^2\beta^2}H_1(\mathcal{E},\alpha)\right]-\frac{8mH_1(\mathcal{E},\alpha)}{\hbar^2\beta^2+8mH_1(\mathcal{E},\alpha)}}{1+\alpha\mathcal{E}}$,

$H_7^0(\mathcal{E},a,\Delta,\alpha_1,\alpha_2) = \sqrt{H_1(\mathcal{E}+a,\alpha_1)H_1(\mathcal{E}+a+\Delta,\alpha_2)}[1+2\alpha_1(\mathcal{E}+a)] \times [1+2\alpha_2(\mathcal{E}+a+\Delta)]$,

$H_8^0(\mathcal{E},a,\Delta,\alpha_1,\alpha_2) = \frac{1+2\alpha_2(\mathcal{E}+a+\Delta)}{[1+2\alpha_1(\mathcal{E}+a)]}\sqrt{H_1(\mathcal{E}+a,\alpha_1)^3H_1(\mathcal{E}+a+\Delta,\alpha_2)}$,

$H_7^1(\mathcal{E},a,\Delta,\alpha_1,\alpha_2,m_1,m_2) = [m_1H_1(\mathcal{E}+a,\alpha_1)+m_2H_1(\mathcal{E}+a+\Delta,\alpha_2)] \times H_7^0(\mathcal{E},a,\Delta,\alpha_1,\alpha_2)$,

$H_8^1(\mathcal{E}, a, \Delta, \alpha_1, \alpha_2, m_1, m_2) = [m_1 H_1(\mathcal{E} + a, \alpha_1) + m_2 H_1(\mathcal{E} + a + \Delta, \alpha_2)] \times H_8^0(\mathcal{E}, a, \Delta, \alpha_1, \alpha_2)$,

$H_9(\mathcal{E}, a, \Delta, \alpha_1, \alpha_2) = [H_1(\mathcal{E} + a, \alpha_1) H_1(\mathcal{E} + a + \Delta, \alpha_2)]^{\frac{3}{2}}$.

Appendix B

In this section we report the functions which appear in the various production terms in Chapter 4.

$$H_{11}(x) := \sqrt{x}\ \frac{\gamma(x) - x\,\dot{\gamma}(x)}{\gamma(x)^{\frac{5}{2}}},$$

$$H_{12,\,i}(x,y) := \frac{g^2(x)\,H_1(y)}{\gamma(x)H_1(x)} \int_{S^2} G^{\,s,p}(x,y,\mathbf{n})\eta_i^2(\mathbf{n})\,n_i^2\,\psi^{\frac{3}{2}}(\mathbf{n})\,d\,\Omega,$$

$$H_{13,\,i}(x,y) := e^{\hbar\omega^{(p)}\left(\frac{1}{k_B T_L}-\lambda_W\right)}\,\frac{g^2(y)\,H_1(x)}{\gamma(y)H_1(y)} \int_{S^2} G^{\,s,p}(y,x,\mathbf{n})\eta_i^2(\mathbf{n})\,n_i^2\,\psi^{\frac{3}{2}}(\mathbf{n})\,d\,\Omega,$$

$$H_{14,\,i}(x,y) := \frac{g(x)\,g(y)}{\sqrt{\gamma(x)\,\gamma(y)}}\,\sqrt{x\,y} \int_{S^2} G_i^{\,v,p}(x,y,\mathbf{n})\eta_i(\mathbf{n})\,n_i\,\psi^{\frac{3}{2}}(\mathbf{n})\,d\,\Omega,$$

$$H_{15}(x) := \int_{S^2} \left[G^{\,s,im}(x,\mathbf{n})\,\eta_i^2(\mathbf{n})\,n_i^2\,\psi^{\frac{3}{2}}(\mathbf{n}) - G_i^{\,v,im}(x,\mathbf{n})\,\eta_i(\mathbf{n})\,n_i\,\psi^{\frac{3}{2}}(\mathbf{n})\right] d\,\Omega,$$

$$H_{16,AB}(x,y,z) := H_{1,A}(x+y)H_{1,B}(x+y+z),$$

$$H_{17,B}(x,y,z) := \frac{8\,m_e\,(x+y)^2}{\hbar^2} H_{1,B}(x+y+z)$$

Bibliography

[1] C.Jacoboni, Theory of Electron Transport in Semiconductors, Springer, 2010

[2] N.W. Ashcroft, N.D. Mermin, Solid State Physics, 1976

[3] F.Bassani, U.N. Grassano, Fisica dello stato solido, Bollati Boringhieri, 2000

[4] P. Degond, Mathematical modelling of microelectronics semiconductor devices, Lecture notes

[5] Tuckerman, The Born-Oppenheimer Approximation, Lecture notes

[6] A.M. Anile, G. Alì, G. Mascali, Modellistica per i dispositivi a semiconduttore, Lecture notes

[7] V. Arnold, Metodi matematici della meccanica classica, 2004

[8] C. Cercignani, The Boltzmann equation and its applications, Springer, 1998

[9] G.Alì, G. Mascali, V.Romano, R.C. Torcasio, A Hydrodynamic Model for Covalent Semiconductors with Applications to Gan and SiC,Acta Applicandae Mathematicae, **122**, 1 (2012), Page 335-348

[10] Fawcett, W., Boardman, A.D., Swain S.: Monte Carlo determination of electron transport properties in gallium arsenide, J. Phys. Chem. Solids , **31** (9), 1963 (1970)

[11] G. Mascali, V. Romano, Hydrodynamical model of charge transport in GaAs based on the maximum entropy principle, Contin. Mech. Thermodyn., **14**, 405, 2002

[12] Chen, S., Wang G.: High-field properties of carrier transport in bulk wurtzite GaN: A Monte Carlo perspective, J. Appl. Phys., **103**, 023703 (2008)

[13] U.V. Bhapkar, M.S. Shur, Monte Carlo calculations of velocity-field characteristics of wurzite GaN. J. Appl. Phys. **82**(4), 1649 (1997)

[14] S. La Rosa, G. Mascali, V. Romano, Exact maximum entropy closure of the hydrodynamical model for Si semiconductors: the 8-moment case. SIAM J. Appl. Math. **70**, 710 (2009)

[15] A.M. Anile, V. Romano, Non parabolic band transport in semiconductors: closure of the moment equations, Contin. Mech. Thermodyn, **11**, 307 (1999)

[16] V. Romano, Non parabolic band transport in semiconductors: closure of the production terms in the moment equations, Contin. Mech. Thermodyn. **12**,31 (2000)

[17] G.Mascali, V. Romano, J.M.Sellier, MEP parabolic hydrodynamical model for holes in silicon semiconductors. Nuovo Cimento B **120** (2), 197 (2005)

[18] G. Pennington, N. Goldsman, Consistent calculations for n-type hexagonal SIC inversion layers. J. Appl. Phys. **95** (8), 4223-4234 (2004)

[19] T.-H. Yu, K. F. Brennan, Monte Carlo calculation of two-dimensional electron dynamics in GaN-AlGaN heterostructures. J. Appl. Phys. **91** (6), 3730 (2002)

[20] O. Muscato, R.M. Pidatella, M. V. Fischetti, Monte Carlo and hydrodynamic simulation of a one dimensional $n^+ - n - n^+$ silicon diode. VLSI Des. **6** (1-4), 247 (1998)

[21] A. Majorana, Equilibrium solutions of the non-linear Boltzmann equation for an electron gas in a semiconductor. Il nuovo cimento B **108** (8), 871-877 (1993)

[22] O. Muscato, The Onsager reciprocity principle as a check of consistency fro semiconductor carrier transport models. Physica A **289** (3-4), 422 (2001)

[23] G. Mascali, V. Romano, Si and GaAs mobility derived from a hydrodynamical model for semiconductor based on the maximum entropy principle. Physica A **352** (2-4), 459 (2005)

[24] C. Cercignani, R. Illner, M. Pulvirenti, The Mathematical Theory of Dilute Gases, 1994

[25] Mickevicius, R., Zhao, J. H.: Monte Carlo study of electron transport in SiC, J. Appl. Phys. **83**(6), 3161 (1998)

[26] G.Alì, G. Mascali, V.Romano, R.C. Torcasio, A Hydrodynamical model for covalent semiconductors with a generalized energy dispersion relation, in pubblication (2013)

[27] Jacoboni, C., Lugli, P.: The Monte Carlo Method for Semiconductor Device Simulation. Springer-Verlag, Wien–New York (1989)

[28] Nilsson, H.E., Hjelm, M., Fröjdh, C., Persson, C., Sannemo, U., and Petersson,C.S.: Full band Monte Carlo simulation of electron transport in 6H-SiC, J. Appl. Phys. **86**, 965 (1999)

[29] Zhao, J. H., Gruzinskis, V., Luo, Y., Weiner, M., Pan, M., Shiktorov, P., Starikov, E.: Monte Carlo simulation of 4H-SiC IMPATT diodes, Semicond. Sci. Technol. **15**, 1093 (2000)

[30] Hjelm, M., Nilsson, H.-E., Martinez, A., Brennan, K.F., Bellotti, E.: Monte Carlo study of high-field carrier transport in 4H-SiC including band-to-band tunneling, J. Appl. Phys. **93** (2), 1099 (2003)

[31] Tomizawa, K.: Numerical Simulation of Submicron Semiconductor Devices. Artech House, Boston–London (1993)

[32] Dreyer, W.: Maximisation of the Entropy in Non-Equilibrium, J. Phys. A: Math. Gen. **20**, 6505 (1987).

[33] Jaynes, E. T.: Information theory and Statistical Mechanics, Phys. Rev. **106**, 620 (1957).

[34] Mascali, G.: Maximum entropy principle in relativistic radiation hydrodynamics II: Compton and double Compton scattering, Continuum Mech. Thermodyn., **14**(6), 549 (2002)

[35] Mascali, G., Romano, V.: Hydrodynamic subband model for semiconductors based on the maximum entropy principle, Il Nuovo Cimento C **33**(1), 155–163 (2010)

[36] Muscato, O., Di Stefano, V.: Local equilibrium and off-equilibrium thermoelectric effects in silicon semiconductors, J. Appl. Phys. **110**(9), 093706 (2011)

[37] Muscato, O., Di Stefano, V.: Modeling heat generation in a submicrometric $n^+ - n - n^+$ silicon diode, J. Appl. Phys., **104**(12), 124501 (2008)

[38] Mascali, G., Romano, V.: A hydrodynamical model for holes in silicon semiconductors: The case of non-parabolic warped bands, Math. Comp. Modelling **53**(1-2), 213 (2011)

[39] von Muench, W., Pettenpaul J.: Saturated electron drift velocity in 6H silicon carbide, J. Appl. Phys., **48**, 4823 (1977)

[40] Baccarani G, Wonderman M R, An investigation on steady- state velocity overshoot in silicon, Solid-state electronics 29: 970-977 (1982)

[41] Muller I , Ruggeri T, Rational Extended Thermodynamics, Berlin, Springer- Verlag (1998)

[42] A. Majorana, R.M. Pidatella, A finite difference scheme solving the Boltzmann-Poisson system, Journal of Computational Physics, 174: 649-668 (2001)

Sintesi del lavoro di tesi

I materiali semiconduttori sono impiegati in diversi campi, quali ad esempio i dispositivi elettronici e microelettronici, i laser e le celle solari. In particolare in microelettronica hanno un vasto campo di applicazione, che include, ad esempio, i computer, le telecomunicazioni, ecc.
Il silicio è il materiale più comunemente usato per le applicazioni in microelettronica. Esistono molti esempi in letteratura riguardanti la descrizione delle sue proprietà fisiche. Inoltre sono stati sviluppati modelli matematici per riprodurre le proprietà fisiche che caratterizzano i fenomeni di trasporto in questo semiconduttore. Poichè però i comuni dispositivi al silicio operano in un range di potenze basso, sono in continuo sviluppo attività di ricerca relative a tecnologie e dispositivi di potenza che considerano materiali innovativi adatti alle suddette applicazioni. In questo scenario hanno trovato largo uso i semiconduttori composti. Fra i semiconduttori composti, uno dei primi ad essere utilizzato è stato il GaAs, per esempio nei LED a infrarossi, nei laser e nelle celle solari. Il vantaggio del GaAs rispetto al Si è che ha una velocità di saturazione degli elettroni più elevata e una più alta mobilità, e quindi è importante per il funzionamento a frequenze più alte di 250 GHz.
Recentemente semiconduttori con bandgap più ampi, come GaN e SiC, hanno attratto un grande interesse poichè hanno un elevato campo di breakdown, un basso tasso di generazione termica, e una buona conducibilità e stabilità termica. Queste proprietà sono utili per dispositivi ad alta potenza e alta temperatura.
Negli ultimi anni c'è quindi una crescente richiesta di modelli di simulazione

che prevedano accuratamente le performance dei dispositivi, analizzando i processi fisici coinvolti in questi nuovi materiali.
L'impiego di questi modelli risulta strategico anche da un punto di vista industriale, in quanto le simulazioni fatte utilizzando questi modelli permettono di risparmiare sui costi di produzione. Per tutti questi semiconduttori ci sono dei modelli Monte Carlo, ma c'è una certa carenza di modelli macroscopici, computazionalmente meno dispendiosi.
Lo scopo di questo lavoro è appunto lo sviluppo di modelli idrodinamici per il trasporto di cariche nei semiconduttori composti.
Questi modelli possono essere ottenuti a partire dalla descrizione cinetica del trasporto di cariche, tenendo conto della struttura a bande del particolare semiconduttore considerato. Nello specifico, bisogna considerare un numero di popolazioni di portatori di carica pari al numero di valli vicine presenti nella struttura a bande del materiale. Lo stato di ogni popolazione di portatori di carica può essere descritto da una equazione del trasporto di Boltzmann, a cui è accoppiata l'equazione di Poisson per il potenziale elettrico autoconsistente. L'equazione di Boltzmann è un'equazione integro-differenziale che deve essere risolta numericamente. Poichè i modelli Monte Carlo e gli schemi alle differenze finite sono computazionalmente molto dispendiosi, sono stati introdotti i modelli idrodinamici. Questi modelli, partendo dall'equazione di Boltzmann, considerano un certo numero di momenti della funzione di distribuzione, ottenuti moltiplicando la funzione di distribuzione per una opportuna funzione peso e integrando sulla prima zona di Brillouin. Le funzioni peso, di solito, vengono scelte in modo che abbiano un significato fisico, come ad esempio la densità, la velocità media, ecc.
L'insieme delle equazioni di evoluzione legate ai momenti ottenuti dall' integrazione dell'equazione di Boltzmann, non è un sistema chiuso, poichè il numero di incognite è maggiore del numero di equazioni.
In passato, la chiusura di questi modelli idrodinamici era ottenuta con relazioni di chiusura ad hoc, carenti di giustificazioni fisiche consistenti. Per questa ragione sono stati cercati metodi di chiusura alternativi, basati su

principi primi. Tra questi vi è il principio di massima entropia. Questo principio afferma che, se è noto un dato numero di momenti, le funzioni di distribuzione, che possono essere usate per valutare i momenti non noti, sono quelle che massimizzano l'entropia del sistema, sotto il vincolo che riproducano i momenti noti.

Questa tesi è composta da quattro capitoli. Per meglio comprendere la derivazione dei modelli, nei primi due capitoli sono brevemente presentati i concetti base della fisica dei semiconduttori e della teoria del trasporto di cariche.

In particolare il capitolo 1 inizia con le definizioni di reticoli e cristalli, proseguendo con la derivazione e la descrizione della struttura a bande di energia del cristallo, che permette di introdurre le bande di conduzione e di valenza. Dall'ampiezza del gap tra queste due bande, è possibile classificare i materiali in isolanti, conduttori e semiconduttori. Il capitolo si conclude con l'introduzione delle principali approssimazioni analitiche impiegate per l'energia dei portatori di carica nelle valli e con i concetti di vibrazioni reticolari e fononi, questi ultimi fondamentali per la descrizione del trasporto di cariche.

Nel capitolo 2 viene derivata l'equazione di Boltzmann per gli elettroni, dapprima in assenza di collisioni, poi tenendo conto dei principali processi di scattering, che possono essere descritti tramite l'operatore di collisione. Vengono infatti presentati i principali meccanismi di interazione tra elettroni e fononi e tra elettroni e impurezze. A conclusione del capitolo vengono introdotti il metodo dei momenti ed il metodo di chiusura basato sul principio di massima entropia.

Negli ultimi due capitoli sono descritti due modelli idrodinamici, sviluppati rispettivamente in [9] e in [26]. L'obiettivo di entrambi i capitoli è la costruzione di modelli macroscopici in grado di descrivere il trasporto di cariche in un generico semiconduttore composto. Infatti questi modelli sono costruiti in modo da poter essere applicati ad un qualsiasi materiale semiconduttore con poche modifiche, una volta identificati i parametri fisici del

materiale e il numero di valli nelle bande di conduzione. Nel capitolo 3 viene presentato un modello isotropo, mentre nel capitolo 4 uno anisotropo. Questi modelli considerano i principali meccanismi di scattering nei semiconduttori polari, cioè le interazioni delle cariche con i fononi acustici, ottici polari e impurezze per quanto riguarda gli scattering intravalle, e con i fononi ottici non polari per i processi intervalle.

Nei semiconduttori, le cariche che contribuiscono maggiormente alla conduzione sono gli elettroni che occupano gli stati attorno ai minimi delle bande di conduzione più basse e le lacune attorno ai massimi delle bande di conduzione più alte. E' quindi di fondamentale importanza costruire modelli che utilizzino le migliori approssimazioni possibili per le relazioni di dispersione dell'energia per queste cariche. Nel capitolo 3 è considerata una relazione di dispersione isotropa. L'approssimazione è sferica e non parabolica. In questo capitolo sono mostrati i risultati delle simulazioni numeriche per i casi del GaN e del 4H-SiC. I risultati ottenuti sono in buon accordo con quelli presenti in letteratura, basati su modelli cinetici.

Per semiconduttori altamente anisotropi sono comunque necessarie approssimazioni migliori.

Per questo motivo, nel capitolo 4 è impiegata una relazione di dispersione dell'energia piú generale, considerando l'approssimazione ellissoidale. Questa approssimazione è utile per descrivere il trasporto di cariche nei semiconduttori in cui le masse degli elettroni lungo gli assi principali sono molto differenti, implicando diverse velocità di drift degli elettroni lungo direzioni diverse. Alla fine del capitolo, sono mostrati i risultati delle simulazioni numeriche per il 4H-SiC e per il 6H-SiC. Anche in questo caso i risultati sono in buon accordo con quelli presenti in letteratura. Il modello presentato in questo capitolo può essere considerato un miglioramento del precedente, descritto nel capitolo 3. I due modelli, isotropo e anisotropo, sono stati infatti confrontati per il caso del 4H-SiC. L'importanza di tenere in considerazione l'anisotropia è mostrata dalle differenze trovate per quanto riguarda l'occupazione delle valli, l'energia media totale e soprattutto la velocità di

drift totale.